Journal of Ophthalmology

Pathogenesis of Common Ocular Diseases

Guest Editors: Jun Zhang, Jingsheng Tuo, Zhongfeng Wang, Aiqin Zhu, Anna Machalińska, and Qin Long

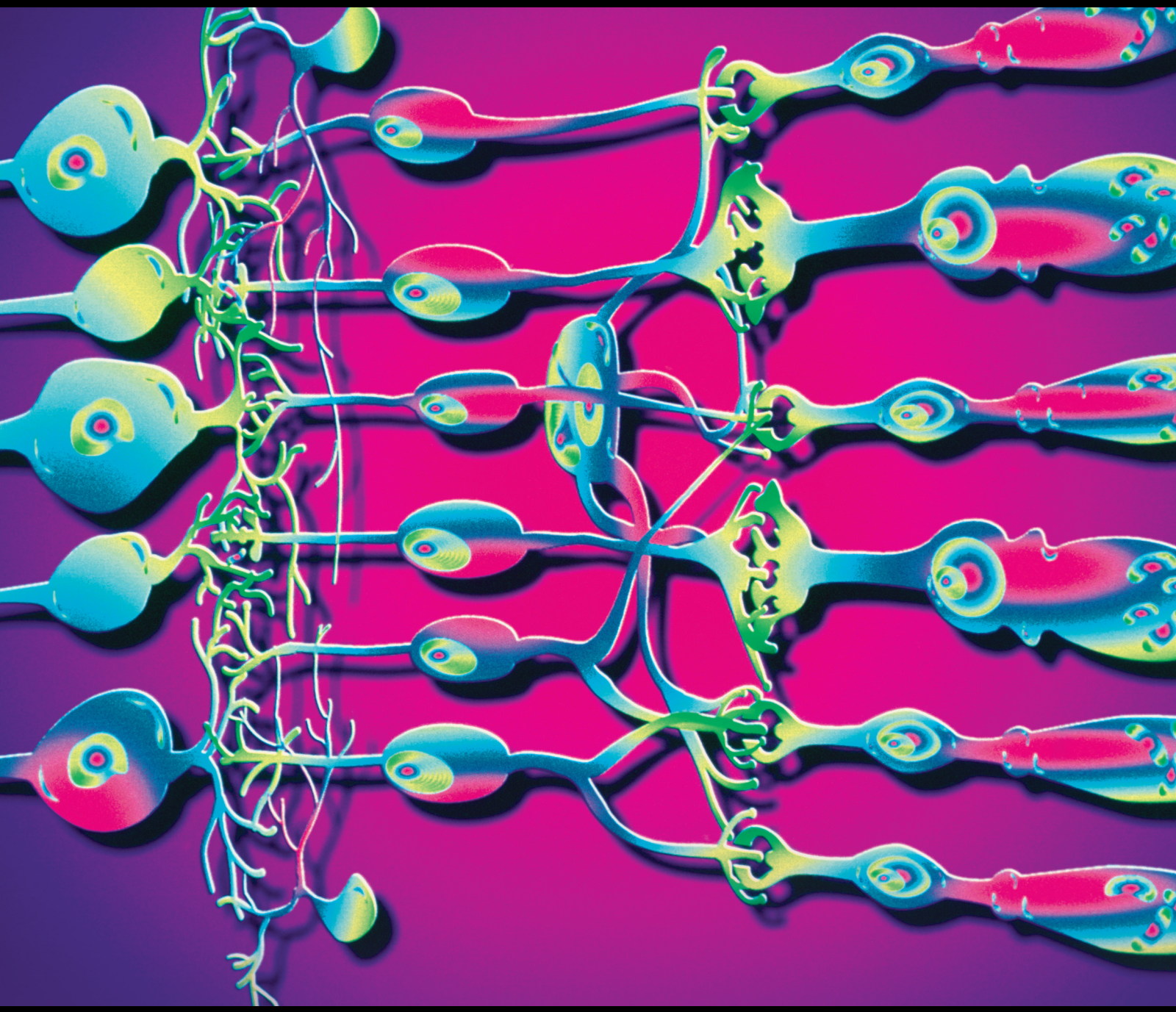

Pathogenesis of Common Ocular Diseases

Journal of Ophthalmology

Pathogenesis of Common Ocular Diseases

Guest Editors: Jun Zhang, Jingsheng Tuo, Zhongfeng Wang, Aiqin Zhu, Anna Machalinska, and Qin Long

Copyright © 2015 Hindawi Publishing Corporation. All rights reserved.

This is a special issue published in "Journal of Ophthalmology." All articles are open access articles distributed under the Creative Commons Attribution License, which permits unrestricted use, distribution, and reproduction in any medium, provided the original work is properly cited.

Editorial Board

Hee B. Ahn, Republic of Korea
Luis Amselem, Spain
Usha P. Andley, USA
Siamak Ansari-Shahrezaei, Austria
Taras Ardan, Czech Republic
Francisco Arnalich-Montiel, Spain
Takayuki Baba, Japan
Paul Baird, Australia
Antonio Benito, Spain
Mehmet Borazan, Turkey
David J. Calkins, USA
Francis Carbonaro, Malta
Chi-Chao Chan, USA
Lingyun Cheng, USA
Chung-Jung Chiu, USA
Daniel C. Chung, USA
Colin Clement, Australia
Miguel Cordero-Coma, Spain
Ciro Costagliola, Italy
Vasilios F. Diakonis, USA
Priyanka P. Doctor, India
Michel E. Farah, Brazil
Giulio Ferrari, Italy
Paolo Fogagnolo, Italy
Farzin Forooghian, Canada
Joel Gambrelle, France
M.-Andreea Gamulescu, Germany
Santiago Garcia-Lazaro, Spain
Ian Grierson, UK
Vlassis Grigoropoulos, Greece
Takaaki Hayashi, Japan
Takeshi Ide, Japan
Vishal Jhanji, Hong Kong
Thomas Klink, Germany
Laurent Kodjikian, France
Naoshi Kondo, Japan
Ozlem G. Koz, Turkey
Rachel W. Kuchtey, USA
Hiroshi Kunikata, Japan
Toshihide Kurihara, Japan
George Kymionis, Greece
Neil Lagali, Sweden
Achim Langenbucher, Germany
Van C. Lansingh, USA
Paolo Lanzetta, Italy
Theodore Leng, USA
Marco Lombardo, Italy
Tamer A. Macky, Egypt
David Madrid-Costa, Spain
Edward Manche, USA
Flavio Mantelli, USA
Enrique Mencía-Gutiérrez, Spain
Marcel N. Menke, Switzerland
Lawrence S. Morse, USA
Darius M. Moshfeghi, USA
Majid M. Moshirfar, USA
Hermann Mucke, Austria
Ramon Naranjo-Tackman, Mexico
Magella M. Neveu, UK
Neville Osborne, UK
Ji-jing Pang, USA
Enrico Peiretti, Italy
David P. Piñero, Spain
Jesús Pintor, Spain
Gordon Terence Plant, UK
Pawan Prasher, India
Antonio Queiros, Portugal
Anthony G. Robson, UK
Mario R. Romano, Italy
Dirk Sandner, Germany
Ana R. Santiago, Portugal
Patrik Schatz, Sweden
Kin Sheng Lim, UK
Wisam A. Shihadeh, USA
Bartosz Sikorski, Poland
Katsuyoshi Suzuki, Japan
Shivalingappa K. Swamynathan, USA
Suphi Taneri, Germany
Christoph Tappeiner, Switzerland
Stephen Charn Beng Teoh, Singapore
Panagiotis G. Theodossiadis, Greece
Biju B. Thomas, USA
Lisa Toto, Italy
Manuel Vidal-Sanz, Spain
Gianmarco Vizzeri, USA
David A. Wilkie, USA
Suichien Wong, UK
Victoria W Y Wong, Hong Kong
Wai T. Wong, USA
Terri L. Young, USA
Hyeong Gon Yu, Republic of Korea
Vicente Zanon-Moreno, Spain

Contents

Hindawi Publishing Corporation
Journal of Ophthalmology
Volume 2015, Article ID 734527, 2 pages
http://dx.doi.org/10.1155/2015/734527

Editorial

Pathogenesis of Common Ocular Diseases

Jun Zhang,[1] Jingsheng Tuo,[2] Zhongfeng Wang,[3] Aiqin Zhu,[4] Anna Machalińska,[5] and Qin Long[6]

[1]*Synaptic Physiology Section, National Institute of Neurological Disorders and Stroke, National Institutes of Health, Bethesda, MD, USA*
[2]*Laboratory of Immunology, National Eye Institute, National Institutes of Health, Bethesda, MD, USA*
[3]*Institutes of Brain Science, State Key Laboratory of Medical Neurobiology, Collaborative Innovation Center for Brain Science, Fudan University, Shanghai, China*
[4]*Institute of Geriatrics, Qinghai Provincial Hospital, Xining, Qinghai, China*
[5]*Department of Ophthalmology and Department of Histology and Embryology, Pomeranian Medical University, Szczecin, Poland*
[6]*Department of Ophthalmology, Peking Union Medical College Hospital, Chinese Academy of Medical Sciences & Peking Union Medical College, Beijing, China*

Correspondence should be addressed to Jun Zhang; junzhang@ninds.nih.gov

Received 13 December 2015; Accepted 13 December 2015

Copyright © 2015 Jun Zhang et al. This is an open access article distributed under the Creative Commons Attribution License, which permits unrestricted use, distribution, and reproduction in any medium, provided the original work is properly cited.

The most common diseases resulting in irreversible blindness or vision impairment include age-related macular degeneration (AMD), glaucoma, diabetic retinopathy, cataract, and dry eye. These diseases seriously affect the quality of life in elderly people worldwide. Therefore, understanding their pathogenesis and the development of strategies allowing earlier detection and treatment demands more effort and attention from both basic and clinical fields. This issue focuses on different aspects of these diseases in elderly population.

AMD is one of the most common diseases resulting in irreversible blindness worldwide in the elderly population. Among multifactorial pathogenesis, immune dysregulations are leading theories of AMD pathogenesis. Recently IL-17 pathway was reported to be involved in AMD pathogenesis. In the original article "Responses of Multipotent Retinal Stem Cells to IL-1β, IL-18, or IL-17" by S. Chen et al., the authors investigated the responses of multipotent retinal stem cells (RSCs), isolated from mice, to the proinflammatory signaling molecules including IL-1β, IL-18, and IL-17A. They found that the addition of IL-1β, IL-18, or IL-17A in the cultured cell decreased RSC viability but increased pyroptotic and/or necroptotic cells. The study is innovative and unique, because, instead of RPE19, a new cell type was used as the model system. Additionally, the results fill gaps in understanding immunological mechanism of AMD pathogenesis.

Like AMD, glaucoma and diabetic retinopathy are common causes of blindness in older adults. Glaucoma is often caused by damage to the optic nerve due to an abnormally high pressure in your eye, while diabetic retinopathy is a diabetes complication, caused by damage to the retinal blood vessels. However, both of them have no symptoms or warning signs at early stage. Thus, it is important to have regular eye exams to measure intraocular pressure and ocular blood flow. In the review paper "Ocular Blood Flow Autoregulation Mechanisms and Methods" by X. Luo et al., the authors summarized the methods for ocular blood flow evaluating and discussed mechanism and treatment of ocular blood flow regulation, particular in glaucoma and diabetic retinopathy.

Cataract is one of the major causes of visual impairment of elderly people. Although recent bioinformatics studies revealed susceptibility genes, such as EPHA2, for age-related cataract, the mechanism underlying its pathogenesis remains elusive. In the original paper "The Polymorphisms with Cataract Susceptibility Impair the EPHA2 Receptor Stability and Its Cytoprotective Function" by J. Yang et al., the authors found that EPHA2 signaling can protect the lens epithelial cells from oxidative stress-induced cell death. In the original paper "Epigenetic Regulation of Werner Syndrome Gene in Age-Related Cataract" by X. Zhu et al., the authors investigated the promotor methylation and histone medication of

Werner syndrome gene (WRN). They found that both mRNA and protein levels of WRN were significantly decreased only in anterior lens capsules in age-related cataract, suggesting that the strategies to intervene epigenetic alteration in this disease should aim to anterior lens capsules. By investigating very large cataract patient population in rural China, X. Cao et al. presented a normative ocular biometry of adult cataract patients in rural China. They found that the axial length is normally distributed with a positive skew and a big kurtosis and corneal astigmatism may affect rural Chinese vision acuity.

Dry eye is a multifactorial disorder of the tears and ocular surface and is a common and often unrecognized disease affecting tens of millions of individuals worldwide. Q. Long et al. evaluated the biomechanical behavior of the cornea in dry eye using, for the first time, Corneal Visualization Scheimpflug Technology (CorVis ST), a new noncontact tonometry system. Their results provide insight into its full usefulness for dry eye patients. B. Wang et al. compared dry eye disease that resulted from two refractive surgeries [small-incision lenticule extraction (SMILE) versus femtosecond laser in situ keratomileusis (FS-LASIK)] in high myopia. They found that SMILE is a safe and successful alternative for the correction of refractive error and may provide a more superior and safer refractive outcome than FS-LASIK in the first six months following surgery. CorVis ST, the very latest technology, has been used by J. Wang et al. to assess the biomechanical parameters of the cornea in myopic and emmetropic eyes.

Vitreous hemorrhage (VH) is one of the ophthalmologic emergency situations. In the paper contributed by D. Y. Kim and colleagues, the authors analyzed causes and prognosis of acute-onset preoperatively unknown origin VH in 169 eyes and found that retinal vein occlusion, retinal break, and AMD are the most common causes. In addition, aging may be an important factor for influencing visual prognosis following vitrectomy.

Optic neuritis is one of the common optic neuropathies and is highly associated with multiple sclerosis. In the original paper "Evaluation of Retinal Nerve Fiber Layer and Ganglion Cell Complex in Patients with Optic Neuritis or Neuromyelitis Optica Spectrum Disorders Using Optical Coherence Tomography in a Chinese Cohort" by G. Tian et al., the authors reported that spectral-domain optical coherence tomography, SD-OCT, is a very useful and objective method to evaluate the thickness of the peripapillary retinal nerve fiber layer and macular ganglion cell complex in optic neuritis and neuromyelitis optica.

Common age-related ocular diseases demand attention as a global health problem. This special issue covered pathogenesis, diagnosis, and treatment of most of these diseases.

Jun Zhang
Jingsheng Tuo
Zhongfeng Wang
Aiqin Zhu
Anna Machalińska
Qin Long

Hindawi Publishing Corporation
Journal of Ophthalmology
Volume 2015, Article ID 401894, 9 pages
http://dx.doi.org/10.1155/2015/401894

Research Article

The Polymorphisms with Cataract Susceptibility Impair the EPHA2 Receptor Stability and Its Cytoprotective Function

Jin Yang,[1,2] Dan Li,[2,3] Qi Fan,[1,2] Lei Cai,[1,2] Xiaodi Qiu,[1,2] Peng Zhou,[4] and Yi Lu[1,2]

[1] *Department of Ophthalmology, Eye and ENT Hospital, Fudan University, 83 Fenyang Road, Shanghai 200031, China*
[2] *Myopia Key Laboratory of Health PR China, Shanghai 200031, China*
[3] *Research Center, Eye and ENT Hospital, Fudan University, 83 Fenyang Road, Shanghai 200031, China*
[4] *Department of Ophthalmology, Parkway Health Hong Qiao Medical Center, Shanghai 200336, China*

Correspondence should be addressed to Yi Lu; luyieent@126.com

Received 27 June 2015; Revised 20 October 2015; Accepted 22 October 2015

Academic Editor: Jun Zhang

Copyright © 2015 Jin Yang et al. This is an open access article distributed under the Creative Commons Attribution License, which permits unrestricted use, distribution, and reproduction in any medium, provided the original work is properly cited.

Despite accumulating evidence revealing susceptibility genes for age-related cataract, its pathophysiology leading to visual impairment at the cellular and molecular level remains poorly understood. Recent bioinformatic studies uncovered the association of two single nucleotide polymorphisms in human EPHA2, rs2291806 and rs1058371, with age-related cataract. Here we investigated the role of EPHA2 in counteracting oxidative stress-induced apoptosis of lens epithelial cells. The cataract-associated missense mutations resulted in the destabilization of EPHA2 receptor without altering the mRNA transcription. The cytoprotective and antiapoptotic function of EPHA2 in lens epithelial cells was abolished by the functional polymorphisms. Furthermore, our results suggest that the downstream signaling of activated EPHA2 promotes the antioxidative capacity of lens epithelial cells to eradicate the overproduction of reactive oxygen species. In contrast, the overexpression of EPHA2 with nonsynonymous mutations in the lens epithelial cells offered limited antioxidative protection against oxidative stress. Thus, our study not only sheds the light on the potential cytoprotective function of EPHA2 signaling in lens but also provides the cellular mechanisms underlying the pathogenesis of age-related cataract.

1. Introduction

Cataract, the opacity of crystalline lens, is the leading cause of blindness and visual impairment worldwide. While congenital cataract is largely inherited in a Mendelian manner with high penetrance, both genetic risk and environmental factors contribute to age-related cataract [1, 2]. Cumulative damage of environmental insults exerts oxidative stress on lens epithelial cells with genetic susceptibility and induces cellular apoptosis, a common cellular mechanism underpinning noncongenital cataract [3–5]. Recent genetic and epidemiological studies suggest the association of Eph-receptor tyrosine kinase-type A2 (EPHA2) with human age-related cataract in distinct populations [6–9]. Despite the bioinformatic screening of nonsynonymous single nucleotide polymorphism (SNP) in *EPHA2* gene as potential risk variants for cataract [10], the cellular and molecular mechanisms underlying its pathogenesis remain elusive.

As a member of the Eph superfamily of receptor tyrosine kinases, the forward signaling cascade of EPHA2 is primarily mediated by its corresponding ephrin-A ligands [11, 12]. Genetic and pharmacological inhibition of EPHA2 induces apoptosis and abrogates tumorigenic growth of tumor cells [13–16]. EPHA2 protein is expressed in human and mouse lens [6], implying its potential role in maintaining lens clarity during aging by promoting cell viability. The combined application of bioinformatic tools including Soft Intolerant from Tolerant (SIFT), Polymorphism Phenotype (PolyPhen), and I-Mutant identified nonsynonymous rs2291806 and rs1058371 as potential functional polymorphisms [10].

The accrual of oxidative damage to lens epithelial cells at least partially causes age-related cataract [17–19]. Under physiological conditions, reactive oxygen species (ROS) are scavenged and eliminated by superoxide dismutase (SOD) in the mitochondria [20]. Either the overproduction of ROS or the dysfunction of endogenous antioxidants disrupts the redox homeostasis and thus triggers the apoptotic process and pathogenesis of the disease [21, 22]. It was shown that the induction of ROS activated EPHA2 receptor to promote virus entry during Kaposi's sarcoma-associated herpesvirus (KSHV) infection [23], which raises questions about the antioxidant role of EHPA2 signaling. Here we show the cytoprotective function by EPHA2 against oxidative stress-mediated damages as well as the antioxidative capacity of EPHA2 polymorphisms rs2291806 and rs1058371 which predispose the individuals to age-related cataract.

2. Materials and Methods

2.1. Cell Culture. The human lens epithelial cell (HLEC) line SRA 01/04 (transformed by Simian virus 40 large T antigen) was purchased from the American Type Culture Collection [24]. For maintenance, HLECs were cultured in Dulbecco's modified eagle's medium (DMEM; Invitrogen, Carlsbad, CA, USA) with 10% of heat inactivated fetal bovine serum (Invitrogen), 100 U/mL of penicillin (Sigma, St. Louis, MO, USA), and 100 μg/mL of streptomycin (Sigma) in humidified 5% CO_2 at 37°C.

2.2. Plasmid Construction and Cell Transfection. The wild-type human *EPHA2* gene (NM_004431.3) was generated by PCR using the following primers:

forward primer: 5′-CTAGCTAGCATGGAGCTCCAGGCAGCCCGC-3′,

reverse primer: 5′-ACGCGTCGACTCAGATGGGGATCCCCACAGT-3′.

The PCR product was then subcloned into Ubi-MCS-3FLAG-SV40-EGFP-IRES-puromycin lentiviral vector. The plasmids encoding EPHA2 polymorphism: rs1058371 (286A>T; forward primer: 5′-GAGGCTGAGCGTATCTTCTTTGAGCTCAAGTTTACTG-3′, and reversed primer: 5′-CAGTAAACTTGAGCTCAAAGAAGATACGCTCAGCCTC-3′), rs2291806 (2473G>A; forward primer: 5′-TGGGAGTTGTCCAACCACAAGGTGATGAAAGCCATCA-3′, and reversed primer: 5′-TGATGGCTTTCATCACCTTGTGGTTGGACAACTCCCA-3′), and rs3754334 (2874C>T; forward primer: 5′-CGGCCACCAGAAGCGCATTGCCTACAGCCTGCTGGGA-3′, and reversed primer: 5′-TCCCAGCAGGCTGTAGGCAATGCGCTTCTGGTGGCCG-3′), were constructed using Multipoints Mutagenesis Kit (Takara, Dalian, Liaoning, China). The lentiviral plasmid encoding WT or mutated EPHA2 was cotransfected with pMDL, pRev, and pVSVG into 293gp cells to generate high-titers of lentivirus, followed by ultracentrifugation of viral supernatants [25]. HLECs were infected with diluted lentivirus and the green fluorescence signal was examined under a fluorescence light microscope (Olympus Inc., Tokyo, Japan) with digital images captured.

2.3. Real-Time PCR. Total RNA was extracted with Trizol reagent (Invitrogen) from the HLECs 72 h after infection. First strand cDNAs were synthesized from 1.0 μg total RNA by reverse transcription using the RevertAid H Minus First Strand cDNA Synthesis Kit (Hanover, MD, USA). Real-time PCR was performed using the following primers: forward primer 5′-TGGCTCACACACCCGTATG-3′ and reversed primer 5′-GTCGCCAGACATCACGTTG-3′. As an internal control, *β-actin* was amplified using 5′-CATTAAGGAGAAGCTGTGCT-3′ and 5′-GTTGAAGGTAGTTTCGTGGA-3′ as forward and reverse primers, respectively.

2.4. Western Blotting Analysis. Cell lysates were collected from the HLECs 72 h after infection with lentivirus expressing wild-type EPHA2 or mutants. The protein concentration was determined by BCA assay. The proteins were separated by electrophoresis and transferred to a nitrocellulose membrane. The blocked membrane was incubated overnight with primary antibodies against EPHA2, GFP, or GAPDH (Santa Cruz, CA, USA) at 4°C. Following washing three times in TBST, the membrane was incubated with goat anti-mouse HRP-conjugated secondary antibodies for 30 min at room temperature. After washes with TBST, immunoreactive signals were detected using enhanced chemiluminescence reagent (Pierce). Images were captured with the ChemiDocT-MMP imaging system (Bio-Rad, Hercules, CA, USA). The densitometric intensity of the imaged bands was analyzed by Image-Pro Plus 5.0 (Media Cybernetics, Silver Spring, EUA). Triplicate experiments were performed.

2.5. Cell Viability Assay. Cell viability and proliferation were determined using a Cell Counting Kit-8 (CCK-8) assay (Dojindo Laboratories, Kumamoto, Japan), which is a sensitive measurement of the survival status of cells. HLECs in the logarithmic growth phase were collected and seeded in 96-well plates (1×10^4 cells/well). After culture in the absence of antibiotics for 24 h, cells were infected with lentivirus encoding wild-type EPHA2 or SNP mutants for 72 h. To each well, 100 μL CCK8 solution dissolved in DMEM was added. After incubation for 3 h, the optical density of formazan crystals was measured in an X Mark microplate spectrophotometer (Bio-Rad) at 450 nm. Eight duplicate wells were used for measurement. Triplicate experiments were performed.

2.6. Measurement of Lipid Peroxidation Products. Lipid peroxidation was assessed with malondialdehyde (MDA) assay using Lipid Peroxidation MDA Assay Kit from Beyotime. Briefly, HLECs with lentiviral infection were lysed in 0.1 M Tris/HCl buffer (pH 7.4 containing 0.5% Triton X-100, 5 mM β-mercaptoethanol, and 0.1 mg/mL PMSF) 72 h after transfection. The lysate supernatant (0.1 mL) was mixed with trichloroacetic acid (15%, w/vol), thiobarbituric acid (0.375%, w/vol), and hydrochloric acid (0.25 M) at a 1 : 1 : 1 : 1 ratio. The mixture was heated at 100°C for 30 min, immediately cooled, and then centrifuged (3,500 ×g for 5 min). The absorbance of the supernatant was measured at 532 nm. The amount of thiobarbituric-acid-reacting substance (TBARS) was calculated MDA equivalents as previously described [26]. Triplicate experiments were performed.

2.7. Superoxide Dismutase (SOD) Activity Assay. In this assay, a water-soluble formazan dye is produced from WST-1 upon its reduction by superoxide anion. The rate of the superoxide anion-mediated reduction is linearly related to the xanthine oxidase activity and is inhibited by SOD, and the inhibitory activity of SOD can be determined by a colorimetric method. To perform this assay, HLECs were seeded on 6-well plates, infected with lentivirus, and lysed in ice-cold 0.1 M Tris/HCl buffer 72 h later. The lysates were centrifuged at 14000 ×g at 4°C for 5 min and the supernatant was collected. The SOD activity in the supernatants was determined by measuring the absorbance at 450 nm in a spectrophotometer. Triplicate experiments were performed.

2.8. Total Antioxidant Capacity (TAC) Assay. Total Antioxidant Capacity (TAC) Colorimetric Assay Kit from BioVision was used to measure the endogenous antioxidants. Briefly, HLECs cells were infected with lentivirus in 6-well plates and collected with ice-cold 0.1 M PBS. Cell lysates were centrifuged at 14000 ×g at 4°C for 4 min and the supernatant was harvested. The absorbance of the supernatant was measured at 570 nm in an X Mark microplate spectrophotometer (Bio-Rad). Triplicate experiments were performed.

2.9. Flow Cytometric Detection of Apoptosis Assay. Apoptosis was evaluated by APC-annexin V/7-AAD (BD Pharmingen, California, USA) staining followed by flow cytometric analysis. Cells were plated in 6-well plates at a density of 1×10^5/well and cultured for 48 h with reagents. Then, the cells were gently trypsinized and washed twice with ice-cold PBS. At least 10,000 cells were resuspended in 100 μL 1x binding buffer, stained with 5 μL 7-AAD (25 μg/mL) and 5 μL APC-annexin V at 4°C for 30 min, and immediately analyzed with a FACScanto flow cytometer (BD Bioscience, USA). Each measurement was carried out in triplicate.

2.10. Statistical Analysis. Data were expressed as mean ± standard error and analyzed by one-way ANOVA and *post hoc* Bonferroni's test. The statistical software, Prism 5 (GraphPad software Inc., San Diego, CA, USA), was used. The criterion for statistical significance was $p < 0.05$.

3. Results

3.1. Impaired Protein Stability Caused by Missense Mutation in EPHA2. There are a total of 134 nonsynonymous SNPs identified within the coding region of *EPHA2* gene. A previous bioinformatic analysis suggests that rs2291806 (E825K) and rs1058371 (I96F) are potential functional polymorphisms involved in susceptibility to cataract formation [10]. Multiple sequence alignment of human, macaque, rat, and mouse EPHA2 showed that both amino acids with missense mutations are evolutionarily conserved (Figure 1(a)). To investigate the cytoprotective role of EPHA2 in lens epithelial cells and the molecular mechanism underlying the association of EPHA2 mutation with age-related cataract, we generated the lentiviral plasmids encoding wild-type EPHA2, $EPHA2^{E825K}$, and $EPHA2^{I96F}$ and prepared the high-titers of corresponding lentivirus for infection. The human lens epithelial cells (HLECs) were subsequently infected with lentivirus expressing either wild-type or mutant EPHA2. The quantification by counting the green fluorescent protein-(GFP-) positive cells showed that ~85% of cells on average were overexpressed by EPHA2 and its missense mutants 72 h after infection (Figures 1(b) and 1(c)).

The abundance of *EPHA2* mRNA in each group after lentiviral infection was evaluated with real-time PCR. There was a 2.5-fold increase in the level of *EPHA2* mRNA following lentivirus-mediated overexpression, as compared with non-infected cells and vector control (Figures 2(a) and 2(b)). Our previous study showed that a synonymous polymorphism within *EPHA2* gene, named rs3754334, is associated with the risk of age-related cataract [27]. Using the synonymous substitution as negative control, we compared the level of mRNA transcripts encoding the wild-type and mutant EPHA2 and found no difference in the transcription (Figure 2(b)).

The missense mutations with apparent effects on function are dominated by compromised protein stability [28]. Thus, we further examined the protein level of EPHA2 without or with amino acid substitution in HLECs by western blot. The results showed that $EPHA2^{I96F}$ and $EPHA2^{E825K}$ mutation significantly impaired the receptor stability while synonymous SNP rs3754334 did not affect the protein expression of EPHA2 (Figure 2(c)). Taken together, these results suggest that the missense mutations in EPHA2 are potentially associated with age-related cataract via compromising the macromolecular stability and its functional network.

3.2. Loss of Cytoprotective Function by Cataract-Associated Mutation in EPHA2. Eph receptors have been shown to play critical roles in tissue boundary formation, neural crest cell migration, axon guidance, bone remodeling, and vascular organization [12]. However, whether the EPHA2 signaling pathway provides cytoprotective effects against oxidative challenge remains largely unclear. To decipher the cellular functions of EPHA2, we overexpressed wild-type EPHA2 in HLECs and examined the cell viability before and after the treatment with 200 μM H_2O_2 to induce oxidative stress (Figure 3(a)). The relative index of cell death was evaluated by

$$\text{Absorbance index} = \frac{\text{The number of starter cells}}{\text{Absorbance value} \times 10000},$$
$$\text{Relative index} = \frac{\text{Absorbance index of experimental group}}{\text{Avergae absorbance index of vector group}}. \quad (1)$$

The absorbance value at 450 nm was determined using CCK8 assay. The relative results of cell viability assay without H_2O_2 stimulation imply that EPHA2 overexpression may enhance the proliferation of lens epithelial cells (Figure 3(b)). The quantitative analysis also showed that overexpression of EPHA2 in HLECs reduced the relative index of cell death and especially ameliorated H_2O_2-induced apoptosis (Figures 3(b) and 3(c)), suggesting the cytoprotective function of EPHA2 in the cultured lens epithelial cells. In addition, we found that

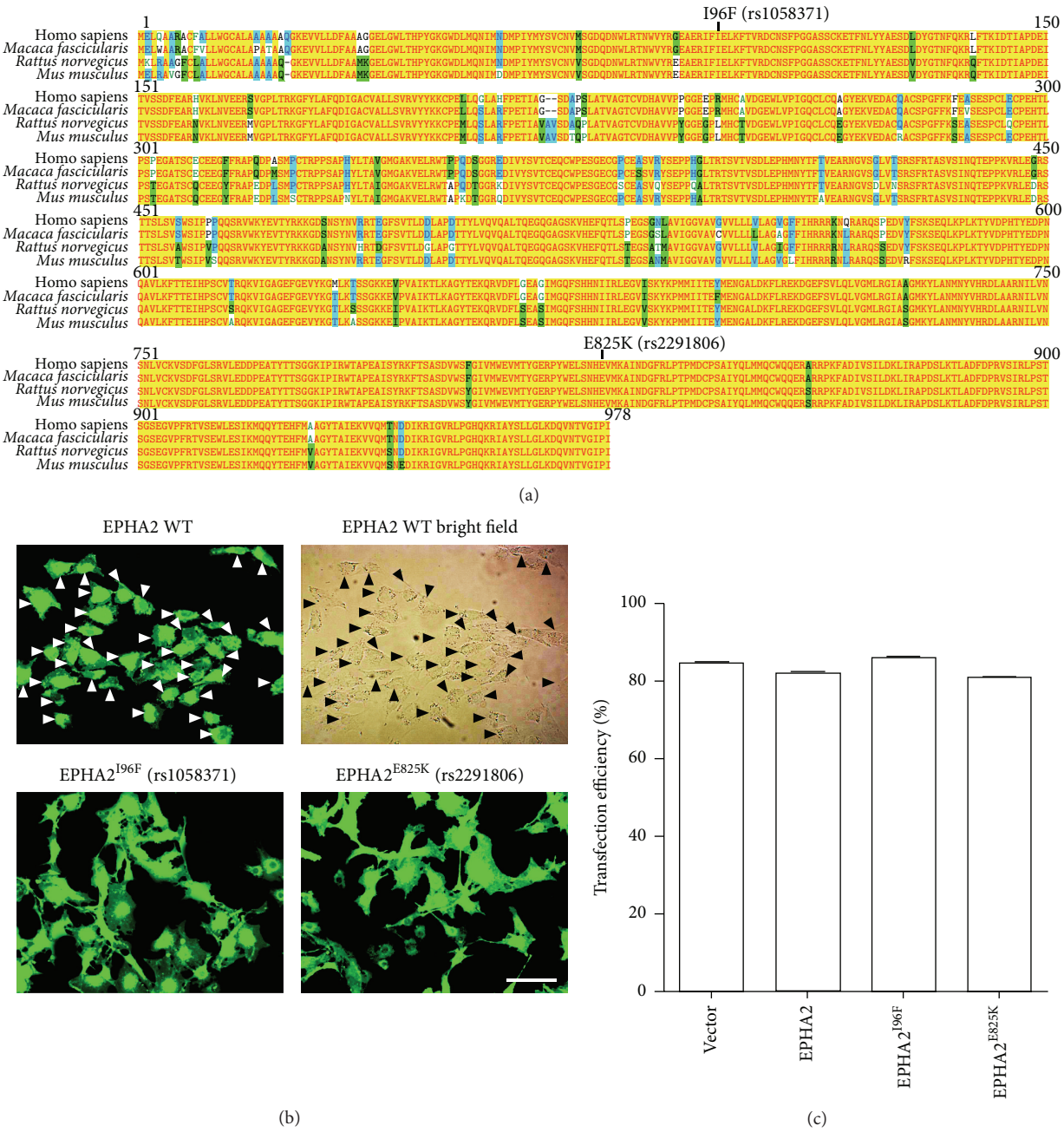

Figure 1: The evolutional conservation of cataract-associated SNP and the overexpression of EPHA2 in lens epithelial cells. (a) The protein sequences of human, macaque, rat, and mouse EPHA2 were aligned for multiple comparison. The functional polymorphisms rs1085371 and rs2291806 are highlighted here to show the missense mutation in EPHA2. The sequence alignment shows the evolutional conservation of both amino acids with substitution. (b) The human lens epithelial cells (HLECs) were infected with lentivirus encoding wild-type EPHA2, $EPHA2^{I96F}$, or $EPHA2^{E825K}$. The images captured with fluorescent microscopy 72 h after infection are shown here. Scale bar: 50 μm. (c) The infection efficiency was quantified by counting GFP-positive cells and total number of cells. Data are shown as the mean ± SEM.

the cytoprotective effect on oxidative stress was abolished by either $EPHA2^{I96F}$ or $EPHA2^{E825K}$ mutation (Figure 3(c)).

To specifically determine the antiapoptotic effect of EPHA2 in HLECs in vitro, we further performed the staining with APC-annexin V or vital dye 7-AAD on the dissociated cells, followed by fluorescent flow cytometry to analyze the proportion of H_2O_2-induced early and apoptotic cells. The data indicated that HLECs with wild-type EPHA2 overexpression displayed a striking reduction in both early and late apoptosis, as compared with control cells undergoing cell death together with the diminishing GFP signal (Figure 4). As expected, ectopic expression of either $EPHA2^{I96F}$ or $EPHA2^{E825K}$ in HLECs showed reduced cytoprotective effects against H_2O_2-induced cell death (Figure 4). These data

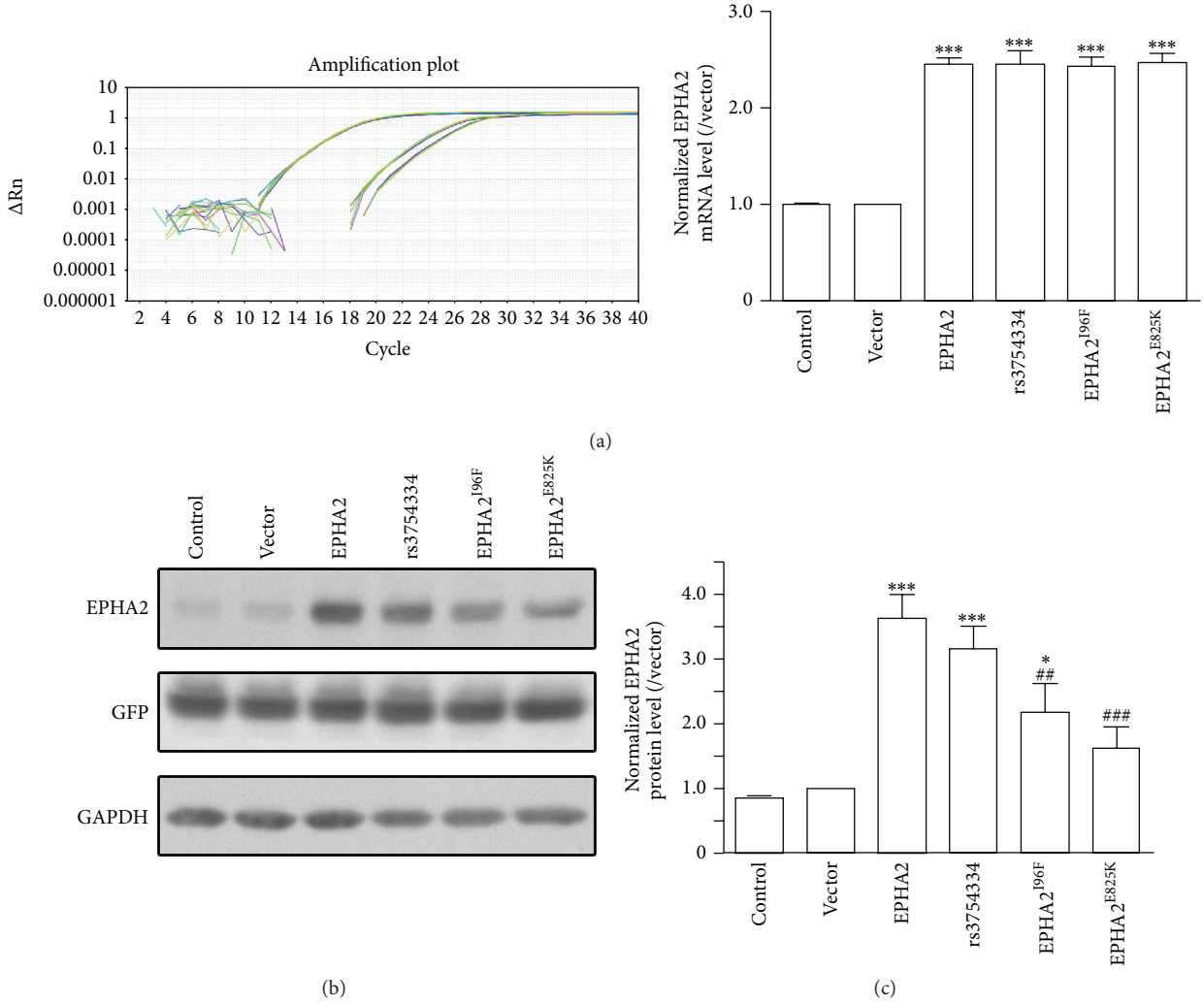

FIGURE 2: The protein destabilization caused by cataract-associated missense mutation. (a) The *EPHA2* mRNA transcriptional level was measured with real-time PCR after HLECs were overexpressed with wild-type or mutant EPHA2 for 48 h. The *EPHA2* mRNA level was normalized with the internal control β-actin and the data are presented as ratio of vector control. (b) The EPHA2 protein expression was tested with western blotting after the lentivirus-mediated overexpression in HLECs. (c) Quantitative analysis shows the impaired protein stability of EPHA2 with missense mutation. The EPHA2 protein level was normalized with the internal control *GAPDH*. Data are shown as the mean ± SEM. $^{*}P < 0.05$, $^{***}P < 0.001$ versus vector control; $^{\#\#}P < 0.01$, $^{\#\#\#}P < 0.001$ versus wild-type EPHA2.

combined demonstrated the protective function of EPHA2 in lens epithelial cells through preventing apoptosis and the neutralization of antiapoptotic effect by two functional polymorphisms.

3.3. Abrogated Antioxidative Effect by Nonsynonymous Polymorphisms with Risk of Cataract. The ROS generated endogenously or induced by environmental stress have long been implicated in cell death and tissue injury in the context of age-related cataract [3–5, 17, 18, 22]. The most efficient enzymatic antioxidants in the lens include SOD, catalase, glutathione peroxidase, and cytosolic glutathion-S-transferase [22, 29]. To investigate the mechanisms underlying the antiapoptotic effect of EPHA2 in the lens, we assessed the levels of lipid peroxidation in the HLECs by MDA assay. Despite the undetectable effect by EPHA2 overexpression under basal conditions, we found that the activation of EPHA2 signaling significantly declined the H_2O_2-induced oxidation of lipids in the lens epithelial cells (Figures 5(a) and 5(b)). Moreover, the SOD activity and the total antioxidative potency were upregulated by overexpression of EPHA2 to counterbalance the production of ROS in HLECs (Figures 5(c) and 5(d)). Interestingly, the antioxidative effect of EPHA2 was consistently abrogated by the identified functional polymorphisms rs2291806 and rs1058371 (Figure 5). Our results showed the antioxidative role of EPHA2 in the lens epithelial cells under the exposure of extrinsic oxidative stress.

4. Discussion

Although genetic studies have hitherto provided a deep insight into the understanding of genetic framework involved

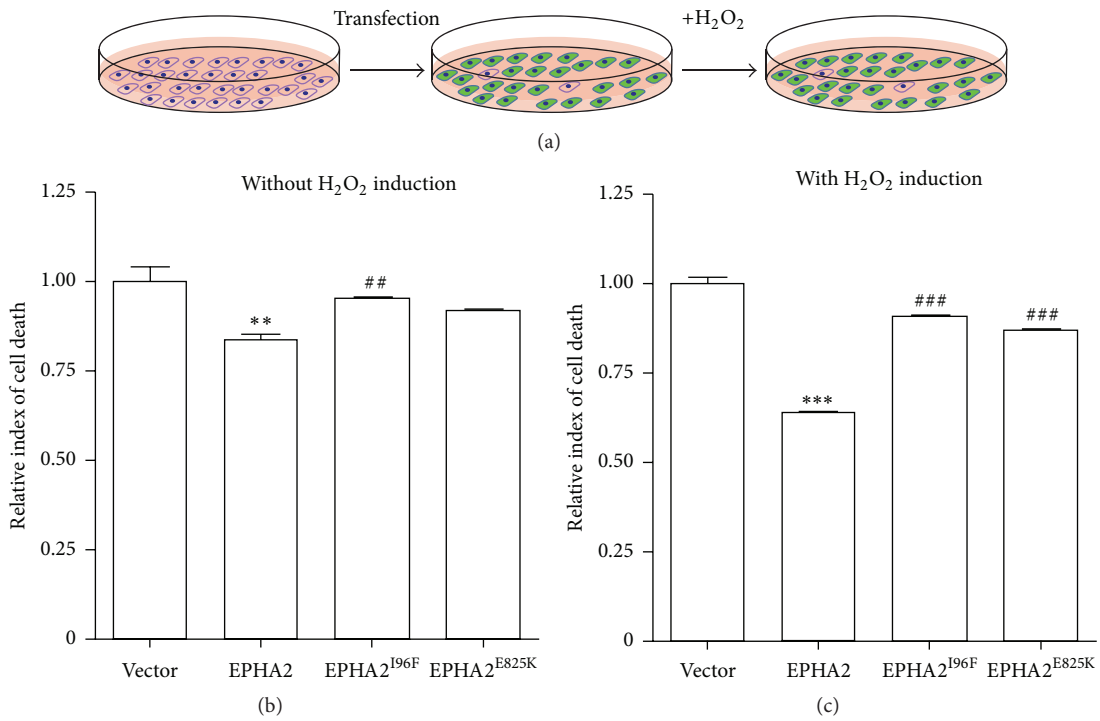

Figure 3: The functional polymorphisms abolish EPHA2-mediated cytoprotective effect. (a) The experimental paradigm. The HLECs were seeded and infected with lentivirus expressing wild-type EPHA2, EPHA2^{I96F}, or EPHA2^{E825K}. The infected cells were treated with 200 μM H_2O_2 to mimic the light-induced oxidative stress in lens. (b-c) The cell viability was assayed before and after H_2O_2 treatment following lentivirus-based gene overexpression. The quantification reveals the cytoprotective effect of wild-type EPHA2 and the loss of function in cataract-associated mutants. Data are shown as the mean ± SEM. $^{**}p < 0.01$, $^{***}p < 0.001$ versus vector control; $^{\#\#}p < 0.01$, $^{\#\#\#}p < 0.001$ versus wild-type EPHA2.

in the age-related cataract, its pathophysiology remains to be elucidated. The putative role of EPHA2 in the etiopathogenesis of age-related cataract has attracted much attention regarding the molecular mechanisms involved in maintaining the clarity of lens by EPHA2. Here we report that EPHA2 signaling protects the lens epithelial cells from oxidative stress-induced cell death. Furthermore, the loss of protein stability in two of the nonsynonymous polymorphisms compromises the antioxidative and antiapoptotic effect of EPHA2.

The previously identified cataract-associated mutations in EPHA2 basically reside in kinase and sterile alpha motif (SAM) domains [2, 12]. It is hypothesized that the loss of EPHA2 function may directly or indirectly impair cellular structural stability, cell-to-cell crosstalk, protein folding, and transcriptional activation, which cause congenital or age-related cataract [6, 12]. Impaired development of lens fiber cells or equatorial cells caused by loss of function in EPHA2 may lead to hereditary cataract, whereas accumulating oxidative stress resulting from both environmental insults and age-dependent reduction of EPHA2 expression in lens could contribute to age-related cataract [6, 12, 17, 30, 31]. Our data suggests that EPHA2 plays a cytoprotective role in lens epithelial cells by promoting cell viability under oxidative stress. In spite of the established regulatory role of Eph/ephrin role in the epithelial morphogenesis and homeostasis [32], we did not find conspicuous differences in the morphology of lens epithelial cells between control and overexpressing cells. Consistent with bioinformatic analysis showing that both rs2291806 and rs1058371 are the least stable among varieties of SNPs [10], our biochemical data confirms that both functional polymorphisms in EPHA2 lead to the destabilization of the receptor and thus neutralize its antiapoptotic role. The decay of mutant EPHA2 is possibly caused by reduced protein solubility and ubiquitin-mediated proteasomal degradation [33]. These results further support that the genetic mutation-mediated protein degradation contributes to apoptosis in age-related degenerative diseases [34, 35].

We further identified the antioxidative effect of EPHA2 by gain-of-function analysis, which underlies its cytoprotective function against environmental insult. Activation of Nrf2 increases the elimination of both exogenous and endogenous toxic chemicals including ROS and Nrf2-dependant signaling regulates the gene expression of EPHA2 [36, 37]. Indeed, our data revealed the upregulation of antioxidative SOD activity and the neutralization of lipid oxidation by EPHA2 activation in the lens epithelial cells. However, the complex transcriptional activation mediated by overexpression of EPHA2 to increase antioxidative capacity still remains to be determined. Importantly, the missense mutations in EPHA2 associated with age-related cataract abolished the EPHA2-mediated enhancement of antioxidative capacity, suggesting the loss of function in both polymorphisms.

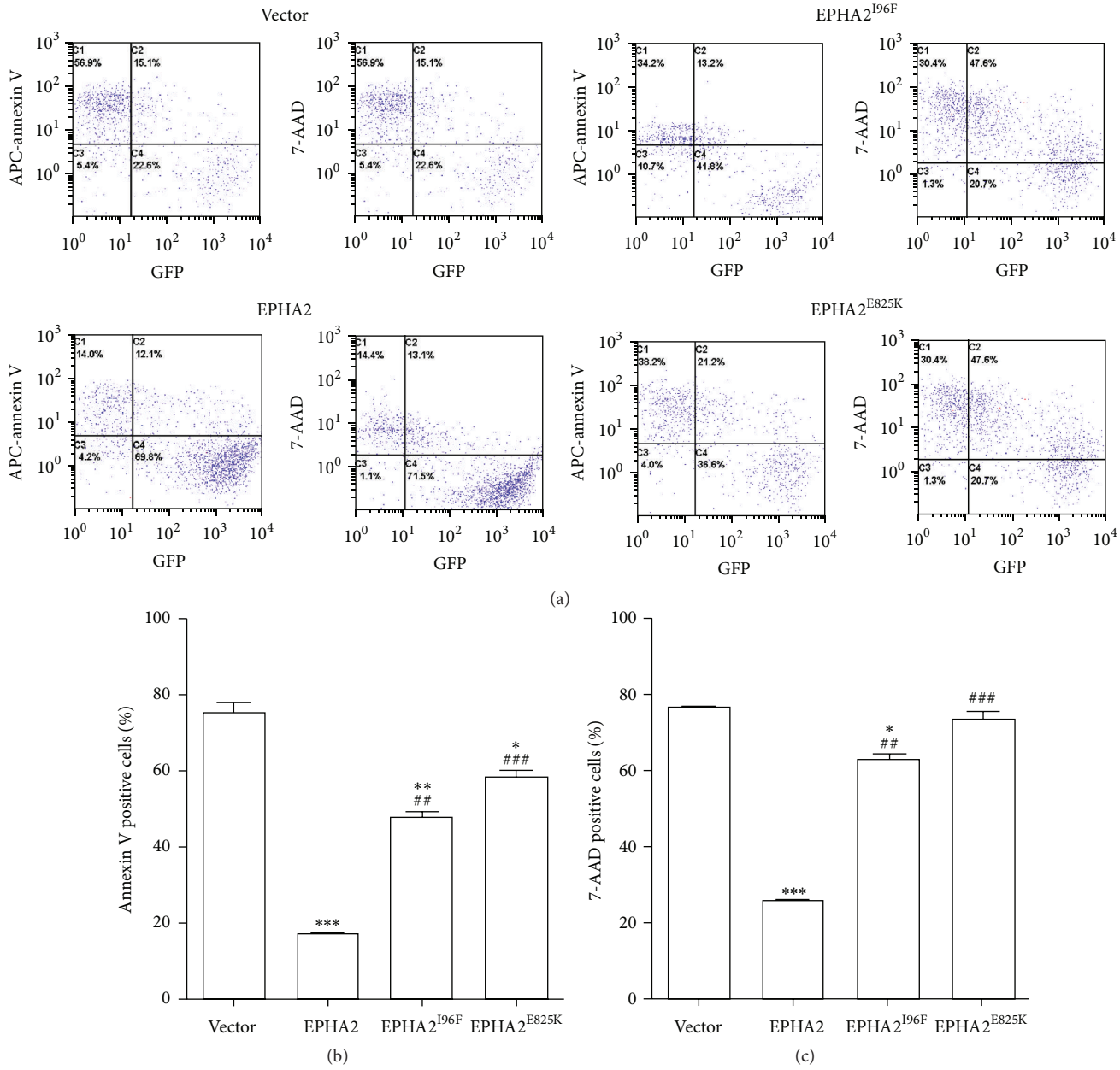

Figure 4: Compromised antiapoptotic function in cataract-associated genetic mutants. (a) After lentiviral infection to introduce control vector, EPHA2, EPHA2^{I96F}, or EPHA2^{E825K} into the cells and the administration with 200 μM H_2O_2, the HLECs were digested, dissociated, and stained with either APC-annexin V or 7-AAD, followed by the fluorescence activated cell sorting to analyze the early and late apoptosis. The GFP signal intensity was compromised if the HLECs undergo oxidative stress-induced apoptosis. (b-c) The statistical analysis shows that overexpression of wild-type EPHA2 reduces the proportion of both early and late apoptotic cells. The missense mutations abolish the antiapoptotic effect against oxidative damage. $^{*}p < 0.05$, $^{**}p < 0.01$, and $^{***}p < 0.001$ versus vector control; $^{\#\#}p < 0.01$, $^{\#\#\#}p < 0.001$ versus wild-type EPHA2.

5. Conclusion

In summary, our study revealed the cytoprotective and antioxidative function of EPHA2 in lens epithelial cells, which coordinate and maintain the lens epithelial structural integrity. The nonsynonymous polymorphisms rs2291806 and rs1058371 disrupt the protein stability and diminish the antiapoptotic effect of EPHA2 in human lens during aging, contributing to age-related cataract. The bioinformatic prediction helps us to identify the functional SNP in disease. The future gain- and loss-of-function studies in the animal model will further elucidate the cytoprotective and antioxidative role of EPHA2 in vivo.

Disclaimer

The authors are responsible for the content and writing of the paper.

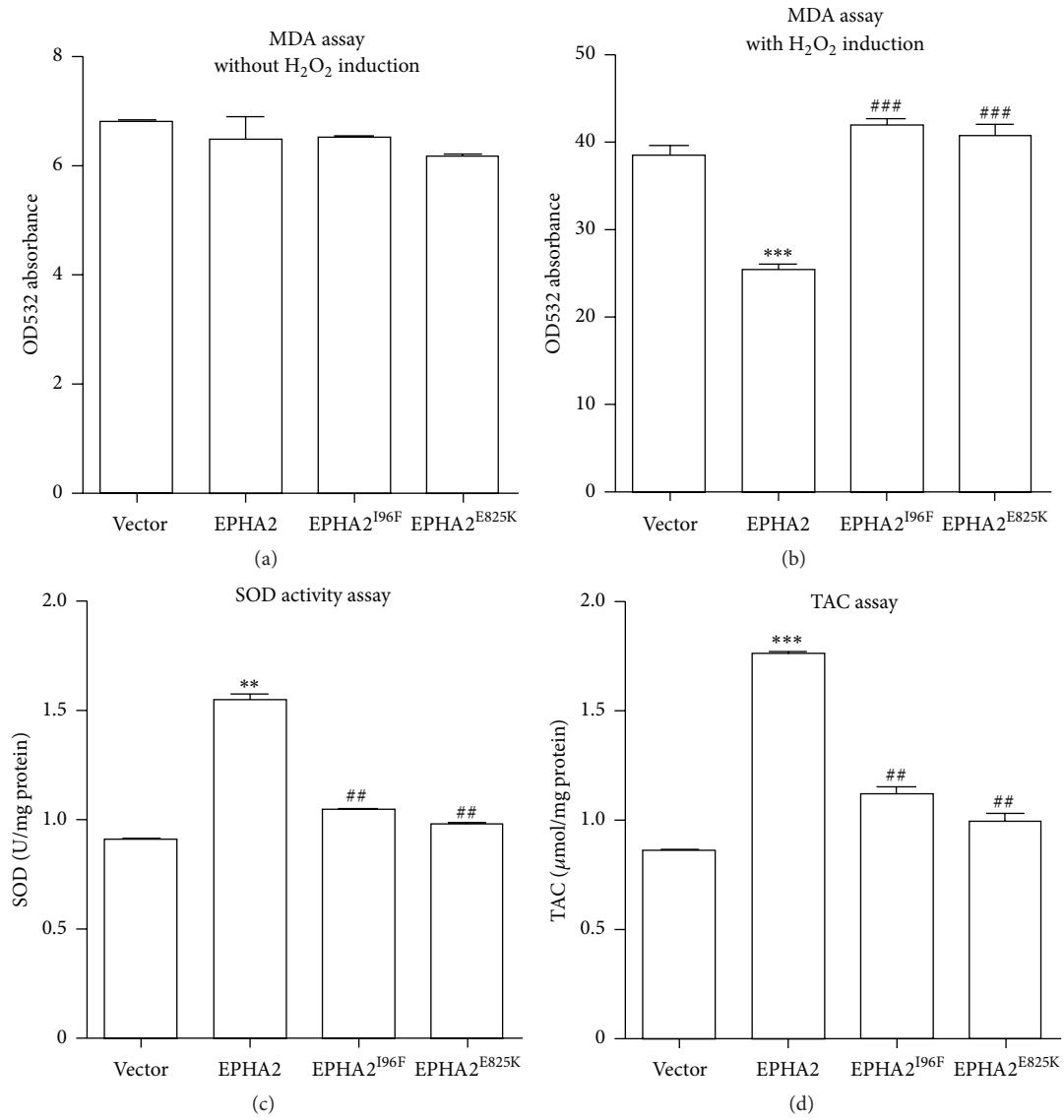

Figure 5: The nonsynonymous polymorphisms nullify the antioxidative capacity of EPHA2. (a-b) The lipid oxidation was evaluated with MDA assays in the HLECs before and after H_2O_2 treatment. The overexpression of EPHA2 reduces the absorbance value of cell lysate with H_2O_2 treatment, while the introduction of EPHA2^{I96F} or EPHA2^{E825K} mutant does not decline the lipid oxidation. (c-d) The SOD activity and the total antioxidative capacity were tested with SOD and TAC assay kit, respectively. The data are presented as U/mg or μmol/mg proteins. The upregulation of SOD level and total antioxidant content by EPHA2 is abrogated by the cataract-associated SNPs. $^{*}p < 0.05$, $^{**}p < 0.01$, and $^{***}p < 0.001$ versus vector control; $^{\#\#}p < 0.01$, $^{\#\#\#}p < 0.001$ compared with wild-type EPHA2.

Conflict of Interests

The authors declare no conflict of interests.

Authors' Contribution

Jin Yang and Dan Li contributed equally to this work.

Acknowledgments

This work was supported by the National Natural Science Foundation of China (NSFC) Grants (81270989 and 81200668) and the Research Fund for the Doctoral Program of Higher Education of China (no. 20120071120089).

References

[1] A. T. Moore, "Understanding the molecular genetics of congenital cataract may have wider implications for age related cataract," *British Journal of Ophthalmology*, vol. 88, no. 1, pp. 2–3, 2004.

[2] J. F. Hejtmancik and M. Kantorow, "Molecular genetics of age-related cataract," *Experimental Eye Research*, vol. 79, no. 1, pp. 3–9, 2004.

[3] A. Charakidas, A. Kalogeraki, M. Tsilimbaris, P. Koukoulomatis, D. Brouzas, and G. Delides, "Lens epithelial apoptosis and cell proliferation in human age-related cortical cataract," *European Journal of Ophthalmology*, vol. 15, no. 2, pp. 213–220, 2005.

[4] G. J. Harocopos, K. M. Alvares, A. E. Kolker, and D. C. Beebe, "Human age-related cataract and lens epithelial cell death," *Investigative Ophthalmology & Visual Science*, vol. 39, no. 13, pp. 2696–2706, 1998.

[5] W.-C. Li, J. R. Kuszak, K. Dunn et al., "Lens epithelial cell apoptosis appears to be a common cellular basis for non-congenital cataract development in humans and animals," *The Journal of Cell Biology*, vol. 130, no. 1, pp. 169–181, 1995.

[6] G. Jun, H. Guo, B. E. K. Klein et al., "EPHA2 is associated with age-related cortical cataract in mice and humans," *PLoS Genetics*, vol. 5, no. 7, Article ID e1000584, 2009.

[7] D. Celojevic, A. Abramsson, M. S. Palmér et al., "EPHA2 polymorphisms in Estonian patients with age-related cataract," *Ophthalmic Genetics*, 2014.

[8] P. Sundaresan, R. D. Ravindran, P. Vashist et al., "EPHA2 polymorphisms and age-related cataract in India," *PLoS ONE*, vol. 7, no. 3, Article ID e33001, 2012.

[9] W. Tan, S. Hou, Z. Jiang, Z. Hu, P. Yang, and J. Ye, "Association of EPHA2 polymorphisms and age-related cortical cataract in a Han Chinese population," *Molecular Vision*, vol. 17, pp. 1553–1558, 2011.

[10] T. A. Masoodi, S. A. Shammari, M. N. Al-Muammar, T. M. Almubrad, and A. A. Alhamdan, "Screening and structural evaluation of deleterious non-synonymous SNPs of ePHA2 gene involved in susceptibility to cataract formation," *Bioinformation*, vol. 8, no. 12, pp. 562–567, 2012.

[11] E. B. Pasquale, "Eph receptors and ephrins in cancer: bidirectional signalling and beyond," *Nature Reviews Cancer*, vol. 10, no. 3, pp. 165–180, 2010.

[12] J. E. Park, A. I. Son, and R. Zhou, "Roles of EphA2 in development and disease," *Genes*, vol. 4, no. 3, pp. 334–357, 2013.

[13] K. R. Amato, S. Wang, A. K. Hastings et al., "Genetic and pharmacologic inhibition of EPHA2 promotes apoptosis in NSCLC," *The Journal of Clinical Investigation*, vol. 124, no. 5, pp. 2037–2049, 2014.

[14] J.-W. Lee, R. L. Stone, S. J. Lee et al., "EphA2 targeted chemotherapy using an antibody drug conjugate in endometrial carcinoma," *Clinical Cancer Research*, vol. 16, no. 9, pp. 2562–2570, 2010.

[15] K. A. Mohammed, X. Wang, E. P. Goldberg, V. B. Antony, and N. Nasreen, "Silencing receptor EphA2 induces apoptosis and attenuates tumor growth in malignant mesothelioma," *American Journal of Cancer Research*, vol. 1, no. 3, pp. 419–431, 2011.

[16] B. Miao, Z. Ji, L. Tan et al., "EPHA2 is a mediator of vemurafenib resistance and a novel therapeutic target in melanoma," *Cancer Discovery*, vol. 5, no. 3, pp. 274–287, 2015.

[17] S. Ottonello, C. Foroni, A. Carta, S. Petrucco, and G. Maraini, "Oxidative stress and age-related cataract," *Ophthalmologica*, vol. 214, no. 1, pp. 78–85, 2000.

[18] O. Ates, H. H. Alp, I. Kocer, O. Baykal, and I. A. Salman, "Oxidative DNA damage in patients with cataract," *Acta Ophthalmologica*, vol. 88, no. 8, pp. 891–895, 2010.

[19] R. J. W. Truscott, "Age-related nuclear cataract—oxidation is the key," *Experimental Eye Research*, vol. 80, no. 5, pp. 709–725, 2005.

[20] K. Kannan and S. K. Jain, "Oxidative stress and apoptosis," *Pathophysiology*, vol. 7, no. 3, pp. 153–163, 2000.

[21] J. P. Kehrer, "Cause-effect of oxidative stress and apoptosis," *Teratology*, vol. 62, no. 4, pp. 235–236, 2000.

[22] R. Thiagarajan and R. Manikandan, "Antioxidants and cataract," *Free Radical Research*, vol. 47, no. 5, pp. 337–345, 2013.

[23] V. Bottero, S. Chakraborty, and B. Chandran, "Reactive oxygen species are induced by Kaposi's sarcoma-associated herpesvirus early during primary infection of endothelial cells to promote virus entry," *Journal of Virology*, vol. 87, no. 3, pp. 1733–1749, 2013.

[24] J. Yang, T.-J. Liu, Y.-X. Jiang, and Y. Lu, "ATRA enhances the bystander effect of suicide gene therapy driven by the specific promoter LEP 503 in human lens epithelial cells," *Molecular Vision*, vol. 18, pp. 2053–2066, 2012.

[25] G. Tiscornia, O. Singer, and I. M. Verma, "Production and purification of lentiviral vectors," *Nature Protocols*, vol. 1, no. 1, pp. 241–245, 2006.

[26] D. Chang, X. Zhang, S. Rong et al., "Serum antioxidative enzymes levels and oxidative stress products in age-related cataract patients," *Oxidative Medicine and Cellular Longevity*, vol. 2013, Article ID 587826, 7 pages, 2013.

[27] J. Yang, J. Luo, P. Zhou, Q. Fan, Y. Luo, and Y. Lu, "Association of the ephreceptor tyrosinekinase-type A2 (EPHA2) gene polymorphism rs3754334 with age-related cataract risk: a meta-analysis," *PLoS ONE*, vol. 8, no. 8, Article ID e71003, 2013.

[28] Z. Wang and J. Moult, "SNPs, protein structure, and disease," *Human Mutation*, vol. 17, no. 4, pp. 263–270, 2001.

[29] K. Rahman, "Studies on free radicals, antioxidants, and co-factors," *Clinical Interventions in Aging*, vol. 2, no. 2, pp. 219–236, 2007.

[30] C. Cheng, M. M. Ansari, J. A. Cooper, and X. Gong, "EphA2 and Src regulate equatorial cell morphogenesis during lens development," *Development*, vol. 140, no. 20, pp. 4237–4245, 2013.

[31] M. A. Coopera, A. I. Sona, D. Komlosb, Y. Suna, N. J. Kleimanc, and R. Zhoua, "Loss of ephrin-A5 function disrupts lens fiber cell packing and leads to cataract," *Proceedings of the National Academy of Sciences of the United States of America*, vol. 105, no. 43, pp. 16620–16625, 2008.

[32] H. Miao and B. Wang, "Eph/ephrin signaling in epithelial development and homeostasis," *International Journal of Biochemistry and Cell Biology*, vol. 41, no. 4, pp. 762–770, 2009.

[33] J. E. Park, A. I. Son, R. Hua, L. Wang, X. Zhang, and R. Zhou, "Human cataract mutations in EPHA2 SAM domain alter receptor stability and function," *PLoS ONE*, vol. 7, no. 5, Article ID e36564, 2012.

[34] E. H. Rannikko, L. B. Vesterager, J. H. A. Shaik et al., "Loss of DJ-1 protein stability and cytoprotective function by Parkinson's disease-associated proline-158 deletion," *Journal of Neurochemistry*, vol. 125, no. 2, pp. 314–327, 2013.

[35] J. A. Sommers, A. N. Suhasini, and R. M. Brosh, "Protein degradation pathways regulate the functions of helicases in the DNA damage response and maintenance of genomic stability," *Biomolecules*, vol. 5, no. 2, pp. 590–616, 2015.

[36] N. M. Reddy, S. R. Kleeberger, M. Yamamoto et al., "Genetic dissection of the Nrf2-dependent redox signaling-regulated transcriptional programs of cell proliferation and cytoprotection," *Physiological Genomics*, vol. 32, no. 1, pp. 74–81, 2007.

[37] Q. Ma, "Advances in mechanisms of anti-oxidation," *Discovery Medicine*, vol. 17, no. 93, pp. 121–130, 2014.

Hindawi Publishing Corporation
Journal of Ophthalmology
Volume 2015, Article ID 832784, 6 pages
http://dx.doi.org/10.1155/2015/832784

Research Article

Evaluation of Retinal Nerve Fiber Layer and Ganglion Cell Complex in Patients with Optic Neuritis or Neuromyelitis Optica Spectrum Disorders Using Optical Coherence Tomography in a Chinese Cohort

Guohong Tian,[1] Zhenxin Li,[2] Guixian Zhao,[2] Chaoyi Feng,[1] Mengwei Li,[1] Yongheng Huang,[1] and Xinghuai Sun[1]

[1]*Department of Ophthalmology, Eye, Ear, Nose, and Throat Hospital, Fudan University, Shanghai 200031, China*
[2]*Department of Neurology, Huashan Hospital, Fudan University, Shanghai 200040, China*

Correspondence should be addressed to Guohong Tian; valentian99@hotmail.com

Received 20 June 2015; Revised 28 September 2015; Accepted 1 October 2015

Academic Editor: Jun Zhang

Copyright © 2015 Guohong Tian et al. This is an open access article distributed under the Creative Commons Attribution License, which permits unrestricted use, distribution, and reproduction in any medium, provided the original work is properly cited.

We evaluate a cohort of optic neuritis and neuromyelitis optica (NMO) spectrum disorders patients in a territory hospital in China. The peripapillary retinal nerve fiber layer (RNFL) and macular ganglion cell complex (GCC) were measured using spectral-domain OCT after 6 months of acute onset. The results showed that both the peripapillary RNFL and macular GCC were significantly thinner in all optic neuritis subtypes compared to controls. In addition, the recurrent optic neuritis and NMO groups showed more severe damage on the RNFL and GCC pattern.

1. Introduction

Acute optic neuritis may be the first manifestation of both multiple sclerosis (MS) and neuromyelitis optica (NMO), or some unknown etiology of disorders [1, 2]. In Chinese, the demographic and clinical features of optic neuritis spectrum disorder are less well-defined than that in Caucasus [3–5].

During the past few years, numerous studies showed that peripapillary RNFL and macular thickness analysis may be used to detect axonal loss in optic neuritis, neuromyelitis optica, and other forms of chronic relapsing optic neuritis [6–9]. In addition, it has been suggested that OCT abnormalities can help differentiate MS from NMO on the severity of axonal loss [10–14].

Due to the ethnic differences, optic neuritis in China shows more atypical features than those in western countries and the prognosis is not clearly described. The propose of this study was to evaluate the thickness of the RNFL and macular GCC using SD-OCT in different forms of optic neuritis in a cohort of Chinese patients and compare the pattern of damage in MS-ON, NMO-ON, and R-ON group.

2. Materials and Methods

2.1. Patients. The current study was a cross-sectional study. Patients who presented with acute optic neuritis in Neuroophthalmology Division in Eye Ear Nose and Throat hospital, Fudan University, Shanghai, between May 2013 and January 2014, were recruited. Paper consent forms were obtained for participation through a study protocol that was approved by the hospital institutional review board. All patients had their diagnosis confirmed by referred neurologists and neuroophthalmologists. After thorough ancillary tests and at least one-year of follow-up, patients were divided into 3 groups for evaluating the involved eye: MS-ON, R-ON, and NMO-ON.

MS-ON group patients included typical acute demyelinating optic neuritis with brain lesions fulfilling the revised McDonald criteria or clinical isolate syndrome (CIS) [15, 16]. Recurrent isolated optic neuritis (R-ON) was defined as unilateral or bilateral recurrence affecting optic nerves in patients whose clinical evidence showed no other brain lesion and seronegative AQP4-Ab. A diagnosis of NMO-ON was

Table 1: Demographics and clinical characteristics for MS-ON, R-ON, and NMO-ON group and control.

Group	Patients (n)	Age (year) (mean ± SD)	Course (month) (mean ± SD)	Bilateral%	Female%
MS-ON	62	30.47 ± 16.71	6.2 ± 3.0	33.3%	58.1%
R-ON	19	31.26 ± 11.20	20.0 ± 22.6	100%	68.4%
NMO-ON	37	40.54 ± 13.64	25.0 ± 33.4	34.7%	83.8%
Control	68	31.96 ± 13.78	NA	NA	64.7%
P value		$P = 0.007^{a}$	$P = 0.02^{b}$	$P = 0.01^{c}$	$P = 0.07^{d}$

NA: not applicable; a: the statistical difference between NMO-ON and other groups; b: the statistical difference between MS-ON and other ON subtypes; NMO-ON and other groups; c: the statistical difference between R-ON group and other ON subtypes; d: the statistical difference between ON subtypes and control.

given to patients who met established diagnostic criteria for NMO or NMO spectrum disorders (NMO-SD) published by Wingerchuk et al. [17]. The new onset eyes in three groups were included for OCT evaluating. As for acute bilateral involved patients, only one affected eye was randomly chosen for OCT evaluation. As for R-ON patients, the new attack eye was evaluated. All enrolled patients underwent the routine blood test including the infectious panel, the rheumatology panels. All patients underwent serum AQP4 antibody test in neurobiology laboratory using the ELISA methods (kit from ElisaRSR AQP4-Ab, RSR limited, UK). Neuroimaging was required to confirm the acute attack of the optic neuritis, evaluate brain demyelinating, and exclude the compressive optic neuropathy and anterior ischemic optic neuropathy.

Exclusion criteria included patients with pathologic myopia with spherical equivalent of the refractive error >6.0 diopters, a previous history of ocular disease (including macular degeneration, diabetic retinopathy, uveitis, and glaucoma), and neurodegenerative conditions that could impact OCT testing results (Parkinson's disease, Alzheimer's disease), and subjects with poor vision having difficulty maintaining fixation were excluded from analyses.

The group of control was recruited from volunteers of hospital staffs and patient's companions at the time duration of the follow-up. Inclusion criteria included best-corrected visual acuity of at least 20/20, spherical equivalent of the refractive error <6.0 diopters (highly myopic), without presence of any ophthalmic or neurological diseases known to affect RNFL thickness. One eye was randomly chosen for evaluation.

2.2. Optical Coherence Tomography. Spectral-domain optical coherence tomography (SD-OCT) was performed using 3D Disc, ONH, GCC protocols provided by the RTVue-100 4.0.7.5 version (Optovue Inc, Fremont, CA). An internal fixation target was used to improve reproducibility. Scan was accepted only if the images with a signal strength index were greater than 35. The peripapillary RNFL thickness was measured automatically using a RNFL 3.45 scan mode, where 4 circular scans (1024 A-scans/scan) acquired 3.45 mm from the center of the optic disc. The RNFL was divided into temporal (316°–45°), superior (46°–135°), nasal (136°–225°), and inferior (226°–315°) quadrants. A RNFL progression analysis is also available for follow-up.

The GCC scan technique provides inner retinal thickness values which consist of ganglion cell layer (GCL) and inner plexiform layer (IPL). Scan mode for GCC analysis, which acquires 14 928A scans over a 7 mm square area in 0.58 seconds with 15 vertical scans collected at 0.5-mm intervals. The center of the scan was shifted 1.0 mm temporally to improve sampling of the temporal periphery. The GCC within the central 6 mm diameter area of the macular was calculated. All the data were measured and collected in acute optic neuritis patients 6 month after attack.

2.3. Statistical Analysis. Demographic variants were described and compared by ANOVA test (numeration variables) if the variance was homogeneity or chi-square test (categorical variables). The peripapillary RNFL data measured according to 4 quadrants was analyzed using repeat measurement analysis of variance due to the correlation intereye within patient. The difference between each group was statistic and compared with controls. GCC values were analyzed by independent-samples t test between groups. A P value of less than 0.05 was considered statistically significant. All analyses were conducted using IBM SPSS statistics for windows, Version 19.0 (IBM Corp, Chicago, USA).

3. Results

3.1. Demographics. A total of 118 patients, including MS-ON ($n = 62$), R-ON ($n = 19$), NMO-ON ($n = 37$), and 68 healthy controls were evaluated. The demographic and clinical characteristics are summarized in Table 1. Among the MS-ON group, 6 patients were diagnosed with clinical definite MS with optic neuritis; 4 patients had presented with CIS with brain or brainstem demyelinated lesion and subsequently got optic neuritis; the other 52 patients presented with isolated acute optic neuritis fulfilling the idiopathic demyelinating etiology after thorough ancillary work-up. Among the 19 R-ON patients, the recurrent times differ from 8 to 3. Among the 37 NMO-ON patients, 5 had previous myelitis and all patients showed a seropositive for AQP4-Ab.

The mean age in NMO-ON group was significantly older than other groups ($P = 0.01$), whereas there was no difference in age between MS-ON, R-ON, and control. The mean disease duration was significantly longer in R-ON and NMO-ON groups compared to MS-ON ($P = 0.02$). R-ON group showed high prevalence of bilateral involvement than MS-ON and NMO-ON group ($P = 0.01$). There was no statistic difference in female prevalence in all groups.

Table 2: Peripapillary RNFL thicknesses (μm) for eyes of patients in each group.

RNFL	MS-ON	R-ON	NMO-ON	Control
Average	79.12 ± 15.64	56.06 ± 9.83	63.94 ± 11.86	112.01 ± 10.93
Temporal	57.94 ± 14.57	48.37 ± 11.25	46.59 ± 12.10	139.93 ± 19.27
Superior	100.43 ± 22.51	80.74 ± 9.50	79.45 ± 16.47	120.43 ± 30.71
Nasal	59.84 ± 17.59	48.37 ± 8.90	48.91 ± 14.08	81.28 ± 13.05
Inferior	98.29 ± 21.57	82.76 ± 17.87	80.82 ± 17.40	141.76 ± 20.19

3.2. RNFL Measurement. Because age is known to influence retinal thickness parameters, first of all, covariance was analyzed using a linear regression model and the results showed there was no significant relation between age and RNFL thickness in our groups of subjects. Peripapillary RNFL thickness measured in 3 optic neuropathy groups was significantly thinning compared to healthy controls (Table 2). After repeat measurement of variance of 4 quadrants in each group, the mean difference showed an average of RNFL loss in MS-ON, R-ON, and NMO-ON groups of 32.8 μm, 46.9 μm, and 43.8 μm, respectively, compared to healthy control (Table 3). Furthermore, the R-ON and NMO-ON patients showed significant decreased RNFL in eyes in all quadrants compared with MS-ON, whereas there was no significant difference between R-ON and NMO-ON group.

3.3. Macular GCC Measurement. For the macular GCC, the tendency was the same as the peripapillary RNFL pattern, which showed significantly reduced in 3 optic neuritis groups compared to control (Figure 1). An average GCC thinning in MS-ON, R-ON, and NMO-ON groups was of 24.2 μm, 28.5 μm, and 28.5 μm, respectively, compared to healthy control. There were no statistic differences for the GCC between R-ON and NMO-ON.

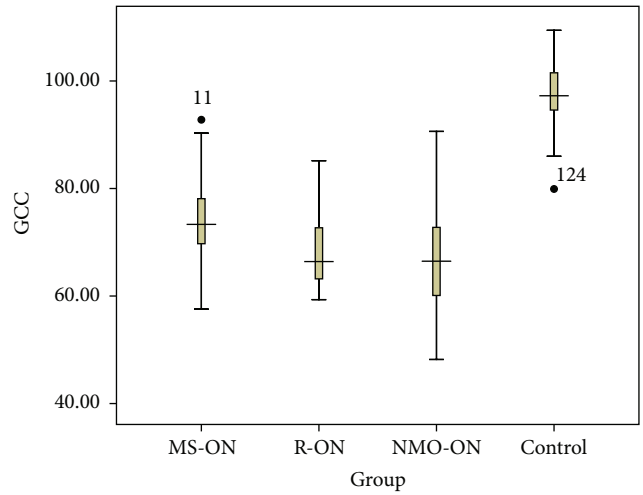

Figure 1: The boxplot analysis representing the macular GCC thickness in MS-ON, R-ON, NMO-ON, and control group. Mean values and 5% and 95% percentiles are shown. The difference between the 4 groups was statistically significant ($P < 0.001$), whereas there was no significant difference between R-ON and NMO-ON group ($P = 0.725$).

4. Discussion

Optic neuritis is one of the common optic neuropathies, which lead to visual loss in young Chinese and the underline etiologies have not been full clarified [1]. Our cohort study composed of a group of typical MS related optic neuritis patients, as well as atypical forms like R-ON and NMO-ON. Most of these patients presented as first attack which can be a manifestation of MS, NMO, or other unknown inflammatory disorders. Although the clinical characteristics and laboratory tests can help differentiating some of the etiology, the board spectrum of optic neuritis made it difficult to a definite diagnosis in a short term after one optic neuritis episode.

SD-OCT is a very useful and objective method to provide data on RNFL and macular GCC thickness and volumes. Also the eye tracking systems permit perfect repositioning in longitudinal studies for investigators to capture subtle changes on the order of a few micrometers.

The up to date cross-sectional studies and longitudinal investigations on OCT showed a significant alteration pattern in NMOSD patients with optic neuritis compared to MS-ON and healthy controls [18, 19]. A meta-analysis showed a loss of approximately 20 m in the affected eye in relapsing-remitting MS compared to healthy controls [20]. Bichuetti et al. [12] research also showed that, in patients with NMO and chronic relapsing inflammatory optic neuritis, the RNFL tend to have significantly lower thickness than patients with MS-ON. Our findings also demonstrate the same OCT pattern that the peripapillary RNFL and macular GCC thickness decreased significantly 6 months after once attack of optic neuritis compared to healthy controls. Furthermore, the R-ON and NMO-ON groups showed more severe damage compared to patients with MS (Figure 2). Approximately 40 μm thinning of RNFL was found in NMO-ON and R-ON eyes compared to controls (approximately 30 μm thinning in MS-ON). The temporal quadrant damage tendency in MS-ON was not shown in our cohort according to Naismith et al. study [11].

The GCC measured in our study by RTVue-100 protocol provided a value of combined macular ganglion cell layer and inner plexiform layer, which can help estimate the retrograde of optic nerve after damage. Six months after attack, the GCC showed an nearly 30 μm thinning in NMO-ON and R-ON groups, as well as approximately 20 μm in MS-ON compared to controls. The profound loss of GCC, which is closely associated with visual disability in MS [21], can also help in differentiating NMO or R-ON from MS-ON in early stage, where the true peripapillary RNFL will not be available due to the swell of optic disc.

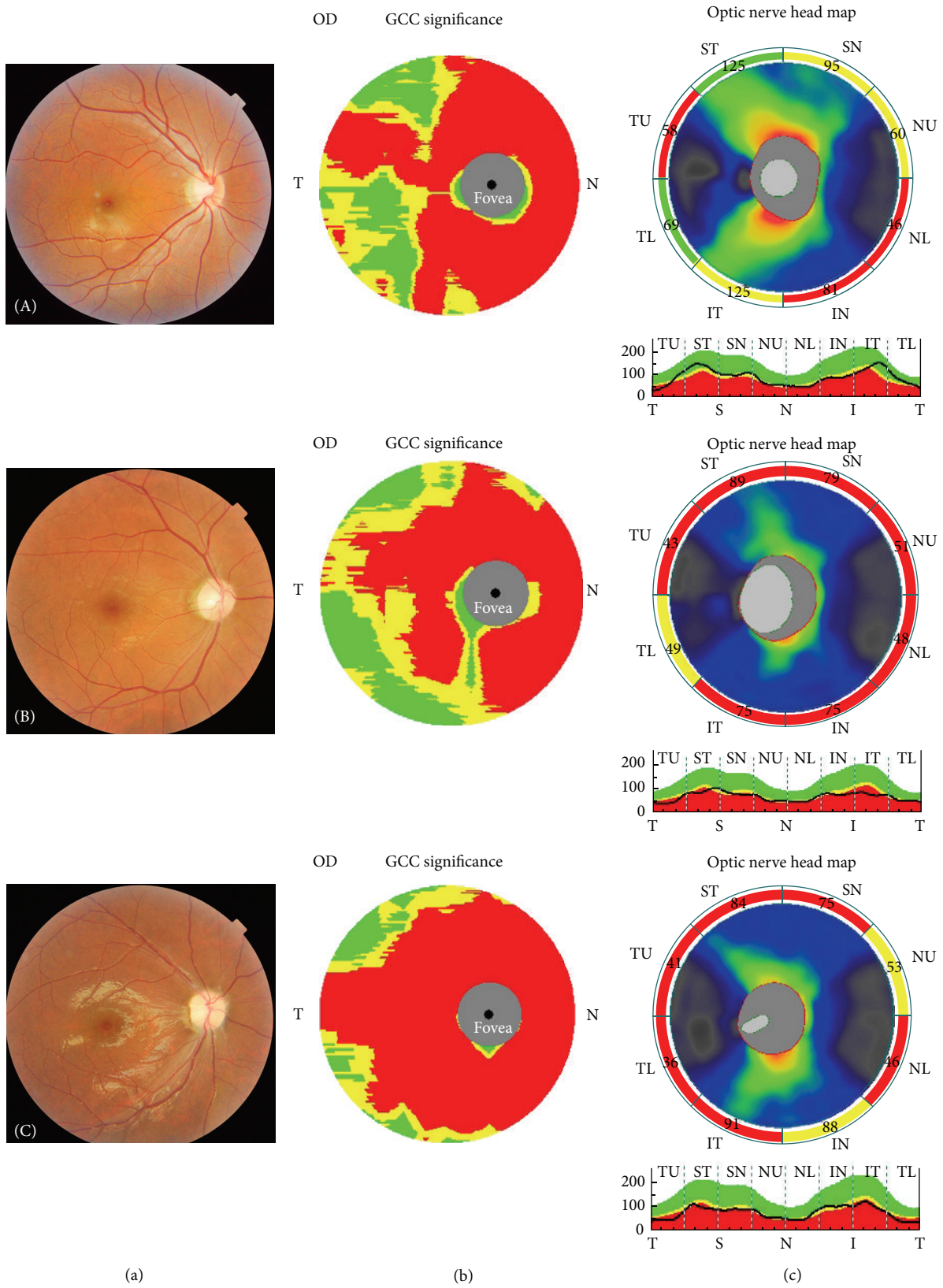

Figure 2: The fundus photograph (a) together with the corresponding macular GCC (b) and RNFL (c) measurements in MS-ON (A), R-ON (B), and NMO-ON (C) groups are showed, respectively.

Table 3: Repeated measures ANOVA of multiple comparisons of each group.

(I) group	(J) group	Mean difference ($I - J$)	Std. error	Sig.	95% confidence interval	
					Lower bound	Upper bound
MS-ON	R-ON	14.087*	3.558	.000	7.066	21.108
	NMO-ON	10.998*	3.336	.001	4.415	17.581
	Control	−32.795*	2.312	.000	−37.358	−28.232
R-ON	NMO-ON	−3.089	4.278	.471	−11.531	5.353
	Control	−46.882*	3.547	.000	−53.881	−39.882
NMO-ON	Control	−43.793*	3.309	.000	−50.322	−37.263

*The mean difference is significant at the 0.05 level.

The profound loss of peripapillary RNFL and macular GCC in R-ON group, whose pattern is similar to NMO-ON, to some extent, indicate that they share the some underline etiology. In addition, the OCT technique makes it possible to measure the single layer of ganglion cell around macular, which will give accurate thickness of the neurons. Further prospective longitudinal investigations will be needed to illustrate the change in OCT pattern as a structure marker for axonal degeneration and neuronal loss.

Conflict of Interests

The authors have no proprietary or commercial interest in any of the materials discussed in this paper.

Acknowledgment

The authors thank Ms. Heng Fan (Department of Biostatistics, School of Public Health, Fudan University) for statistical analysis consultation.

References

[1] A. T. Toosy, D. F. Mason, and D. H. Miller, "Optic neuritis," *The Lancet Neurology*, vol. 13, no. 1, pp. 83–99, 2014.

[2] F. A. Warren, "Atypical optic neuritis," *Journal of Neuro-Ophthalmology*, vol. 34, no. 4, pp. e12–e13, 2014.

[3] J. T. Peng, H. R. Cong, R. Yan et al., "Neurological outcome and predictive factors of idiopathic optic neuritis in China," *Journal of the Neurological Sciences*, vol. 349, no. 1-2, pp. 94–98, 2015.

[4] C. Lai, G. Tian, W. Liu, W. Wei, T. Takahashi, and X. Zhang, "Clinical characteristics, therapeutic outcomes of isolated atypical optic neuritis in China," *Journal of the Neurological Sciences*, vol. 305, no. 1-2, pp. 38–40, 2011.

[5] A. C. O. Cheng, N. C. Y. Chan, and C. K. M. Chan, "Acute and subacute inflammation of the optic nerve and its sheath: clinical features in Chinese patients," *Hong Kong Medical Journal*, vol. 18, no. 2, pp. 115–122, 2012.

[6] S. B. Syc, S. Saidha, S. D. Newsome et al., "Optical coherence tomography segmentation reveals ganglion cell layer pathology after optic neuritis," *Brain*, vol. 135, no. 2, pp. 521–533, 2012.

[7] D. B. Fernandes, A. S. Raza, R. G. Nogueira et al., "Evaluation of inner retinal layers in patients with multiple sclerosis or neuromyelitis optica using optical coherence tomography," *Ophthalmology*, vol. 120, no. 2, pp. 387–394, 2013.

[8] M. L. R. Monteiro, D. B. Fernandes, S. L. Apóstolos-Pereira, and D. Callegaro, "Quantification of retinal neural loss in patients with neuromyelitis optica and multiple sclerosis with or without optic neuritis using fourier-domain optical coherence tomography," *Investigative Ophthalmology and Visual Science*, vol. 53, no. 7, pp. 3959–3966, 2012.

[9] H. Merle, S. Olindo, A. Donnio, R. Richer, D. Smadja, and P. Cabre, "Retinal peripapillary nerve fiber layer thickness in neuromyelitis optica," *Investigative Ophthalmology and Visual Science*, vol. 49, no. 10, pp. 4412–4417, 2008.

[10] J. N. Ratchford, M. E. Quigg, A. Conger et al., "Optical coherence tomography helps differentiate neuromyelitis optica and MS optic neuropathies," *Neurology*, vol. 73, no. 4, pp. 302–308, 2009.

[11] R. T. Naismith, N. T. Tutlam, J. Xu et al., "Optical coherence tomography differs in neuromyelitis optica compared with multiple sclerosis," *Neurology*, vol. 72, no. 12, pp. 1077–1082, 2009.

[12] D. B. Bichuetti, A. S. de Camargo, A. B. Falcão, F. F. Gonçalves, I. M. Tavares, and E. M. L. de Oliveira, "The retinal nerve fiber layer of patients with neuromyelitis optica and chronic relapsing optic neuritis is more severely damaged than patients with multiple sclerosis," *Journal of Neuro-Ophthalmology*, vol. 33, no. 3, pp. 220–224, 2013.

[13] E. Schneider, H. Zimmermann, T. Oberwahrenbrock et al., "Optical coherence tomography reveals distinct patterns of retinal damage in neuromyelitis optica and multiple sclerosis," *PLoS ONE*, vol. 8, no. 6, Article ID e66151, 2013.

[14] K.-A. Park, J. Kim, and S. Y. Oh, "Analysis of spectral domain optical coherence tomography measurements in optic neuritis: Differences in neuromyelitis optica, multiple sclerosis, isolated optic neuritis and normal healthy controls," *Acta Ophthalmologica*, vol. 92, no. 1, pp. e57–e65, 2014.

[15] C. H. Polman, S. C. Reingold, B. Banwell et al., "Diagnostic criteria for multiple sclerosis: 2010 revisions to the McDonald criteria," *Annals of Neurology*, vol. 69, no. 2, pp. 292–302, 2011.

[16] D. H. Miller, D. T. Chard, and O. Ciccarelli, "Clinically isolated syndromes," *The Lancet Neurology*, vol. 11, no. 2, pp. 157–169, 2012.

[17] D. M. Wingerchuk, V. A. Lennon, C. F. Lucchinetti, S. J. Pittock, and B. G. Weinshenker, "The spectrum of neuromyelitis optica," *The Lancet Neurology*, vol. 6, no. 9, pp. 805–815, 2007.

[18] L. J. Balk and A. Petzold, "Current and future potential of retinal optical coherence tomography in multiple sclerosis with and without optic neuritis," *Neurodegenerative Disease Management*, vol. 4, no. 2, pp. 165–176, 2014.

[19] J. Bennett, J. de Seze, M. Lana-Peixoto et al., "Neuromyelitis optica and multiple sclerosis: seeing differences through optical

coherence tomography," *Multiple Sclerosis Journal*, vol. 21, no. 6, pp. 678–688, 2015.

[20] A. Petzold, J. F. de Boer, S. Schippling et al., "Optical coherence tomography in multiple sclerosis: a systematic review and meta-analysis," *The Lancet Neurology*, vol. 9, no. 9, pp. 921–932, 2010.

[21] S. D. Walter, H. Ishikawa, K. M. Galetta et al., "Ganglion cell loss in relation to visual disability in multiple sclerosis," *Ophthalmology*, vol. 119, no. 6, pp. 1250–1257, 2012.

Hindawi Publishing Corporation
Journal of Ophthalmology
Volume 2015, Article ID 132417, 8 pages
http://dx.doi.org/10.1155/2015/132417

Research Article

Dry Eye Disease following Refractive Surgery: A 12-Month Follow-Up of SMILE versus FS-LASIK in High Myopia

Bingjie Wang,[1] Rajeev K. Naidu,[2] Renyuan Chu,[1] Jinhui Dai,[1] Xiaomei Qu,[1] and Hao Zhou[1]

[1]*Key Myopia Laboratory of Chinese Health Ministry, Department of Ophthalmology, Eye & ENT Hospital, Fudan University, No. 83, Fenyang Road, Shanghai 200031, China*
[2]*The University of Sydney, Camperdown, NSW 2006, Australia*

Correspondence should be addressed to Hao Zhou; zhouhaoeent@163.com

Received 2 July 2015; Revised 7 October 2015; Accepted 8 October 2015

Academic Editor: George Kymionis

Copyright © 2015 Bingjie Wang et al. This is an open access article distributed under the Creative Commons Attribution License, which permits unrestricted use, distribution, and reproduction in any medium, provided the original work is properly cited.

Purpose. To compare dry eye disease following SMILE versus FS-LASIK. *Design.* Prospective, nonrandomised, observational study. *Patients.* 90 patients undergoing refractive surgery for myopia were included. 47 eyes underwent SMILE and 43 eyes underwent FS-LASIK. *Methods.* Evaluation of dry eye disease was conducted preoperatively and at 1, 3, 6, and 12 months postoperatively, using the Salisbury Eye Evaluation Questionnaire (SEEQ) and TBUT. *Results.* TBUT reduced following SMILE at 1 and 3 months ($p < 0.001$) and at 1, 3, and 6 months following FS-LASIK ($p < 0.001$). TBUT was greater following SMILE than FS-LASIK at 3, 6, and 12 months ($p < 0.001$, $p < 0.001$, and $p = 0.009$, resp.). SEEQ scores increased (greater symptoms) following SMILE at 1 month ($p < 0.001$) and 3 months ($p = 0.003$) and at 1, 3, and 6 months following FS-LASIK ($p < 0.001$). SMILE produced lower SEEQ scores (fewer symptoms) than FS-LASIK at 1, 3, and 6 months ($p < 0.001$). *Conclusion.* SMILE produces less dry eye disease than FS-LASIK at 6 months postoperatively but demonstrates similar degrees of dry eye disease at 12 months.

1. Introduction

Dry eye disease is a common ocular surface disease and plays a significant role in the ocular comfort and visual performance of patients, with the potential to have a great impact on their quality of life [1–6]. Dry eye is known to be a frequently reported and observed finding following refractive surgery, particularly in the period immediately following surgery [7–12]. With refractive surgery cases increasing in number, dry eye is becoming an increasing challenge for refractive surgeons to overcome, with a large proportion of patients experiencing dry eye symptoms to varying degrees [3, 10, 13–18]. Dry eye has also been associated with a delayed wound healing response and may predispose patients to refractive regression in moderate to severe cases [7, 15].

While the pathophysiology of this complication is still evolving, a number of theories have been proposed to explain why dry eye occurs following refractive surgery, including exacerbation of preexisting dry eye disease [12], medicamentosa from postoperative medications [19, 20], and damage to conjunctival goblet cells increasing tear hyperosmolarity and inflammation [19, 21–23]. The interaction between the ocular surface and eyelids is an important factor in maintaining tear production and flow, which is also altered following surgery [10, 24]. Perhaps the biggest factor, however, is the impact surgery has on corneal nerves and sensation [19, 21, 25, 26]. Intact corneal sensation is required for adequate blink frequency and tear production, and corneal denervation resulting from disruption and damage to corneal nerves has been shown to play a significant role in the development of dry eye disease following refractive surgery [27–29].

Laser-assisted in situ keratomileusis (LASIK) continues to be a popular refractive surgical option [18, 30]; however, almost half of all LASIK patients continue to report dry eye symptoms following surgery [8]. The introduction of the femtosecond laser (FS) has seen FS-LASIK become a more accurate and safe surgical option, with a reduced rate of dry eye disease, which is likely due to reduced neurotrophic effects on the corneal nerves during formation of the corneal flap [22]. A recent advancement in refractive surgery has been small-incision lenticule extraction (SMILE), which was established as a "flapless" procedure in which an intrastromal

lenticule is cut by a femtosecond laser and manually extracted through a peripheral corneal tunnel incision. The refractive predictability, safety, and patient satisfaction of SMILE are comparable to FS-LASIK. SMILE has the benefit of being minimally invasive, with a lesser degree of damage to the cornea and corneal nerves, and may therefore result in fewer complications and reduced symptoms of dry eye [9]. The key difference between FS-LASIK and SMILE and their impact on corneal innervation may lie in the fact that FS-LASIK affects the epithelium and anterior stroma, thus resulting in greater resection of the sensory nerves of the cornea [19–21], while SMILE affects the posterior stromal bed with relatively greater preservation of the corneal subbasal nerve plexus [9].

Few studies exist in the literature investigating the long-term effects of refractive surgery, specifically comparing both SMILE and FS-LASIK, on the development of dry eye syndromes. In this prospective observational study, we present the findings of the objectively measured clinical signs and subjective reporting of dry eye symptoms following SMILE versus FS-LASIK for the correction of myopia in a large group of demographically similar patients over a period of 12 months postoperatively.

2. Methods

2.1. Setting and Design. This institutional, prospective, observational study was approved prospectively by the institutional review board of The Eye and ENT Hospital of Fudan University. Written informed consent was obtained from all patients prior to participating in the study. The study adhered to the guidelines and principles of the Declaration of Helsinki.

2.2. Patients. Patients who attended The Eye and ENT Hospital of Fudan University, Shanghai, China, between the period of January 2012 and January 2014, for refractive treatment of their myopia were recruited.

Inclusion criteria included patient aged over 18 years, Spherical Equivalent (SE) refractive error ≥ -6.00 D, a stable refractive error in the last 2 years, no contraindications to laser refractive surgery, and no previous history of dry eye disease. Additionally, prior to surgery, patients completed a dry eye questionnaire (The Salisbury Eye Evaluation) and only those who yielded a total score of 0 were included. Patients were excluded if they had undergone any ocular surgery in the past 6 months or were using medication that could interfere with the ocular surface. A complete dilated ophthalmic examination was performed to assess the patient's suitability for either SMILE or FS-LASIK. Central corneal thickness (CCT) was determined with a Pentacam system (Typ70700; Oculus; Wetzlar, Germany). After the nature of the two procedures was explained, the patients chose the type of surgery they wished to undergo.

In total, 90 patients who completed 12 months of follow-up were included in this study. 47 patients underwent SMILE procedures (SMILE group) while 43 patients underwent FS-LASIK procedures (FS-LASIK group). The mean age of patients undergoing SMILE was 25.21 ± 6.51 years old, which was not significantly different to the mean age of patients undergoing FS-LASIK, which was 24.72 ± 6.53 years old ($p = 0.722$). The mean preoperative SE was -7.46 ± 1.11 D in the SMILE group and -7.44 ± 1.13 D in the FS-LASIK group, with no significant difference between the two groups. The mean preoperative TBUT was 9.87 ± 1.57 seconds in the SMILE group and 9.56 ± 1.35 seconds in the FS-LASIK group, again with no significant difference between the two groups ($p = 0.948$). Written informed consent was obtained from each patient after the details of the study were fully explained.

2.2.1. Tear-Film Breakup Time (TBUT). TBUT was assessed prior to surgery and was repeated at 1 month, 3 months, 6 months, and 12 months after surgery. TBUT was assessed with fluorescein paper strips that were wetted with unpreserved saline solution. One drop was instilled in each eye in the lower conjunctival sac, and the patient was instructed to blink several times. A cobalt filter was attached to a slit-lamp biomicroscope, and the time it took from a complete blink until the first signs of a break in the tear film was recorded. The test was repeated 3 times and averaged. The same observer performed the test.

2.2.2. The Salisbury Eye Evaluation Questionnaire for Dry Eye Symptoms. The Salisbury Eye Evaluation Questionnaire, translated into Chinese, was given to each subject for self-evaluation of dry eye symptoms before operation and at 1, 3, 6, and 12 months after operation. The questionnaire contains 6 items pertaining to dry eye symptoms. Questions include the following: (1) Do your eyes ever feel dry? (2) Do you ever feel a gritty or sandy sensation in your eye? (3) Are your eyes ever red? (4) Do your eyes ever have a burning sensation? (5) Do you notice much crusting on your lashes? (6) Do your eyes ever get stuck shut in the morning? The subject answers each question on the questionnaire based on how often they experience these symptoms as rarely, sometimes, often, or all the time. Symptoms that were experienced often or all the time were given a score of 1, and the other two responses were given a score of 0. The scores were added up to give a total score for each subject.

2.3. Surgical Technique. All surgeries were performed under local anesthesia by one surgeon (Hao Zhou) with patients undergoing either SMILE or FS-LASIK.

SMILE was performed using the VisuMax femtosecond laser system (Carl Zeiss Meditec) with a repetition rate of 500 kHz, pulse energy of 185–190 nJ, intended cap thickness of 100–120 μm, cap diameter of 7.5 mm, lenticule diameter of 6.1 to 6.6 mm (depending on the refractive error), and a 90°-angle side cut with a circumferential length of 2.1 mm at the superior position.

FS-LASIK was performed with the VisuMax system for flap creation followed by Mel 80 excimer laser (Carl Zeiss Meditec) for stromal ablation, with an intended flap thickness of 95 μm and pulse energy of 185 nJ. The hinge was located at the superior position.

A standard postoperative topical steroid (Fluorometholone 0.1%) was tapered over 30 days; topical antibiotic

Table 1: Demographic data of the subjects included in this study.

	Mean ± standard deviation		p value
	SMILE ($n = 47$)	FS-LASIK ($n = 43$)	
Age (y)	25.21 ± 6.51	24.72 ± 6.53	0.722
Gender (F/M)	30/17	27/16	0.157
Preop SE (D)	−7.46 ± 1.11	−7.44 ± 1.13	0.948
Preop CCT (μm)	546.49 ± 25.52	544.88 ± 24.28	0.761
Preop TBUT (sec)	9.87 ± 1.57	9.56 ± 1.35	0.313

Table 2: Lenticule thickness/ablation depth.

	Mean ± standard deviation		p value
	SMILE ($n = 47$)	FS-LASIK ($n = 43$)	
Lenticule thickness/ Ablation depth (μm)	138.63 ± 8.56	137.77 ± 13.31	0.711

(Tobramycin 0.003%) QID for 7 days, and unpreserved ocular lubricant 4 times a day was prescribed for a month.

2.4. Statistical Analysis. In all cases, only data from the first eye (right eye) on which the procedure was performed was used in the statistical analysis. The sample size of this study was determined based on the standard deviation reported from a previous study [9], with the significance level set at $\alpha = 0.05$ (two tailed) and a power of 90%, and a sample size of at least 38 was required in each group. Allowing for a 10% dropout rate, at least 84 subjects were required. All statistical analyses were performed with a statistics program (SPSS 19.0 IBM Corporation, Armonk, NY, USA). Independent-samples t-test was used to compare the differences between groups. One-way repeated measures ANOVA test was used to compare TBUT change and SEEQ score change within groups over time. Tukey's honestly significant difference (HSD) post hoc test was performed to evaluate the differences in parameters between groups. Spearman's correlation test was used to assess relationship between TBUT and SEEQ scores. $p < 0.05$ was considered significant.

3. Results

In total, 90 patients were recruited for the study, with a total of 90 eyes (the first eye to have surgery performed for each patient) included in the analysis. There were a total of 47 eyes in the SMILE group and 43 eyes in the FS-LASIK group. There were no significant differences between the two groups preoperatively in terms of age, SE refractive error, central corneal thickness (CCT), or preoperative TBUT. Demographic data for all subjects included in this study is outlined in Table 1.

Objective surgical changes in corneal parameters were similar between the two groups, with no significant difference in lenticule thickness/ablation depth between the two groups (Table 2).

3.1. Tear-Film Breakup Time (TBUT). Preoperatively, there was no significant difference in TBUT between the SMILE and FS-LASIK groups (9.87 ± 1.57 seconds and 9.56 ± 1.35 seconds, resp., $p = 0.313$). One-way ANOVA showed that there was a statistically significant difference in TBUT between preoperative values and the different follow-up time periods, for both SMILE ($F(4, 230) = 79.673$, $p < 0.001$) and FS-LASIK ($F(4, 210) = 55.531$, $p < 0.001$).

Table 3: TBUT between SMILE and FS-LASIK.

Postop TBUT (sec)	Mean ± standard deviation		p value
	SMILE ($n = 47$)	FS-LASIK ($n = 43$)	
1 month	6.28 ± 1.35	6.53 ± 1.24	0.348
3 months	8.21 ± 0.95	7.42 ± 0.96	<0.001
6 months	9.57 ± 0.93	8.19 ± 1.45	<0.001
12 months	9.83 ± 0.99	9.30 ± 0.89	0.009

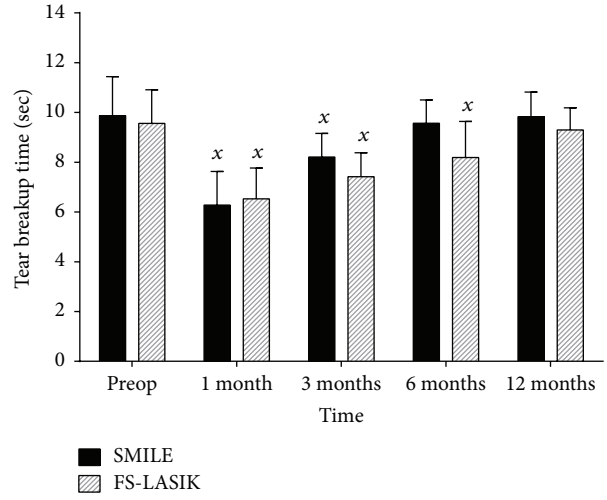

Figure 1: Tear-film breakup time (TBUT) in SMILE and FS-LASIK groups before operation, 1, 3, 6, and 12 months after operation. "x": statistically significantly less than preoperative values, $p < 0.05$.

Post hoc tests showed that, at 1 and 3 months after operation, there was a statistically significant decrease in TBUT from preoperative values in the SMILE group (6.28 ± 1.35, $p < 0.001$, and 8.21 ± 0.95, $p < 0.001$, resp.), before returning to preoperative values by 6 and 12 months (9.57 ± 0.93, $p = 0.740$, and 9.83 ± 0.99, $p = 1.00$, resp.). In the FS-LASIK group, TBUT was statistically significantly reduced from preoperative values at 1 month, 3 months, and 6 months postoperatively (6.53 ± 1.24, $p < 0.001$, 7.41 ± 0.96, $p < 0.001$, and 8.18 ± 1.45, $p < 0.001$, resp.), before returning to preoperative values at 12 months (9.30 ± 0.89, $p = 0.826$) (Figure 1).

Between the two procedures, TBUT was not statistically significantly different at 1 month postoperatively ($p = 0.348$); however, at 3, 6, and 12 months postoperatively, TBUT was statistically significantly greater in the SMILE group than the FS-LASIK group ($p < 0.001$, $p < 0.001$, and $p = 0.009$, resp.) (Table 3).

3.2. Salisbury Eye Evaluation Questionnaire. The Salisbury Eye Evaluation Questionnaire (SEEQ) was used to assess a patient's subjective reporting of dry eye symptoms, with a

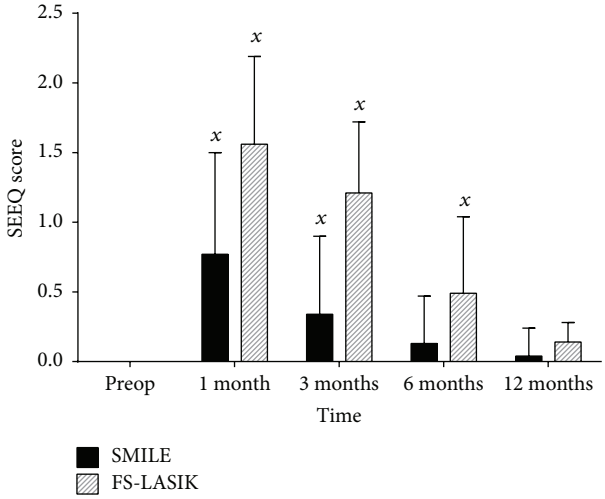

Figure 2: Salisbury Eye Evaluation Questionnaire results in SMILE and FS-LASIK groups at 1, 3, 6, and 12 months after operation. "x": statistically significantly greater than preoperative values, $p < 0.05$.

higher score indicating a greater degree of experienced dry eye symptoms. Preoperative scores were 0, per the inclusion criteria. One-way ANOVA testing found a statistically significant difference in SEEQ scores within groups over the time period of review for both SMILE ($F(4, 230) = 23.127$, $p < 0.001$) and FS-LASIK ($F(4, 210) = 91.161$, $p < 0.001$).

Post hoc tests showed that, in the SMILE group, SEEQ scores were statistically significantly higher at 1 month ($p < 0.001$) and 3 months ($p = 0.003$) after operation than preoperative values. By 6 and 12 months, this difference was no longer statistically significant ($p = 0.640$ and $p = 0.991$, resp.). For FS-LASIK, post hoc test evaluation found that SEEQ scores at 1 month, 3 months, and 6 months after operation were statistically significantly higher than preoperative values ($p < 0.001$ for all 3 follow-up time periods). By 12 months, this difference was no longer found ($p = 0.636$) (Figure 2).

Postoperatively at the 1-, 3-, and 6-month follow-up intervals, the SEEQ score was higher in the FS-LASIK group than the SMILE group ($p < 0.001$ for all 3 follow-up time intervals). 12 months after operation, this difference was no longer statistically significant ($p = 0.109$) (Table 4).

Spearman's correlation test revealed a moderate negative correlation between SEEQ scores and TBUT at 1 month after operation for the SMILE group ($r_s = -0.599$, $p < 0.001$) as well as in the FS-LASIK group ($r_s = -0.518$, $p < 0.001$).

4. Discussion

Dry eye disease continues to be a common complication of refractive surgery, affecting not only the ocular comfort of patients, but also their visual quality [8, 31]. This can have a direct impact on their overall satisfaction and quality of life following surgery. Although a frequently noted condition, dry eye disease remains a complex syndrome with a wide-ranging spectrum of clinical signs and subjective symptoms that do not always show a great degree of correlation [4, 32].

Table 4: SEEQ scores between SMILE and FS-LASIK.

Postop SEEQ	Mean ± standard deviation		p value
	SMILE ($n = 47$)	FS-LASIK ($n = 43$)	
1 month	0.77 ± 0.73	1.56 ± 0.63	<0.001
3 months	0.34 ± 0.56	1.21 ± 0.51	<0.001
6 months	0.13 ± 0.34	0.49 ± 0.55	<0.001
12 months	0.04 ± 0.20	0.14 ± 0.14	0.109

While there exist several clinical measures to diagnose and monitor the severity of dry eye disease, it is difficult to fully understand the impact it has on a patient, as many patients that show early clinical signs of dry eye disease may be asymptomatic, while others may report symptoms greater than their clinical signs may suggest, or without any tissue damage at all [32]. Assessment of dry eye disease should, therefore, consist of both clinical examination and subjective self-reporting of symptoms by patients, ideally through the use of a dry eye questionnaire. The purpose of this study was to investigate and compare the long-term dry eye outcomes up to 12 months following SMILE and FS-LASIK for the correction of high myopia, using both clinical (TBUT) and subjective (SEEQ) measures of dry eye disease.

Dry eye symptoms are often considered a transient occurrence, occurring in the vast majority of patients in the short-term following refractive surgery [9, 15, 17]. Many studies have shown an increase in dry eye symptoms in the period immediately following refractive surgery, which often improves within three to nine months postoperatively [7, 9–11, 13–17, 19, 21, 22, 30, 31, 33–36]. In the present study, we investigated the objectively measured clinical signs and subjective reporting of dry eye symptoms following SMILE and FS-LASIK for the correction of high myopia in a large group of demographically similar patients over a longer period of 12 months postoperatively. The main outcome measures of interest were the TBUT as a clinical marker for dry eye disease and the Salisbury Eye Evaluation Questionnaire as a subjective indicator of a patient's experience of dry eye symptoms, with a comparison of both measures between two highly affective refractive procedures, SMILE and FS-LASIK. The use of both of these measures provides a good representation of dry eye disease. TBUT has been shown to be both sensitive and accurate as a noninvasive method of dry eye diagnosis [37], and dry eye questionnaires have been shown to represent the true degree of morbidity of the disease as experienced by patients [2, 4, 32, 37].

The present study demonstrated that both the SMILE and FS-LASIK procedures resulted in changes in both the clinical and subjective markers of dry eye, with a transient increase in dry eye disease in both groups. A reduction in TBUT was observed for both the SMILE and FS-LASIK groups following surgery at 1 and 3 months postoperatively. However, this change was only transient, as the TBUT had recovered to preoperative levels for patients that underwent SMILE by 6 months postoperatively, whereas for patients that underwent FS-LASIK, this recovery did not occur until 12 months postoperatively.

These results suggest that SMILE may be superior to FS-LASIK, inducing a shorter duration of tear-film disturbance and leading to a quicker recovery of tear-film function postoperatively. Our results also indicate that this advantage of the SMILE procedure was noted subjectively with the patient's experience of dry eye symptoms, as demonstrated by the results of the SEEQ. Patients in the SMILE group reported lower SEEQ scores (fewer dry eye symptoms) compared to patients in the FS-LASIK group at 1, 3, and 6 months postoperatively, before equalizing at 12 months postoperatively. Therefore, patients who underwent SMILE were less prone to dry eye symptoms, as assessed with both clinical and subjective measures, than those who underwent FS-LASIK in the first 6 months following surgery, but they demonstrated similar degrees of dry eye disease after 12 months of follow-up.

Several hypotheses have been proposed to explain the pathophysiology underlying the development of dry eye disease following refractive surgery. Changes in corneal innervation and sensitivity induced by refractive surgery are key in understanding the pathogenesis of dry eye disease and revolve around the idea that corneal sensitivity is reduced due to transection of the corneal nerves, thus resulting in dysfunction of the cornea-lacrimal gland functional unit [19, 21]. Transection of the sensory nerves of the cornea, as it occurs during FS-LASIK, is thought to lead to a decrease in the innervation to the autonomic nerve fibres supplying the lacrimal gland that would otherwise stimulate tear production via the neural reflex arc [19, 21]. This change may result in tear-film dysfunction via a number of mechanisms, including changes in the composition of the tears, ocular surface changes, and decreased blink frequency [21, 23].

There has been increasing evidence supporting the theory that damage to the corneal nerve density occurs following refractive surgery, particularly affecting the subbasal nerve plexus [19, 21, 24, 27, 38–40]. The main consequence of this change in nerve density is a reduction in corneal sensitivity. This results in a hypoesthetic cornea and is likely the key factor in the development of postrefractive dry eye disease [13, 23, 25, 26, 35, 41, 42]. With the aid of in vivo confocal microscopy, Denoyer et al. demonstrated that SMILE preserved the corneal subbasal nerve plexus better than LASIK [9]. They found a greater nerve density, number of long nerve fibres and nerve fibre branchings in patients that underwent SMILE compared to those that underwent LASIK. They also found that corneal sensitivity was greater in the SMILE group in the short-term but found no significant difference between SMILE and LASIK after 6 months after surgery [9]. This loss in nerve fibre density does start to regenerate months after surgery, with almost complete recovery by 2 to 5 years postoperatively [21, 43–45].

The degree of injury to corneal nerves is understandably expected to be different between the two surgical procedures, owing to the differing nature of each procedure. The two procedures differ in the method of ablation and the layers of the cornea affected, with FS-LASIK affecting the epithelium and anterior stroma, with the creation of a flap, while SMILE mainly affects the posterior stromal bed, only requiring a small tunnel incision [26]. Our results demonstrated a clear difference in the degree of injury and in the time to recovery of tear function between SMILE and FS-LASIK, as assessed by the TBUT. SMILE not only showed a more rapid recovery of tear function, with a return in TBUT to preoperative levels at 6 months compared to 12 months for FS-LASIK, but also showed a significantly lower degree of loss in TBUT compared to FS-LASIK at 3, 6, and 12 months postoperatively. Recent studies have demonstrated that SMILE preserves corneal sensitivity better than LASIK but demonstrated that both procedures eventually result in the recovery of corneal sensitivity to levels seen in healthy controls [9, 21, 25, 30, 43]. This may help to explain the transient nature and the long-term return of TBUT and SEEQ scores to preoperative levels in both groups after 12 months.

Li et al., who examined corneal sensitivity and dry eye following SMILE and FS-LASIK surgery, found that corneal sensitivity was less reduced and thus better in patients that underwent SMILE at all postoperative time intervals compared to those patients that underwent FS-LASIK [41]. The present study found that patients who underwent SMILE not only recovered tear-film function quicker than those who underwent FS-LASIK, but also were less symptomatic in the first 6 months. We also found a moderate correlation between the TBUT and SEEQ scores at 1 month postoperatively in both the SMILE and FS-LASIK groups; however, this correlation did not persist, suggesting that the clinical signs do not always correlate with reported symptoms. This discrepancy between clinical signs and patient symptoms has been previously noted, as Demirok et al. demonstrated that although both SMILE and FS-LASIK resulted in a decrease in corneal sensation up to 3 months postoperatively, there was no change in dry eye symptoms at any point in their patients [25].

Ocular surface changes, including those to the conjunctiva, induced by the two procedures would also differ. Coupled with the effects of hypoesthesia of the cornea, these changes may help to further explain the difference in the development of dry eye disease between SMILE and FS-LASIK patients. Contour changes may impact the distribution of tears over the corneal surface and are likely to pose a greater problem following FS-LASIK than SMILE due to disruption of the epithelium during the formation of the epithelial flap [11, 22]. Damage to and loss of mucin-producing conjunctival goblet cells have been shown to occur following LASIK, resulting in tear-film instability through a reduction of the mucin layer of the tear film [19, 21, 23]. This change may, however, return to baseline after 6 months and may contribute to the transient nature of the postrefractive dry eye disease. An increase in the osmolarity of tears following refractive surgery has also been demonstrated to occur after LASIK [19, 33, 34]. Hyperosmolarity of the tears occurs due to decreased blinking and increased evaporative loss of tears, reduced secretion of tears from the lacrimal gland, and the loss of goblet cells producing the mucin layer of the tear film [19]. This hyperosmolar environment results in the triggering of an inflammatory cascade with an upregulation of inflammatory cytokines, leading to continuing ocular surface irritation, a reduction in TBUT, and the development of dry eye symptoms [33].

FS-LASIK has been proven to be a safe and successful procedure for the surgical correction of refractive error over a number of years [8, 46]. SMILE, although in its clinical infancy, is now proving to also be a safe and successful alternative for the correction of refractive error and may provide a more superior and safer refractive outcome than FS-LASIK [36]. Extensive literature exists demonstrating the safety, efficacy, and complications of FS-LASIK, including a substantial amount of literature investigating the development of ocular surface and dry eye disease following FS-LASIK [8, 10, 11, 17, 19, 22, 23, 47]. Recently, there have been limited studies investigating the development of dry eye following SMILE, as well as studies comparing the two procedures [9, 25, 36, 41]. The majority of the literature, however, has focused on the short-term dry eye outcomes following SMILE and FS-LASIK, looking at the development of dry eye disease up to 3 to 9 months postoperatively. The present study advances on the current literature by investigating and comparing the clinical and subjective dry eye outcomes of patients undergoing SMILE and FS-LASIK over a longer period of follow-up, with measures up to 12 months postoperatively. One other advantage of the present study is that all patients investigated had a moderate to high degree of myopia prior to surgery. This is significant as the large majority of patients undergoing refractive surgery each year are myopic, and the greater the degree of myopia, the greater the amount of stromal ablation or lenticular extraction required [8, 12, 16]. This is a potential area of future research, investigating the development of dry eye disease in relation to the degree of refractive error.

Future advancements can be made on this study to further investigate both the clinical and subjective dry eye outcomes following SMILE and FS-LASIK. The present study was limited in the scope of assessments it conducted, looking at only 2 clinical indicators of dry eye: one objective measure using the TBUT and one subjective evaluation of patient symptoms using the SEEQ. A more comprehensive combination of assessments, as suggested by the Dry Eye Workshop and other studies, would provide a more accurate diagnosis of dry eye disease [5, 24, 37–39]. This would include a measure of tear osmolarity, corneal sensitivity, TBUT, a measure of tear function such as the Schirmer's test, and with advances in technology even the use of confocal microscopy. Also, a more rigorous questionnaire should be utilised, such as the 12-item Ocular Surface Disease Index (OSDI) or the 57-item Impact of Dry Eye on Everyday Life (IDEEL) questionnaires, which have been shown to be more accurate indicators of dry eye disease [2, 47, 48]. The SEEQ had the advantage of being quick and easy to administer, with only 6 items, but has been shown to be outdated and having a low correlation with dry eye signs [47].

The present study demonstrated that SMILE resulted in a lesser degree of dry eye disease and a faster recovery of tear function compared to FS-LASIK in the short-term following surgery in those patients with no preexisting dry eye disease. This was found using both clinical and subjective measures of dry eye and also demonstrated that the long-term outcome was not significantly different between the two procedures after 12 months of follow-up postoperatively. This short-term change, however, can have a great impact on a patients' overall satisfaction with their surgical and visual outcome and may influence their quality of life. Further studies may aim to determine preventative measures that may be taken to help prevent or reduce the development of dry eye disease in patients undergoing refractive surgery and help better monitor and manage those that do.

Conflict of Interests

The authors declare that there is no conflict of interests regarding the publication of this paper.

Acknowledgment

This study was supported by the Science and Technology Commission of Shanghai Municipality, Grant no. 134119a5100.

References

[1] I. K. Gipson, "Research in dry eye: report of the research subcommittee of the International Dry Eye WorkShop (2007)," *The Ocular Surface*, vol. 5, no. 2, pp. 179–193, 2007.

[2] L. Abetz, K. Rajagopalan, P. Mertzanis, C. Begley, R. Barnes, and R. Chalmers, "Development and validation of the impact of dry eye on everyday life (IDEEL) questionnaire, a patient-reported outcomes (PRO) measure for the assessment of the burden of dry eye on patients," *Health and Quality of Life Outcomes*, vol. 9, article 111, 2011.

[3] H. Brewitt and F. Sistani, "Dry eye disease: the scale of the problem," *Survey of Ophthalmology*, vol. 45, supplement 2, pp. S199–S202, 2001.

[4] J. R. Grubbs Jr., S. Tolleson-Rinehart, K. Huynh, and R. M. Davis, "A review of quality of life measures in dry eye questionnaires," *Cornea*, vol. 33, no. 2, pp. 215–218, 2014.

[5] H. D. Perry and E. D. Donnenfeld, "Dry eye diagnosis and management in 2004," *Current Opinion in Ophthalmology*, vol. 15, no. 4, pp. 299–304, 2004.

[6] M. A. Lemp, C. Baudouin, J. Baum et al., "The definition and classification of dry eye disease: report of the definition and classification subcommittee of the international Dry Eye WorkShop (2007)," *Ocular Surface*, vol. 5, no. 2, pp. 75–92, 2007.

[7] M. V. Netto, R. R. Mohan, R. Ambrósio Jr., A. E. K. Hutcheon, J. D. Zieske, and S. E. Wilson, "Wound healing in the cornea: a review of refractive surgery complications and new prospects for therapy," *Cornea*, vol. 24, no. 5, pp. 509–522, 2005.

[8] K. D. Solomon, L. E. Fernández de Castro, H. P. Sandoval et al., "LASIK world literature review: quality of life and patient satisfaction," *Ophthalmology*, vol. 116, no. 4, pp. 691–701, 2009.

[9] A. Denoyer, E. Landman, L. Trinh, J. Faure, F. Auclin, and C. Baudouin, "Dry eye disease after refractive surgery: comparative outcomes of small incision lenticule extraction versus LASIK," *Ophthalmology*, vol. 122, no. 4, pp. 669–676, 2015.

[10] D. Garcia-Zalisnak, D. Nash, and E. Yeu, "Ocular surface diseases and corneal refractive surgery," *Current Opinion in Ophthalmology*, vol. 25, no. 4, pp. 264–269, 2014.

[11] D. Raoof and R. Pineda, "Dry eye after laser in-situ keratomileusis," *Seminars in Ophthalmology*, vol. 29, no. 5-6, pp. 358–362, 2014.

[12] A. A. M. Torricelli, S. J. Bechara, and S. E. Wilson, "Screening of refractive surgery candidates for lasik and PRK," *Cornea*, vol. 33, no. 10, pp. 1051–1055, 2014.

[13] N. S. Jabbur, K. Sakatani, and T. P. O'Brien, "Survey of complications and recommendations for management in dissatisfied patients seeking a consultation after refractive surgery," *Journal of Cataract and Refractive Surgery*, vol. 30, no. 9, pp. 1867–1874, 2004.

[14] B. A. Levinson, C. J. Rapuano, E. J. Cohen, K. M. Hammersmith, B. D. Ayres, and P. R. Laibson, "Referrals to the Wills Eye Institute Cornea Service after laser in situ keratomileusis: reasons for patient dissatisfaction," *Journal of Cataract and Refractive Surgery*, vol. 34, no. 1, pp. 32–39, 2008.

[15] E. Y. W. Yu, A. Leung, S. Rao, and D. S. C. Lam, "Effect of laser in situ keratomileusis on tear stability," *Ophthalmology*, vol. 107, no. 12, pp. 2131–2135, 2000.

[16] S. D. Hammond Jr., A. K. Puri, and B. K. Ambati, "Quality of vision and patient satisfaction after LASIK," *Current Opinion in Ophthalmology*, vol. 15, no. 4, pp. 328–332, 2004.

[17] A. E. Levitt, A. Galor, J. S. Weiss et al., "Chronic dry eye symptoms after LASIK: parallels and lessons to be learned from other persistent post-operative pain disorders," *Molecular Pain*, vol. 11, article 21, 2015.

[18] M. D. Hammond, W. P. Madigan Jr., and K. S. Bower, "Refractive surgery in the United States Army, 2000–2003," *Ophthalmology*, vol. 112, no. 2, pp. 184–190, 2005.

[19] G. R. Nettune and S. C. Pflugfelder, "Post-LASIK tear dysfunction and dysesthesia," *The Ocular Surface*, vol. 8, no. 3, pp. 135–145, 2010.

[20] A. M. Alfawaz, S. Algehedan, S. S. Jastaneiah, S. Al-Mansouri, A. Mousa, and A. Al-Assiri, "Efficacy of punctal occlusion in management of dry eyes after laser in situ keratomileusis for myopia," *Current Eye Research*, vol. 39, no. 3, pp. 257–262, 2014.

[21] C. Chao, B. Golebiowski, and F. Stapleton, "The role of corneal innervation in LASIK-induced neuropathic dry eye," *The Ocular Surface*, vol. 12, no. 1, pp. 32–45, 2014.

[22] M. Q. Salomão, R. Ambrósio Jr., and S. E. Wilson, "Dry eye associated with laser in situ keratomileusis: mechanical microkeratome versus femtosecond laser," *Journal of Cataract & Refractive Surgery*, vol. 35, no. 10, pp. 1756–1760, 2009.

[23] R. Solomon, E. D. Donnenfeld, and H. D. Perry, "The effects of LASIK on the ocular surface," *The Ocular Surface*, vol. 2, no. 1, pp. 34–44, 2004.

[24] M. S.-B. Zeev, D. D. Miller, and R. Latkany, "Diagnosis of dry eye disease and emerging technologies," *Clinical Ophthalmology*, vol. 8, pp. 581–590, 2014.

[25] A. Demirok, E. B. Ozgurhan, A. Agca et al., "Corneal sensation after corneal refractive surgery with small incision lenticule extraction," *Optometry and Vision Science*, vol. 90, no. 10, pp. 1040–1047, 2013.

[26] S. Wei and Y. Wang, "Comparison of corneal sensitivity between FS-LASIK and femtosecond lenticule extraction (ReLEx flex) or small-incision lenticule extraction (ReLEx smile) for myopic eyes," *Graefe's Archive for Clinical and Experimental Ophthalmology*, vol. 251, no. 6, pp. 1645–1654, 2013.

[27] A. Kheirkhah, U. S. Saboo, T. B. Abud et al., "Reduced corneal endothelial cell density in patients with dry eye disease," *American Journal of Ophthalmology*, vol. 159, no. 6, pp. 1022.e2–1026.e2, 2015.

[28] C. F. Marfurt, J. Cox, S. Deek, and L. Dvorscak, "Anatomy of the human corneal innervation," *Experimental Eye Research*, vol. 90, no. 4, pp. 478–492, 2010.

[29] L. J. Müller, C. F. Marfurt, F. Kruse, and T. M. T. Tervo, "Corneal nerves: structure, contents and function," *Experimental Eye Research*, vol. 76, no. 5, pp. 521–542, 2003.

[30] M. O'Doherty, M. O'Keeffe, and C. Kelleher, "Five year follow up of laser in situ keratomileusis for all levels of myopia," *British Journal of Ophthalmology*, vol. 90, no. 1, pp. 20–23, 2006.

[31] W. Sekundo, K. Bönicke, P. Mattausch, and W. Wiegand, "Six-year follow-up of laser in situ keratomileusis for moderate and extreme myopia using a first-generation excimer laser and microkeratome," *Journal of Cataract and Refractive Surgery*, vol. 29, no. 6, pp. 1152–1158, 2003.

[32] K. K. Nichols, J. J. Nichols, and G. L. Mitchell, "The lack of association between signs and symptoms in patients with dry eye disease," *Cornea*, vol. 23, no. 8, pp. 762–770, 2004.

[33] L. Battat, A. Macri, D. Dursun, and S. C. Pflugfelder, "Effects of laser in situ keratomileusis on tear production, clearance, and the ocular surface," *Ophthalmology*, vol. 108, no. 7, pp. 1230–1235, 2001.

[34] A. Denoyer, G. Rabut, and C. Baudouin, "Tear film aberration dynamics and vision-related quality of life in patients with dry eye disease," *Ophthalmology*, vol. 119, no. 9, pp. 1811–1818, 2012.

[35] J. S. Kung, C. S. Sáles, and E. E. Manche, "Corneal sensation and dry eye symptoms after conventional versus inverted side-cut femtosecond LASIK: a prospective randomized study," *Ophthalmology*, vol. 121, no. 12, pp. 2311–2316, 2014.

[36] Y. Xu and Y. Yang, "Dry eye after small incision lenticule extraction and LASIK for myopia," *Journal of Refractive Surgery*, vol. 30, no. 3, pp. 186–190, 2014.

[37] "Methodologies to diagnose and monitor dry eye disease: report of the Diagnostic Methodology Subcommittee of the International Dry Eye WorkShop (2007)," *The Ocular Surface*, vol. 5, no. 2, pp. 108–152, 2007.

[38] Y. Qazi, S. Aggarwal, and P. Hamrah, "Image-guided evaluation and monitoring of treatment response in patients with dry eye disease," *Graefe's Archive for Clinical and Experimental Ophthalmology*, vol. 252, no. 6, pp. 857–872, 2014.

[39] E. Villani, C. Baudouin, N. Efron et al., "In vivo confocal microscopy of the ocular surface: from bench to bedside," *Current Eye Research*, vol. 39, no. 3, pp. 213–231, 2014.

[40] B. J. Thomas, A. Galor, A. A. Nanji et al., "Ultra high-resolution anterior segment optical coherence tomography in the diagnosis and management of ocular surface squamous neoplasia," *The Ocular Surface*, vol. 12, no. 1, pp. 46–58, 2014.

[41] M. Li, J. Zhao, Y. Shen et al., "Comparison of dry eye and corneal sensitivity between small incision lenticule extraction and femtosecond LASIK for myopia," *PloS ONE*, vol. 8, no. 10, Article ID e77797, 2013.

[42] B. S. Shaheen, M. Bakir, and S. Jain, "Corneal nerves in health and disease," *Survey of Ophthalmology*, vol. 59, no. 3, pp. 263–285, 2014.

[43] M. P. Calvillo, J. W. McLaren, D. O. Hodge, and W. M. Bourne, "Corneal reinnervation after LASIK: prospective 3-year longitudinal study," *Investigative Ophthalmology and Visual Science*, vol. 45, no. 11, pp. 3991–3996, 2004.

[44] J. C. Erie, J. W. McLaren, D. O. Hodge, and W. M. Bourne, "Recovery of corneal subbasal nerve density after PRK and LASIK," *American Journal of Ophthalmology*, vol. 140, no. 6, pp. 1059.e1–1064.e1, 2005.

[45] C. Wang, Y. Peng, S. Pan, and L. Li, "Effect of insulin-like growth factor-1 on corneal surface ultrastructure and nerve regeneration of rabbit eyes after laser in situ keratomileusis," *Neuroscience Letters*, vol. 558, pp. 169–174, 2014.

[46] C. McAlinden, "Corneal refractive surgery: past to present," *Clinical and Experimental Optometry*, vol. 95, no. 4, pp. 386–398, 2012.

[47] "The epidemiology of dry eye disease: report of the Epidemiology Subcommittee of the International Dry Eye WorkShop (2007)," *The Ocular Surface*, vol. 5, no. 2, pp. 93–107, 2007.

[48] S. Vitale, L. A. Goodman, G. F. Reed, and J. A. Smith, "Comparison of the NEI-VFQ and OSDI questionnaires in patients with Sjögren's syndrome-related dry eye," *Health and Quality of Life Outcomes*, vol. 2, article 44, 2004.

Hindawi Publishing Corporation
Journal of Ophthalmology
Volume 2015, Article ID 380624, 7 pages
http://dx.doi.org/10.1155/2015/380624

Research Article

Assessment of Corneal Biomechanical Properties by CorVis ST in Patients with Dry Eye and in Healthy Subjects

Qin Long, Jingyi Wang, Xue Yang, Yumei Jin, Fengrong Ai, and Ying Li

Department of Ophthalmology, Peking Union Medical College Hospital, Chinese Academy of Medical Sciences and Peking Union Medical College, Beijing 100730, China

Correspondence should be addressed to Ying Li; liyingpumch@126.com

Received 28 June 2015; Revised 5 September 2015; Accepted 10 September 2015

Academic Editor: Antonio Queiros

Copyright © 2015 Qin Long et al. This is an open access article distributed under the Creative Commons Attribution License, which permits unrestricted use, distribution, and reproduction in any medium, provided the original work is properly cited.

Purpose. To investigate corneal biomechanical properties in patients with dry eye and in healthy subjects using Corneal Visualization Scheimpflug Technology (CorVis ST). *Methods*. Biomechanical parameters were measured using CorVis ST in 28 eyes of 28 patients with dry eye (dry eye group) and 26 normal subjects (control group). The Schirmer I test value, tear film break-up time (TBUT), and corneal staining score (CSS) were recorded for each eye. Biomechanical properties were compared between the two groups and bivariate correlation analysis was used to assess the relationship between biomechanical parameters and dry eye signs. *Results*. Only one of the ten biomechanical parameters was significantly different between the two groups. Patients in the dry eye group had significantly lower highest concavity time (HC-time) ($P = 0.02$) than the control group. Correlation analysis showed a significant negative correlation between HC-time and CSS with marginal P value ($\rho = -0.39$, $P = 0.04$) in the dry eye group. *Conclusions*. The corneal biomechanical parameter of HC-time is reduced in dry eyes compared to normal eyes. There was also a very weak but significant negative correlation between HC-time and CSS in the dry eye group, indicating that ocular surface damage can give rise to a more compliant cornea in dry eyes.

1. Introduction

Dry eye is a very common condition which is characterized by a lack of tear secretion or excessive tear evaporation that affects tens of millions of people worldwide, with a higher prevalence in Asian population [1, 2]. It is a multifactorial disease of the tears and ocular surface that results in symptoms of discomfort and visual disturbance and signs including tear film instability with potential damage to the ocular surface [3]. Studies show that the cornea is a complex biomechanical composite and that an intact corneal structural component is important for overall corneal biomechanics [4, 5]. Considering the high prevalence of dry eye, its potential influence on corneal biomechanics needs to be clarified.

Many studies have indicated that inflammation plays a key role in the pathogenesis of dry eye related corneal damage [6, 7]. A number of inflammatory cytokines and chemokines have been shown to be consistently elevated in dry eyes [8–10] and may have potential impact on corneal tissue and consequently alter the corneal biomechanical behavior. Some evidence has shown significant corneal biomechanical alterations in eyes with glaucoma and keratoconus [11, 12], which are also considered to have ocular surface inflammation [13, 14] indicating a possible similar mechanism of action in dry eye.

Since dry eye is initially a disorder of the tear film layer, tear secretion value, tear film break-up time (TBUT), and corneal staining score (CSS) are valuable parameters to assess the severity of dry eye and ocular surface integrity. As we mentioned that an intact corneal structural component is essential to maintain the corneal biomechanics, therefore, the above parameters can be applied to evaluate the impact of dry eye on the behavior of corneal biomechanics.

Age is also a potential factor for the corneal biomechanical alterations in dry eyes since it has been reported that the prevalence of dry eye increases significantly with age [2]. Until now, no reports have addressed the relationship between age and corneal biomechanics in dry eyes.

The Ocular Response Analyzer (ORA) (Reichert, Buffalo, NY, USA) was the first commercially available device to measure the in vivo corneal biomechanical properties of corneal hysteresis (CH) and corneal resistance factor (CRF) [15, 16]. In a study using the ORA, Firat and Doganay reported that corneal biomechanical parameters such as CH and CRF were not influenced in dry eye [17].

Corneal Visualization Scheimpflug Technology (CorVis ST) (Oculus Optikgeräte GmbH, Wetzlar, Germany) is a recently developed noncontact tonometry system since 2011. With an integrated ultra-high-speed Scheimpflug Camera, it is able to record real-time dynamic deformation of the cornea, allowing direct description of the corneal biomechanics for clinical evaluation [18]. Until now, biomechanical parameters generated from CorVis ST have been recorded for glaucoma and diabetes mellitus and after refractive procedures [19–22].

Herein, the aims of this study are twofold: (1) to compare the corneal biomechanical parameters of patients with dry eye and normal subjects by the CorVis ST and (2) to assess the correlation between corneal biomechanical parameters and other characteristics, such as age and dry eye parameters.

2. Methods

In this observational comparative study, unrelated Chinese patients with or without dry eye were recruited sequentially from the Department of Ophthalmology, Peking Union Medical College Hospital, Beijing, China. The study was performed according to the Declaration of Helsinki. Informed consent was obtained from all subjects prior to participation in the study.

The inclusion criteria of dry eye were identified according to the consensus of dry eye disease in China (2013): (1) at least 1 of 6 symptoms: dryness, gritty/sandiness, burning, tiredness, discomfort, and blurred vision with TBUT (the time to initial break-up of the tear film following a blink) for less than 5 seconds (s) using FLUOR-STRIP (Tianjin Jingming New Technological Development Co., Ltd., Tianjin, China) or a Schirmer I test (without anesthesia, eye closed during the test) value of less than 5 mm per 5 minutes using SCHIRMER TEAR TEST STRIPS (Tianjin Jingming New Technological Development Co., Ltd., Tianjin, China); (2) at least 1 of 6 symptoms: dryness, gritty/sandiness, burning, tiredness, discomfort, and blurred vision with 5 s < TBUT ⩽ 10 s or 5 mm/5 min < Schirmer I test (without anesthesia) ⩽ 10 mm/5 min, accompanied by CSS (the score evaluated by employing fluorescein) total of +1 or more [scale 0 (none) to 12 (severe)], as described in Table 1. TBUT and CSS were observed using slit lamp biomicroscopy by the same masked investigator; Schirmer I test was performed more than 20 minutes after dye staining by another masked investigator.

Patients were excluded from the study if they had concurrent ocular infectious disease, ocular inflammatory disease other than dry eye, a positive history of ocular surgery, ocular or systemic diseases (e.g., corneal scars, corneal dystrophy, corneal degradation, keratoconus, glaucoma, uveitis, systemic autoimmune diseases, and diabetes mellitus), or local or systemic medication use other than artificial tears. In addition, subjects with a refractive error greater than ±1.00 D or contact lens wearers were excluded from the study.

Table 1: Grading of cornea staining.

Score	Cornea staining (with fluorescein)
0	0 dots
1	1–30 dots
2	>30 dots without confluence
3	>30 dots with confluence, filament, or ulcer

Staining is represented by punctate dots on the cornea, the cornea is divided into four quadrants, and the total cornea staining score is represented by the total score of four cornea quadrants.

Corneal biomechanical parameters were obtained using CorVis ST (Type 72100, Oculus Optikgeräte GmbH, Wetzlar, Germany) by one masked investigator in every case to eliminate any possible interobserver variability more than 20 minutes after Schirmer I test. CorVis ST uses a high speed Scheimpflug camera (4330 frames/s), covering 8.0 mm horizontally, and records 140 images of the corneal deformation in response to a puff of air. Due to the air puff, the cornea underwent three distinct phases: first applanation, the highest concavity, and second applanation, respectively (Figure 1). Ten phase-specific parameters were automatically generated during the process (Table 2) [23]. Intraocular pressure (IOP) and central corneal thickness (CCT) were also obtained during one measurement procedure. Only the acquisitions showing "OK" on quality of scan (QS) were analyzed.

To reduce the potential diurnal variability, all the measurements were performed between 8:00 and 11:00 a.m.

3. Data Analysis

Data were analyzed using IBM SPSS 19.0 for Windows statistical software (SPSS, Chicago, IL) and GraphPad Prism 5 (GraphPad Software, Inc.). Numerical variables were presented as mean ± SD. Shaphiro-Wilk test was used to test normal distribution. Two-tailed Student's t-test and Mann-Whitney U test were used to compare the observational parameters of the two groups depending on data normality. Pearson or Spearman bivariate correlation analysis was used according to data normality to assess the relationship between corneal biomechanical parameters and potential related characteristics, such as age, IOP, CCT, and dry eye parameters. The level of statistical significance was set to $P < 0.05$. Due to the significant correlation between the right and left eyes, only one randomly selected eye from each subject was included in the analysis.

4. Results

Overall, 54 patients were included in the study. The dry eye group ($n = 28$) included 18 female and 10 male patients, with a mean age of 46.82 years (range, 14 to 68 years; mean ± SD, 46.82 ± 14.42 years). 20 female and 6 male patients

Table 2: All biomechanical parameters derived from CorVis ST.

CorVis ST parameters	Means
A1-time	Time from starting until the first applanation
A2-time	Time from starting until the second applanation
A1-length	Cord length of the first applanation
A2-length	Cord length of the second applanation
A1-velocity (A1-V)	Corneal speed during the first applanation moment
A2-velocity (A2-V)	Corneal speed during the second applanation moment
Highest concavity-time (HC-time)	Time from starting until HC is reached
Peak distance (PD)	Distance between the two peaks of the cornea at HC
HC radius	Central concave curvature at HC
Deformation amplitude (DA)	Maximum amplitude at the highest concavity

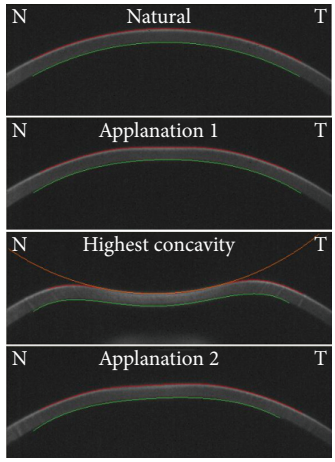

Figure 1: The corneal deformation during air puff from CorVis ST. Due to the air puff, the cornea starts with a natural convex shape and undergoes three distinct phases of first applanation, highest concavity, and second applanation, respectively.

constituted the control group, with a mean age of 40.19 years (range, 24 to 67 years; mean ± SD, 40.19 ± 11.39 years). There were no differences between the two groups in terms of age ($t = 1.50$, $P = 0.15$) and sex ($X^2 = 1.03$, $P = 0.31$). Significant differences were found between the dry eye group and control group in terms of Schirmer I test value (mean ± SD, 2.43 ± 1.85 mm versus 12.65 ± 5.92 mm; Mann-Whitney $U = 2.5$, $P < 0.001$), TBUT (mean ± SD, 3.07 ± 1.76 s versus 7.19 ± 2.38 s; Mann-Whitney $U = 55.5$, $P < 0.001$), and CSS (mean ± SD, 1.11 ± 1.83 versus 0.04 ± 0.20; Mann-Whitney $U = 243.5$, $P = 0.003$).

The corneal biomechanical parameters and IOP and CCT values are shown in Table 3. The differences in IOP and CCT were not statistically significant between the dry eye group and control group (IOP: $t = 0.15$, $P = 0.88$; CCT: $t = 0.13$, $P = 0.90$). Only one of ten biomechanical parameters was significantly different between the dry eye group and control group. Patients in the dry eye group had a significantly lower time at highest concavity (HC-time) (Mann-Whitney $U = 223.0$, $P = 0.02$) compared to the control group (Figure 2).

In the dry eye group, bivariate correlation analysis showed a significant negative correlation between HC-time and CSS with marginal P value (Spearman $\rho = -0.39$, $P = 0.04$) (Figure 3(a)). No correlation was found between HC-time and age, sex, Schirmer I test value, and TBUT (Spearman correlation analysis, all $P > 0.05$). In contrast, bivariate correlation analysis of the control group showed a significant positive correlation between HC-time and age (Spearman $\rho = 0.45$, $P = 0.02$) (Figure 3(b)); however, no correlation was noted between HC-time and sex, Schirmer I test value, TBUT, and CSS (Spearman correlation analysis, all $P > 0.05$). There was no correlation between HC-time and IOP and CCT in both groups (Spearman correlation analysis, all $P > 0.05$). The correlation coefficients and P values are shown in Table 4.

5. Discussion

The integrity of the cornea is dependent on its biomechanical properties of elasticity, viscosity, and viscoelasticity, which in turn can be affected by the integrity of epithelial barrier, collagen fibrils arrangement, regional pachymetry, hydration, and age [24]. Knowledge of the contribution of corneal biomechanics to dry eye is essential to develop appropriate treatment strategies particularly in cases with concurrent conditions, such as glaucoma and keratoconus, as well as predicting the response to clinical procedures, such as corneal transplant, refractive surgery, and corneal collagen cross-linking [24, 25]. To date, there are 2 systems available for clinical use, ORA, and the recently developed CorVis ST, which are able to provide dynamic quantitative information, to precisely evaluate corneal biomechanics. To our knowledge, this is the first study to use CorVis ST to investigate corneal biomechanics in dry eyes.

This study demonstrated that patients in the dry eye group had significantly lower HC-time than age- and sex-matched normal controls. Bivariate correlation analysis showed a significantly negative correlation between HC-time and CSS in the dry eye group and a significantly positive correlation between HC-time and age was noted in control group, but not in the age- and sex-matched dry eye group.

HC-time represents the time from commencement until the highest concavity is reached and reflects the time to maximum deformation. A shorter HC-time may be due to a more compliant cornea reaching the highest concavity. Studies have indicated that HC-time was significantly shorter after laser in situ keratomileusis (LASIK) compared to small incision lenticule extraction (SMILE). Since the major difference between the two refractive procedures is the flap, the lower HC-time after LASIK may result from more collagen fibres being cut during flap creation [26]. For dry

Table 3: All parameters derived from CorVis ST in dry eye group and control group, mean ± SD.

Parameters	Dry eye group (n = 28)	Control group (n = 26)	t/U value	P value
A1-time (ms)	7.38 ± 0.28	7.37 ± 0.16	0.05*	0.96
A2-time (ms)	21.85 ± 0.42	21.95 ± 0.29	0.91*	0.37
A1-length (mm)	1.75 ± 0.05	1.77 ± 0.03	309.0#	0.34
A2-length (mm)	1.71 ± 0.23	1.77 ± 0.19	301.5#	0.28
A1-V (m/s)	0.15 ± 0.02	0.15 ± 0.01	0.22*	0.83
A2-V (m/s)	−0.30 ± 0.07	−0.31 ± 0.05	0.23*	0.82
HC-time (ms)	17.07 ± 0.40	17.55 ± 0.95	223.0#	0.02
PD (mm)	3.92 ± 1.19	3.89 ± 1.16	353.0#	0.86
HC radius (mm)	7.29 ± 0.90	7.15 ± 0.95	317.0#	0.42
DA (mm)	3.92 ± 1.19	3.89 ± 1.16	0.42*	0.68
IOP (mmHg)	13.64 ± 2.76	13.70 ± 1.61	0.15*	0.88
CCT (μm)	534.82 ± 25.64	537.0 ± 35.97	0.13*	0.90

A1-V: A1-velocity; A2-V: A2-velocity; HC-time: highest concavity-time; PD: peak distance; HC radius: radius at HC; DA: deformation amplitude; IOP: intraocular pressure; CCT: central corneal thickness; *t-test value; #Mann-Whitney U test value.

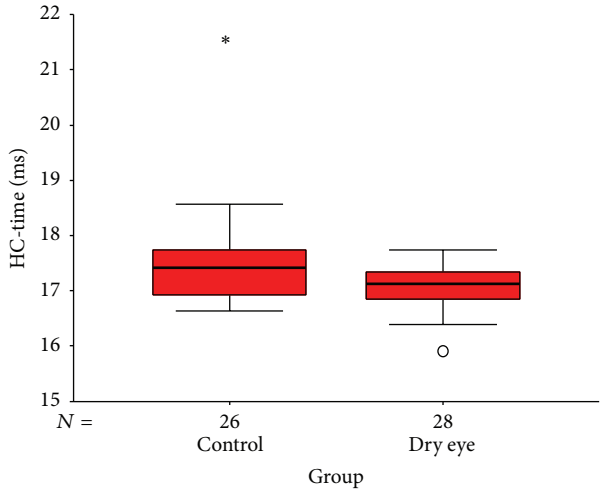

Figure 2: Box plot shows the distribution percentage difference between the dry eye group and control group for HC time (time from starting until the highest concavity is reached). The median for each data set is indicated by the center line, and the first and third quartiles are represented by the edges of the area, which is known as the interquartile range (IQR). The 95%/5% confidence intervals are represented by the ends of the lines extending from the IQR. The circles denote the outliers with values of more than 1.5 IQR from the upper or lower edge of the box.

Table 4: Factors associated with HC-time.

Parameters	Dry eye group (n = 28)		Control group (n = 26)	
	ρ value	P value	ρ value	P value
Age	−0.04	0.82	0.45	0.02
Gender	0.05	0.80	0.33	0.10
Schirmer I test value (mm)	−0.16	0.41	−0.35	0.08
TBUT (s)	0.02	0.90	−0.22	0.28
CSS (score)	−0.39	0.04	0.04	0.85
IOP (mmHg)	0.17	0.38	−0.28	0.17
CCT (μm)	0.06	0.76	0.15	0.46

TBUT: tear break-up time; CSS: corneal staining score; IOP: intraocular pressure; CCT: central corneal thickness; Coeff: the correlation coefficient; ρ: Spearman's correlation coefficient value.

eyes, there is a consensus that dry eye is an inflammation triggered disease, since significantly increased inflammation factors and proteins have been detected in the tear film and ocular surface tissue of dry eye [9, 11, 27], which may have potential impact on corneal biomechanics. For example, matrix metalloproteinase 9 (MMP-9) was shown to be elevated in dry eyes [28, 29]. As a member of matrix metalloproteinases (MMPs) family, MMP-9 is involved in the degradation of extracellular matrix components (ECM) and contributes to inflammation, wound healing, and tissue remodeling [30, 31]. It is thought that the increased MMP-9 expression may cause a more compliant cornea in dry eye, and this hypothesis is supported by our study. We found a lower HC-time in dry eye patients compared to age- and sex-matched normal controls. However, none of the remaining CorVis ST parameters supported this theory. Given that corneal biomechanical behavior is governed by the stroma, therefore, greater alterations would be expected in severe dry eyes which exhibit greater corneal stromal lesions.

Corneal biomechanical properties can be affected by multiple factors, including the integrity of epithelial barrier [5]. Elsheikh et al. showed that an intact corneal epithelium has a very important function over the corneal biomechanics [5]. The integrity of the corneal epithelium can be represented by CSS with fluorescein staining [3]. The negative correlation between HC-time and CSS in dry eye group suggests that greater corneal epithelium damage results in more compliant cornea, resulting in a shorter time to reach the highest concavity. Since only a borderline P value was noted, further studies should be conducted to confirm this significance.

The evaluation of CCT and corneal epithelial damage are essential to study and compare the biomechanical parameters between the dry eye group and control group. In our study,

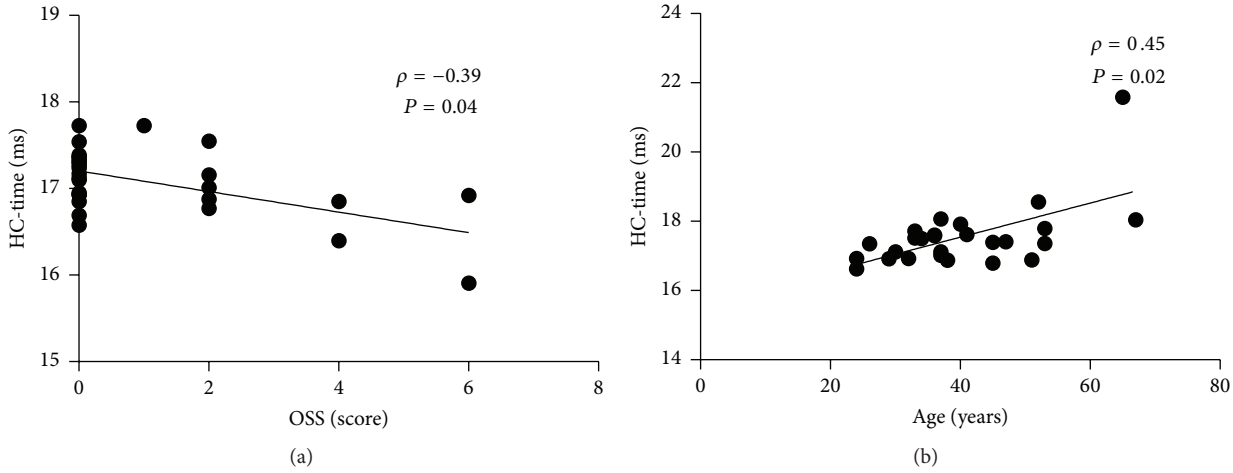

Figure 3: Scatter diagrams of bivariate correlation analysis. (a) Correlation between the HC- time (time from starting until the highest concavity is reached) and CSS (corneal staining score). (b) Correlation between the HC-time and age; ρ: Spearman's correlation coefficient value.

we did not find difference in terms of CCT between two groups; this was consistent with the study by Firat and Doganay [17]. However, CCT was observed to be thinner in dry eyes compared to normal controls by Meyer et al. [32]. With regard to the evaluation of corneal epithelial damage, the measurements of central corneal epithelial thickness (subjective assessment) and CSS (objective assessment) are both used in clinic. Similar to CCT, the results of central corneal epithelial thickness were also contradictory. It showed to be thicker in dry eyes in the study of Kanellopoulos and Asimellis [33] and no difference in Cui's study [34]. Further objective assessment approaches, such as epithelial mapping or tear film osmolarity, should be considered to clarify our results in the future.

Age related alterations in corneal biomechanics are associated with corneal stiffening and decreasing viscoelasticity [35]. Ex vivo and in vivo studies have demonstrated that corneal stiffness changes with age, accompanied with stromal microstructure changes including the more cross-links of collagen fibrils within the cornea [36, 37]. Several studies showed that CH and CRF significantly decreased with age in healthy population [38, 39]. Other authors, however, demonstrated no correlation between corneal biomechanics and age by ORA [40]. With CorVis ST, Valbon et al. reported that only the HC-time correlated significantly with age in healthy eyes [23]. A similar result was seen in our study, and data suggested that older subjects tended to have longer HC-time due to a less compliant cornea. However, we did not find the significant correlation between HC-time and age in dry eye group, which may be due to the neutralization of the impact caused by aging and the integrity of corneal epithelium because of dry eye.

The main limitations of our study are that (1) the sample size is relatively small; (2) not all the subjects had a general examination and we excluded systemic diseases only by the history; (3) we did not test the diurnal variation for the corneal biomechanics, although several studies reported a stable profile during daytime acquisitions by ORA [41] (to date, no study has addressed diurnal variation by CorVis ST; therefore, the importance of this factor in our study is unknown); and (4) biomechanical properties can be affected by corneal hydration, but, in dry eye patients, it is difficult to eliminate the influence caused by the use of artificial tears.

In summary, the present study showed that HC-time was significantly lower in dry eye patients than in age- and sex-matched normal controls. Correlation analysis showed a very weak but significant negative correlation between HC-time and CSS in the dry eye group, indicating that the ocular surface damage can cause a more compliant cornea in dry eyes. As CorVis ST is a relatively new technology, further studies with a larger sample size should be performed to elucidate its full usefulness for dry eye patients, as this might be helpful in clinical practice, especially for planning ophthalmological interventions, such as refractive surgery, which has been reported to alter corneal biomechanical behavior due to corneal tissue removal.

Conflict of Interests

The authors have neither conflict of interests nor commercial interests in the devices mentioned in the paper.

Acknowledgment

This work was supported by grants from the National Natural Science Foundation of China (30600692, 81070755).

References

[1] E. M. Messmer, "The pathophysiology, diagnosis, and treatment of dry eye disease," *Deutsches Ärzteblatt international*, vol. 112, no. 5, pp. 71–82, 2015.

[2] N.-N. Liu, L. Liu, J. Li, and Y.-Z. Sun, "Prevalence of and risk factors for dry eye symptom in mainland China: a systematic review and meta-analysis," *Journal of Ophthalmology*, vol. 2014, Article ID 748654, 8 pages, 2014.

[3] "The definition and classification of dry eye disease: report of the definition and classification Subcommittee of the International Dry Eye WorkShop (2007)," *The Ocular Surface*, vol. 5, no. 2, pp. 75–92, 2007.

[4] T. Huseynova, G. O. Waring IV, C. Roberts, R. R. Krueger, and M. Tomita, "Corneal biomechanics as a function of intraocular pressure and pachymetry by dynamic infrared signal and scheimpflug imaging analysis in normal eyes," *American Journal of Ophthalmology*, vol. 157, no. 4, pp. 885–893, 2014.

[5] A. Elsheikh, D. Alhasso, and P. Rama, "Assessment of the epithelium's contribution to corneal biomechanics," *Experimental Eye Research*, vol. 86, no. 2, pp. 445–451, 2008.

[6] M. Hessen and E. K. Akpek, "Dry eye: an inflammatory ocular disease," *Journal of Ophthalmic & Vision Research*, vol. 9, no. 2, pp. 240–250, 2014.

[7] Y. Wei and P. A. Asbell, "The core mechanism of dry eye disease is inflammation," *Eye & Contact Lens*, vol. 40, no. 4, pp. 248–256, 2014.

[8] M. L. Massingale, X. Li, M. Vallabhajosyula, D. Chen, Y. Wei, and P. A. Asbell, "Analysis of inflammatory cytokines in the tears of dry eye patients," *Cornea*, vol. 28, no. 9, pp. 1023–1027, 2009.

[9] J. Zhang, X. Yan, and H. Li, "Analysis of the correlations of mucins, inflammatory markers, and clinical tests in dry eye," *Cornea*, vol. 32, no. 7, pp. 928–932, 2013.

[10] L. Niu, S. Zhang, J. Wu, L. Chen, and Y. Wang, "Upregulation of NLRP3 inflammasome in the tears and ocular surface of dry eye patients," *PLOS ONE*, vol. 10, no. 5, Article ID e0126277, 2015.

[11] K. Mansouri, M. T. Leite, R. N. Weinreb, A. Tafreshi, L. M. Zangwill, and F. A. Medeiros, "Association between corneal biomechanical properties and glaucoma severity," *American Journal of Ophthalmology*, vol. 153, no. 3, pp. 419–427.e1, 2012.

[12] J. S. Wolffsohn, S. Safeen, S. Shah, and M. Laiquzzaman, "Changes of corneal biomechanics with keratoconus," *Cornea*, vol. 31, no. 8, pp. 849–854, 2012.

[13] J. Chua, M. Vania, C. M. G. Cheung et al., "Expression profile of inflammatory cytokines in aqueous from glaucomatous eyes," *Molecular Vision*, vol. 18, pp. 431–438, 2012.

[14] A. S. Jun, L. Cope, C. Speck et al., "Subnormal cytokine profile in the tear fluid of keratoconus patients," *PLoS ONE*, vol. 6, no. 1, Article ID e16437, 2011.

[15] N. Terai, F. Raiskup, M. Haustein, L. E. Pillunat, and E. Spoerl, "Identification of biomechanical properties of the cornea: the ocular response analyzer," *Current Eye Research*, vol. 37, no. 7, pp. 553–562, 2012.

[16] D. A. Luce, "Determining in vivo biomechanical properties of the cornea with an ocular response analyzer," *Journal of Cataract and Refractive Surgery*, vol. 31, no. 1, pp. 156–162, 2005.

[17] P. G. Firat and S. Doganay, "Corneal hysteresis in patients with dry eye," *Eye*, vol. 25, no. 12, pp. 1570–1574, 2011.

[18] Y. Hon and A. K. C. Lam, "Corneal deformation measurement using scheimpflug noncontact tonometry," *Optometry and Vision Science*, vol. 90, no. 1, pp. e1–e8, 2013.

[19] L. Tian, D. Wang, Y. Wu et al., "Corneal biomechanical characteristics measured by the CorVis Scheimpflug technology in eyes with primary open-angle glaucoma and normal eyes," *Acta Ophthalmologica*, 2015.

[20] L. Tian, Y.-F. Huang, L.-Q. Wang et al., "Corneal biomechanical assessment using corneal visualization scheimpflug technology in keratoconic and normal eyes," *Journal of Ophthalmology*, vol. 2014, Article ID 147516, 8 pages, 2014.

[21] C. Pérez-Rico, C. Gutiérrez-Ortíz, A. González-Mesa, A. M. Zandueta, A. Moreno-Salgueiro, and F. Germain, "Effect of diabetes mellitus on Corvis ST measurement process," *Acta Ophthalmologica*, vol. 93, no. 3, pp. e193–e198, 2015.

[22] Z. Hassan, L. Modis Jr., E. Szalai, A. Berta, and G. Nemeth, "Examination of ocular biomechanics with a new Scheimpflug technology after corneal refractive surgery," *Contact Lens & Anterior Eye*, vol. 37, no. 5, pp. 337–341, 2014.

[23] B. F. Valbon, R. Ambrósio, B. M. Fontes, and M. R. Alves, "Effects of age on corneal deformation by non-contact tonometry integrated with an ultra-high-speed (UHS) scheimpflug camera," *Arquivos Brasileiros de Oftalmologia*, vol. 76, no. 4, pp. 229–232, 2013.

[24] D. P. Piñero and N. Alcón, "In vivo characterization of corneal biomechanics," *Journal of Cataract and Refractive Surgery*, vol. 40, no. 6, pp. 870–887, 2014.

[25] N. Garcia-Porta, P. Fernandes, A. Queiros, J. Salgado-Borges, M. Parafita-Mato, and J. M. González-Méijome, "Corneal biomechanical properties in different ocular conditions and new measurement techniques," *ISRN Ophthalmology*, vol. 2014, Article ID 724546, 19 pages, 2014.

[26] I. B. Pedersen, S. Bak-Nielsen, A. H. Vestergaard, A. Ivarsen, and J. Hjortdal, "Corneal biomechanical properties after LASIK, ReLEx flex, and ReLEx smile by Scheimpflug-based dynamic tonometry," *Graefe's Archive for Clinical and Experimental Ophthalmology*, vol. 252, no. 8, pp. 1329–1335, 2014.

[27] L. Zhu, J. Shen, C. Zhang et al., "Inflammatory cytokine expression on the ocular surface in the Botulium toxin B induced murine dry eye model," *Molecular Vision*, vol. 15, pp. 250–258, 2009.

[28] K. R. Vandermeid, S. P. Su, K. W. Ward, and J.-Z. Zhang, "Correlation of tear inflammatory cytokines and matrix metalloproteinases with four dry eye diagnostic tests," *Investigative Ophthalmology & Visual Science*, vol. 53, no. 3, pp. 1512–1518, 2012.

[29] A. Acera, G. Rocha, E. Vecino, I. Lema, and J. A. Durán, "Inflammatory markers in the tears of patients with ocular surface disease," *Ophthalmic Research*, vol. 40, no. 6, pp. 315–321, 2008.

[30] S. R. Van Doren, "Matrix metalloproteinase interactions with collagen and elastin," *Matrix Biology*, vol. 44–46, pp. 224–231, 2015.

[31] T. Sakimoto and M. Sawa, "Metalloproteinases in corneal diseases: degradation and processing," *Cornea*, vol. 31, no. 11, supplement 1, pp. S50–S56, 2012.

[32] L. M. Meyer, M. Kronschläger, and A. R. Wegener, "Schleimpflug photography detects alterations in corneal density and thickness in patients with dry eye disease," *Der Ophthalmologe*, vol. 111, no. 10, pp. 914–919, 2014.

[33] A. J. Kanellopoulos and G. Asimellis, "In vivo 3-dimensional corneal epithelial thickness mapping as an indicator of dry eye: preliminary clinical assessment," *American Journal of Ophthalmology*, vol. 157, no. 1, pp. 63–68.e2, 2014.

[34] X. Cui, J. Hong, F. Wang et al., "Assessment of corneal epithelial thickness in dry eye patients," *Optometry and Vision Science*, vol. 91, no. 12, pp. 1446–1454, 2014.

[35] A. Kotecha, "What biomechanical properties of the cornea are relevant for the clinician?" *Survey of Ophthalmology*, vol. 52, no. 6, pp. S109–S114, 2007.

[36] N. S. Malik, S. J. Moss, N. Ahmed, A. J. Furth, R. S. Wall, and K. M. Meek, "Ageing of the human corneal stroma: structural

and biochemical changes," *Biochimica et Biophysica Acta—Molecular Basis of Disease*, vol. 1138, no. 3, pp. 222–228, 1992.

[37] A. Elsheikh, B. Geraghty, P. Rama, M. Campanelli, and K. M. Meek, "Characterization of age-related variation in corneal biomechanical properties," *Journal of the Royal Society Interface*, vol. 7, no. 51, pp. 1475–1485, 2010.

[38] K. Kamiya, K. Shimizu, and F. Ohmoto, "Effect of aging on corneal biomechanical parameters using the ocular response analyzer," *Journal of Refractive Surgery*, vol. 25, no. 10, pp. 888–893, 2009.

[39] D. Ortiz, D. Piñero, M. H. Shabayek, F. Arnalich-Montiel, and J. L. Alió, "Corneal biomechanical properties in normal, post-laser in situ keratomileusis, and keratoconic eyes," *Journal of Cataract and Refractive Surgery*, vol. 33, no. 8, pp. 1371–1375, 2007.

[40] M. A. del Buey, L. Lavilla, F. J. Ascaso, E. Lanchares, V. Huerva, and J. A. Cristóbal, "Assessment of corneal biomechanical properties and intraocular pressure in myopic Spanish healthy population," *Journal of Ophthalmology*, vol. 2014, Article ID 905129, 6 pages, 2014.

[41] A. Kotecha, D. P. Crabb, A. Spratt, and D. F. Garway-Heath, "The relationship between diurnal variations in intraocular pressure measurements and central corneal thickness and corneal hysteresis," *Investigative Ophthalmology & Visual Science*, vol. 50, no. 9, pp. 4229–4236, 2009.

Hindawi Publishing Corporation
Journal of Ophthalmology
Volume 2015, Article ID 864871, 7 pages
http://dx.doi.org/10.1155/2015/864871

Review Article

Ocular Blood Flow Autoregulation Mechanisms and Methods

Xue Luo, Yu-meng Shen, Meng-nan Jiang, Xiang-feng Lou, and Yin Shen

Eye Center, Renmin Hospital of Wuhan University, Wuhan University, Wuhan, Hubei 430060, China

Correspondence should be addressed to Yin Shen; yinshen@whu.edu.cn

Received 14 June 2015; Accepted 14 September 2015

Academic Editor: Jun Zhang

Copyright © 2015 Xue Luo et al. This is an open access article distributed under the Creative Commons Attribution License, which permits unrestricted use, distribution, and reproduction in any medium, provided the original work is properly cited.

The main function of ocular blood flow is to supply sufficient oxygen and nutrients to the eye. Local blood vessels resistance regulates overall blood distribution to the eye and can vary rapidly over time depending on ocular need. Under normal conditions, the relation between blood flow and perfusion pressure in the eye is autoregulated. Basically, autoregulation is a capacity to maintain a relatively constant level of blood flow in the presence of changes in ocular perfusion pressure and varied metabolic demand. In addition, ocular blood flow dysregulation has been demonstrated as an independent risk factor to many ocular diseases. For instance, ocular perfusion pressure plays key role in the progression of retinopathy such as glaucoma and diabetic retinopathy. In this review, different direct and indirect techniques to measure ocular blood flow and the effect of myogenic and neurogenic mechanisms on ocular blood flow are discussed. Moreover, ocular blood flow regulation in ocular disease will be described.

1. Introduction

Ocular blood flow regulation compensates for changes in ocular activity, keeping the relative constant ocular temperature and retinal perfusion pressure [1]. Recently, there have been dramatic advances in understanding ocular blood flow (OBF) physiology [2]. Autoregulation of blood flow adjustment can be classified into two types static and dynamic according to responding rate [3]. Static autoregulation involves several diverse factors, including myogenic, neurogenic, and metabolic factors [2, 4, 5]; dynamic autoregulation is an instantaneous process facing up sudden variation in perfusion pressure. Dynamic autoregulation of outer ocular vascular system has been extensively studied and revealed a rich sympathetic innervation in the outer ocular vessels [6–8]. In this review, we will review the techniques for ocular blood flow evaluating and focus on the association between autoregulation of blood flow summarizing present knowledge of autoregulatory processes in the regulation of ocular blood flow and its relevance for ocular disease. More importantly, the need for a comprehensive understanding of the mechanisms regulating retinal blood flow is required to gain further insight into the pathophysiology of ocular disease [9].

2. Ocular Blood Flow and Anatomy

The retina receives its nutrients from both choroidal and retinal blood flow. Researchers characterize retinal blood flow as a high level of oxygen extraction and a low level of blood flow. The choroidal vascular beds supply nutrition to the optic nerve [10]. The interplay among them may be essential for maintaining a healthy optic nerve [4].

The physiology and anatomy of the retinal circulation appear like the brain circulation; meanwhile the retinal circulation does not have autonomic innervation. The presence of endothelial tight junctions results in a blood-retinal barrier, resembling the blood-brain barrier. Large studies indicate that autoregulation may be less effective to the retina but better to the choroid [11–14]. Optimal visual function needs an appropriately regulated environment. As reported, epithelia and vascular endothelium as dynamic structures identify this regulation. These structures quickly respond to changing physiological needs and extrinsic conditions.

Many studies have demonstrated that efficient autoregulation of ocular blood flow in the ocular nerve head (ONH) is potential taken by increasing capacitance of blood vessels. The changing magnitude of the reactive increased vascular

capacitance compensates the decrease of ocular nerve head vascular resistance with intraocular pressure increasing [13].

3. Techniques for Ocular Blood Flow Evaluating

As large methods have been described in previous research, no single vascular indicator can completely evaluate ocular blood flow [15, 16]. Every technique measures its specific aspects of ocular circulation, each with different limitations but providing a view of ocular hemodynamics [14]: pulsatile ocular blood flow, a possible indication of choroidal blood flow [17, 18]; color Doppler imaging (CDI), a widely used assessment to evaluate retrobulbar vascular circulation [19]; scanning laser Doppler flowmeter, for quantifying superficial layers of ONH and retinal vascular circulation [19, 20]; and optical coherence tomography (OCT), for detecting noninvasive vascular mapping at the microcirculation level.

3.1. Color Doppler Imaging. CDI has been widely used to investigate retrobulbar vascular parameters including blood velocity, pulsatility index, and resistive index, in both health and disease [9]. But CDI technology has its own major limitation. CDI quantifies the vascular velocity rather than vessel diameter [21]. However, the consistent correlation between blood flow and vascular velocity has been identified; moreover, the measurements of blood flow are viewed to be reproducible [19, 22]. CDI may be particularly useful in cases with media opacities.

3.2. Doppler Fourier Domain Optical Coherence Tomography (Doppler FD-OCT). One of the main advantages of the technique over the existing methods of measuring retinal blood flow is its ability to rapidly provide the total retinal blood flow (TRBF) by summing all measures around the optic nerve head, thereby assessing the whole retinal blood flow rather than a single point within the retinal vascular tree [23]. There are also still some limitations to the double circular scanning method that need to be addressed in the future development of the technique. These include complete elimination of eye motion, which can resolve possible errors in Doppler angle measurement, and full automation of the software for objective and reliable delineation and detection of vessel area [9].

3.3. Angiography. Fluorescein angiography is the gold standard for *in vivo* evaluation of retinal circulation. It provides useful qualitative information [24]; however, it has its advantage on investigating the superficial ocular nerve head vascular and its limitation on deep ocular nerve head circulation [25]. Although the passage time of fluorescent dyes through ocular vessels may not be highly correlated with OBF, it gives useful information on ocular perfusion [26].

3.4. Split-Spectrum Amplitude-Decorrelation Angiography-(SSADA-) OCT. Very recently, using ultrahigh-speed OCT, researchers developed a new method using 3D angiography algorithm to image ophthalmic microcirculation, which is called split-spectrum amplitude-decorrelation angiography (SSADA) [27]. OCT angiography generated by the latest SSADA measures optic disc perfusion and may be helpful in the evaluation of OBF [28]. The major limitation associated with OCT angiography is that SSADA-OCT only yields a flow index in arbitrary units instead of absolute volumetric flow. Although various methods can be capable of evaluating ophthalmic hemodynamics, like Heidelberg Retinal Flowmeter (HRF) and Laser Doppler Flowmetry (LDF), the direct evaluation of microcirculation is the most promising method in need [29].

4. Mechanism and Modulation of Ocular Blood Flow Regulation

Ocular blood flow autoregulation is known to fit well with changes in OPP, assembling other human organs and tissues. Autoregulation keeps blood flow relatively constant, only increasing blow flow in response to metabolic demands in the eye. However, defective autoregulation may exert its important role in the pathophysiology of ophthalmic vascular diseases [30].

The common method that clinicians use to assess autoregulation ability is artificially elevating or decreasing OPP in accordance with different results of blood flow evaluation. The classic curve of autoregulation describes the relation that the blood flow changes are followed by OPP changes within a certain range [30, 31]. In contrast to the clinic, autoregulation capacity in the eyes of both experimental animals and humans is measured by a "two-point" BF assessment. If blood flow deviates dramatically in response to pressure changes, therefore we can consider autoregulation impaired [32–37].

As discussed above, autoregulation is classified into two types to adjust blood flow changes, namely, static and dynamic. During and after a perturbation, static autoregulation system requires several minutes to induce a new steady balance of blood flow; on the other hand, the dynamic autoregulatory responses occur within 5 s [2, 5]. Various factors, including metabolic, myogenic, and neurogenic factors, are involved in static autoregulation within longer time to regulate the blood flow. On the other hand, factors that are involved in dynamic autoregulation, an instantaneous reaction to sudden changes in perfusion pressure, are found to be quite contractive [38].

Different from choroidal circulation, there is no neuronal innervation in retinal vascular beds. Retinal and ONH blood flow are mainly in the regulation of local mechanisms. Beside myogenic factor, endothelial cells take part in local regulation [39–43]. The mediators of these mechanisms include oxygen, carbon dioxide, angiotensin-II, adenosine, nitric oxide (NO), and endothelin-1 [44]. Among these factors, the role of angiotensin-II and endothelin-1 in regulating the blood flow of retina and ONH is disputable. Due to exclusion by the blood-retinal barrier, circulating hormones like angiotensin-II and endothelin-1 cannot directly be transported to smooth-muscle cells and therefore do not participate in retinal blood flow regulation in healthy persons. But they could diffuse

from choroid into retinal tissue in the incomplete blood-retina barrier.

However, sympathetic innervation plays an important role in choroidal blood flow regulation. Recent research revealed that the choroid mainly controlled by the sympathetic nervous system and metabolic factors [45, 46] can be autoregulated in response to an increase or decrease in OPP.

4.1. Endothelin-1 (ET-1). Endothelin-1 is mostly secreted by the endothelial cell, as the potent vasoconstrictor has been found to affect vascular endothelium and pericyte interactions within the ophthalmologic microcirculation [47]. As reported, in healthy humans, ET-1 affects the regulation of ophthalmologic posterior parts, especially choroidal blood flow regulation [48]. ET-1 has two types of binding sites, ET_A receptor and ET_B receptor, reducing ocular blood flow and mediating preferably binds to the ET_A receptor expressed on vascular smooth-muscle cells mediating vasodilatation by releasing prostacyclin and NO, respectively. Increased ET-1 concentration has been observed in the aqueous humor of glaucoma patients [49]. Moreover, the increased ET-1 levels elevate IOP, inducing decreased ocular blood flow and astrocyte proliferation and therefore may cause the degeneration of retinal ganglion cell in the end [50]. Thus, ET-1, as a major risk factor, exerts function in the process of retinal disease, such as glaucoma and diabetic retinopathy. Because of ET receptor antagonist reducing the retinal blood flow, endothelin antagonism is considered as a promising therapy for glaucoma [51]. In recent decades, calcium channel blockers (CCBs) have been commonly available to improve BF regulation and reduce the vasoconstrictive effect of endothelin-1 [52]. The effect of CCB on OBF has been investigated in numerous studies. But not all studies investigating CCBs indicate an impact on ocular blood flow.

4.2. Nitric Oxide. Nitric oxide (NO) plays a potential role in vascular diastole and protecting vascular endothelial cells from the risk of glaucoma and diabetic retinopathy [53, 54]. Nitric oxide synthase (NOS) is divided into three isoforms to perform dichotomous function, including endothelial nitric oxide synthase (eNOS), neural nitric oxide synthase (nNOS), and inducible nitric oxide synthase (iNOS). Only in allergic or inflammatory conditions is iNOS expressed, while eNOS and nNOS are constitutively expressed in the retina and the choroid. NOS influences both pathological and physiological processes of the eye and regulates ocular blood flow and intraocular pressure (IOP) [54]. Impaired NOS signaling is induced by vascular dysfunction in POAG and diabetic retinopathy [55].

4.3. Estrogen. Estrogens appear to be neuroprotective and also have been shown to improve retrobulbar circulation; recent research indicates significantly improved retinal blood flow and reduced risk for developing glaucoma in postmenopausal women with hormone replacement therapy [44, 56].

4.4. Diurnal Variations. Recently, there is evidence supporting the function of diurnal rhythm in the ophthalmologic blood flow regulation. Compared with retinal and ONH blood flow, diurnal variation of choroidal circulation was more easily affected by systemic environment changes [57]. To our knowledge, the relation between IOP and diurnal variations has been investigated for a long time.

4.5. Adenosine. In healthy humans, there is sufficient evidence that adenosine has been demonstrated to have effect on retinal vasodilatation and modulating IOP [58]. Acting through adenosine A1, A2, and A3 receptors, adenosine has been proposed for stimulating adenylyl cyclase and subsequently regulating the activation of different ion channels such as reducing calcium influx or activating chloride channel [59]. Intravenous administration of adenosine analogs was applied in clinical trials to regulate blood flow [60].

4.6. Carbonic Anhydrase. Carbonic anhydrase especially CAII has been considered as an important factor in retinopathy. Inhibition of this enzyme is thought to reduce IOP by increasing aqueous outflow. Carbonic anhydrase inhibitors (CAIs) have been shown to have a positive effect on ocular blood flow and are utilized to reduce IOP in patients with OAG [61].

4.7. Myogenic Mechanisms. There is disputable evidence on myogenic autoregulation. Most studies predict that myogenic mechanisms do not have significant effect on ocular blood flow autoregulation. Stretching of the vessel wall leads to activating calcium channels resulting in an increase of calcium influx and vascular constriction. With elevating perfusion pressure, inherent responsive vasoconstriction is thought to rapidly adapt to blood flow changes [62].

5. Impaired Autoregulation of Ocular Blood Flow in Ocular Diseases

5.1. Open-Angle Glaucoma. Glaucoma is a progressive optic nerve disease with characteristic changes in the structure of the optic nerve and vision loss. Vascular regulatory plays an important role in the progression of retinopathy such as OAG and DR [63]. There is sufficient evidence indicating a correlation of blood pressure with either ocular vascular diameter or blood velocity in patients with ocular hypertension and OAG, rather than in health, demonstrating impaired autoregulation in OAG [64]. But autoregulation of ocular blood flow is difficult to assess, and clear criteria to classify the status of autoregulation as dysfunctional or functional remain scarce. On the other hand, the majority of studies have demonstrated that individuals with progressive glaucoma have lower blood flow parameters than individuals with stable vision loss; therefore the reduced blood velocity is a risk factor for the progression of OAG [65]. In particular, the disturbed perfusion system, or vascular dysregulation to compensate the blood flow requirement or to fluctuate in perfusion pressure, may result in chronic changes or low ocular perfusion. Many researchers discover the signs of

reduced ocular perfusion in the early and advanced diagnosis of OAG. Fluctuant ocular perfusion, in turn, may cause oxidative stress reaction and ischemic damage, potentially resulting in glaucomatous damage at ONH.

There is evidence indicating that autoregulation is disturbed in glaucoma, resulting in the retinal vascular parameters response to OPP changes to be more passive, elevating to the higher level when the OPP rises or reducing to the lower level if the OPP drops [8, 52, 66–70]. By using CDI, OAG is characterized by damage of retinal nerve fiber layer (RNFL) reduction of vascular circulation and changes of blood rheology [71], while there is debatable evidence that impaired autoregulation of ocular nerve head blood flow has been found in patients with OAG [37, 72].

A lack of autoregulation, a vasospastic reaction to stimuli such as psychological stress or cold, has been considered as a possible contributing factor to OAG [73], particularly without associated IOP [74]. Moreover, the variation range of intraocular pressure before treatment is crucial in observing how effectively this vascular factor is regulated in glaucoma patients [75]. The mentioned therapies in the review, including β-blockers and carbonic anhydrase inhibitor, are most commonly used to lower IOP and subsequently prevent optic nerve damage and progression of the disease.

5.2. Diabetic Retinopathy. Retinopathy is a common complication of diabetes mellitus and one of the leading causes of irreversible blindness in the developed world. In the early stage of diabetic, retinal integral network could successfully adapt to the systemic metabolic changes. But when it progresses, oxygen and nutrient requirements of the retina may lead to eventual loss of ocular homeostasis. The specific characteristic structural changes of DR have focused on damage to the retinal vessels, no matter in nonproliferative diabetic retinopathy (NPDR) or proliferative diabetic retinopathy (PDR) [76]. All vascular lesions of DR include the appearance of microaneurysms, vascular nonperfusion, degeneration, and neovascular stage. However, the effect of ocular blood flow regulation on DR remains unclear. There are several disputable views of dysfunctional flood flow in the orbital vascular in diabetic retinopathy patients. To investigate the blood flow of DR, different vascular parameters were observed in recent studies [77]. As reported, compared with normal individuals, DR patients had a significantly higher resistivity index in the ophthalmic artery and central retinal vein and lower PSV and EDV of the posterior vascular [78]. However, there is conflicting evidence that different blood flow velocity changes were not consistent in different techniques and measurements. Recently antivascular endothelial growth factor (VEGF) is the most popular therapy to interfere with autoregulation of the choroidal and retinal microcirculation, resulting in reducing the progression of neovascularization and the incidence of blindness in patients with DR [79].

Perspective

In future studies, it is critical to develop the measurement of blood flow regulation and further study the effect of ocular blood flow regulation on the incidence and progression of glaucoma and diabetic retinopathy. If relevance to this retinopathy risk or development can be established, the clinical implications for patient management should be considered, particularly for individuals with disturbed ocular vascular circulation [80]. Looking forward, more study of OBF needs to be focused on in the future. The development and up-to-state technology to measure OBF are more precise; we also need more direct data on blood flow in specific tissues of the eye [14].

Conflict of Interests

Xue Luo, Yu-meng Shen, Meng-nan Jiang, Xiang-feng Lou, and Yin Shen, authors of the paper referenced above, declare that there is no conflict of interests regarding the publication of this paper.

Acknowledgment

This work was supported by the National Natural Science Foundation of China (NSFC) (nos. 81270998 and 81470628).

References

[1] J. Flammer and M. Mozaffarieh, "Autoregulation, a balancing act between supply and demand," *Canadian Journal of Ophthalmology*, vol. 43, no. 3, pp. 317–321, 2008.

[2] D. Schmidl, G. Garhofer, and L. Schmetterer, "The complex interaction between ocular perfusion pressure and ocular blood flow—relevance for glaucoma," *Experimental Eye Research*, vol. 93, no. 2, pp. 141–155, 2011.

[3] T. P. Doczi, A. Lam, D. W. Newell, and F. Tiecks, "Comparison of static and dynamic cerebral autoregulation measurements," *Stroke*, vol. 26, no. 12, pp. 2372–2373, 1995.

[4] C. Delaey and J. Van De Voorde, "Regulatory mechanisms in the retinal and choroidal circulation," *Ophthalmic Research*, vol. 32, no. 6, pp. 249–256, 2000.

[5] M. Iester, P. G. Torre, G. Bricola, A. Bagnis, and G. Calabria, "Retinal blood flow autoregulation after dynamic exercise in healthy young subjects," *Ophthalmologica*, vol. 221, no. 3, pp. 180–185, 2007.

[6] J. Kolodjaschna, F. Berisha, S. Lung, H. Schima, E. Polska, and L. Schmetterer, "Comparison of the autoregulatory mechanisms between middle cerebral artery and ophthalmic artery after thigh cuff deflation in healthy subjects," *Investigative Ophthalmology & Visual Science*, vol. 46, no. 2, pp. 636–640, 2005.

[7] S. Kaya, J. Kolodjaschna, F. Berisha, L. Schmetterer, and G. Garhöfer, "Comparison of the autoregulatory mechanisms between central retinal artery and posterior ciliary arteries after thigh cuff deflation in healthy subjects," *Microvascular Research*, vol. 82, no. 3, pp. 269–273, 2011.

[8] A. Alm and A. Bill, "Ocular and optic nerve blood flow at normal and increased intraocular pressures in monkeys (*Macaca irus*): a study with radioactively labelled microspheres including flow determinations in brain and some other tissues," *Experimental Eye Research*, vol. 15, no. 1, pp. 15–29, 1973.

[9] A. M. Shahidi, S. R. Patel, D. Huang, O. Tan, J. G. Flanagan, and C. Hudson, "Assessment of total retinal blood flow using Doppler Fourier Domain Optical Coherence Tomography

during systemic hypercapnia and hypocapnia," *Physiological Reports*, vol. 2, no. 7, Article ID e12046, 2014.

[10] D. J. Spalton, "Microvasculature of the human optic nerve," *American Journal of Ohthalmology*, vol. 121, no. 4, pp. 452–453, 1996.

[11] C. J. Pournaras and C. E. Riva, "Studies of the hemodynamics of the optic head nerve using laser Doppler flowmetry," *Journal Francais d'Ophtalmologie*, vol. 24, no. 2, pp. 199–205, 2001.

[12] A. Movaffaghy, S. R. Chamot, B. L. Petrig, and C. E. Riva, "Blood flow in the human optic nerve head during isometric exercise," *Experimental Eye Research*, vol. 67, no. 5, pp. 561–568, 1998.

[13] C. E. Riva, M. Hero, P. Titze, and B. Petrig, "Autoregulation of human optic nerve head blood flow in response to acute changes in ocular perfusion pressure," *Graefe's Archive for Clinical and Experimental Ophthalmology*, vol. 235, no. 10, pp. 618–626, 1997.

[14] J. Flammer, S. Orgül, V. P. Costa et al., "The impact of ocular blood flow in glaucoma," *Progress in Retinal and Eye Research*, vol. 21, no. 4, pp. 359–393, 2002.

[15] Y. Shiose, Y. Kitazawa, S. Tsukahara et al., "Epidemiology of glaucoma in Japan—a nationwide glaucoma survey," *Japanese Journal of Ophthalmology*, vol. 35, no. 2, pp. 133–155, 1991.

[16] J. Flammer and S. Orgül, "Optic nerve blood-flow abnormalities in glaucoma," *Progress in Retinal and Eye Research*, vol. 17, no. 2, pp. 267–289, 1998.

[17] M. E. Langham, R. A. Farrell, V. O'Brien, D. M. Silver, and P. Schilder, "Blood flow in the human eye," *Acta Ophthalmologica. Supplement*, vol. 191, pp. 9–13, 1989.

[18] G. Pekel, S. Acer, E. N. Çetin, R. Yağcı, A. Kaşikçi, and A. Çevik, "Ocular pulse amplitude and retinal vessel caliber changes after intravitreal ranibizumab," *International Ophthalmology*, vol. 35, no. 5, pp. 657–662, 2015.

[19] E. T. Matthiessen, O. Zeitz, G. Richard, and M. Klemm, "Reproducibility of blood flow velocity measurements using colour decoded Doppler imaging," *Eye*, vol. 18, no. 4, pp. 400–405, 2004.

[20] M. Sehi, "Basic technique and anatomically imposed limitations of confocal scanning laser Doppler flowmetry at the optic nerve head level," *Acta Ophthalmologica*, vol. 89, no. 1, pp. e1–e11, 2011.

[21] E. Polska, K. Kircher, P. Ehrlich, P. V. Vecsei, and L. Schmetterer, "RI in central retinal artery as assessed by CDI does not correspond to retinal vascular resistance," *The American Journal of Physiology: Heart and Circulatory Physiology*, vol. 280, no. 4, pp. H1442–H1447, 2001.

[22] G. Michelson, B. Schmauss, M. J. Langhans, J. Harazny, and M. J. Groh, "Principle, validity, and reliability of scanning laser Doppler flowmetry," *Journal of Glaucoma*, vol. 5, no. 2, pp. 99–105, 1996.

[23] S. Srinivas, O. Tan, S. Wu et al., "Measurement of retinal blood flow in normal chinese-american subjects by Doppler fourier-domain optical coherence tomography," *Investigative Ophthalmology & Visual Science*, vol. 56, no. 3, pp. 1569–1574, 2015.

[24] J. Francois and J. J. de Laey, "Fluorescein angiography of the glaucomatous disc," *Ophthalmologica*, vol. 168, no. 4, pp. 288–298, 1974.

[25] S. S. Hayreh, "Colour and fluorescence of the optic disc," *Ophthalmologica*, vol. 165, no. 2, pp. 100–108, 1972.

[26] L. Tomic, O. Mäepea, G. O. Sperber, and A. Alm, "Comparison of retinal transit times and retinal blood flow: a study in monkeys," *Investigative Ophthalmology and Visual Science*, vol. 42, no. 3, pp. 752–755, 2001.

[27] Y. Jia, J. C. Morrison, J. Tokayer et al., "Quantitative OCT angiography of optic nerve head blood flow," *Biomedical Optics Express*, vol. 3, no. 12, pp. 3127–3137, 2012.

[28] Y. Jia, E. Wei, X. Wang et al., "Optical coherence tomography angiography of optic disc perfusion in glaucoma," *Ophthalmology*, vol. 121, no. 7, pp. 1322–1332, 2014.

[29] L. E. Pillunat, "Ocular blood flow endpoints," *European Journal of Ophthalmology*, vol. 9, supplement 1, pp. S44–S47, 1999.

[30] A. S. Hafez, R. L. G. Bizzarro, M. Rivard, and M. R. Lesk, "Changes in optic nerve head blood flow after therapeutic intraocular pressure reduction in glaucoma patients and ocular hypertensives," *Ophthalmology*, vol. 110, no. 1, pp. 201–210, 2003.

[31] S. S. Hayreh, "Factors influencing blood flow in the optic nerve head," *Journal of Glaucoma*, vol. 6, no. 6, pp. 412–425, 1997.

[32] A. Bill, "Blood circulation and fluid dynamics in the eye," *Physiological Reviews*, vol. 55, no. 3, pp. 383–417, 1975.

[33] G. T. Feke and L. R. Pasquale, "Retinal blood flow response to posture change in glaucoma patients compared with healthy subjects," *Ophthalmology*, vol. 115, no. 2, pp. 246–252, 2008.

[34] G. Michelson, M. J. Groh, and M. Langhans, "Perfusion of the juxtapapillary retina and optic nerve head in acute ocular hypertension," *German Journal of Ophthalmology*, vol. 5, no. 6, pp. 315–321, 1996.

[35] L. E. Pillunat, R. Stodtmeister, I. Wilmanns, and T. Christ, "Autoregulation of ocular blood flow during changes in intraocular pressure. Preliminary results," *Graefe's Archive for Clinical and Experimental Ophthalmology*, vol. 223, no. 4, pp. 219–223, 1985.

[36] M. Best, D. Gerstein, N. Wlad, A. Z. Rabinovitz, and G. H. Hiller, "Autoregulation of ocular blood flow," *Archives of Ophthalmology*, vol. 89, no. 2, pp. 143–148, 1973.

[37] G. Weigert, O. Findl, A. Luksch et al., "Effects of moderate changes in intraocular pressure on ocular hemodynamics in patients with primary open-angle glaucoma and healthy controls," *Ophthalmology*, vol. 112, no. 8, pp. 1337–1342, 2005.

[38] Y. Liang, B. Fortune, G. Cull, G. A. Cioffi, and L. Wang, "Quantification of dynamic blood flow autoregulation in optic nerve head of rhesus monkeys," *Experimental Eye Research*, vol. 90, no. 2, pp. 203–209, 2010.

[39] S. Orgül, K. Gugleta, and J. Flammer, "Physiology of perfusion as it relates to the optic nerve head," *Survey of Ophthalmology*, vol. 43, supplement 1, pp. S17–S26, 1999.

[40] I. O. Haefliger, P. Meyer, J. Flammer, and T. F. Lüscher, "The vascular endothelium as a regulator of the ocular circulation: a new concept in ophthalmology?" *Survey of Ophthalmology*, vol. 39, no. 2, pp. 123–132, 1994.

[41] P. Meyer, J. Flammer, and T. F. Luscher, "Local action of the renin angiotensin system in the porcine ophthalmic circulation: effects of ACE-inhibitors and angiotensin receptor antagonists," *Investigative Ophthalmology and Visual Science*, vol. 36, no. 3, pp. 555–562, 1995.

[42] P. Meyer, J. Flammer, and T. F. Luscher, "Endothelium-dependent regulation of the ophthalmic microcirculation in the perfused porcine eye: role of nitric oxide and endothelins," *Investigative Ophthalmology and Visual Science*, vol. 34, no. 13, pp. 3614–3621, 1993.

[43] I. O. Haefliger, J. Flammer, and T. F. Luscher, "Nitric oxide and endothelin-1 are important regulators of human ophthalmic artery," *Investigative Ophthalmology & Visual Science*, vol. 33, no. 7, pp. 2340–2343, 1992.

[44] M. R. Lesk, M. Wajszilber, and M. C. Deschenes, "The effects of systemic medications on ocular blood flow," *Canadian Journal of Ophthalmology*, vol. 43, no. 3, pp. 351–355, 2008.

[45] P.-I. Chou, D.-W. Lu, and J.-T. Chen, "Bilateral superior cervical ganglionectomy increases choroidal blood flow in the rabbit," *Ophthalmologica*, vol. 214, no. 6, pp. 421–425, 2000.

[46] J. J. Steinle, D. Krizsan-Agbas, and P. G. Smith, "Regional regulation of choroidal blood flow by autonomic innervation in the rat," *The American Journal of Physiology: Regulatory Integrative and Comparative Physiology*, vol. 279, no. 1, pp. R202–R209, 2000.

[47] G. Fuchsjäger-Mayrl, A. Luksch, M. Malec, E. Polska, M. Wolzt, and L. Schmetterer, "Role of endothelin-1 in choroidal blood flow regulation during isometric exercise in healthy humans," *Investigative Ophthalmology and Visual Science*, vol. 44, no. 2, pp. 728–733, 2003.

[48] G. Fuchsjäger-Mayrl, A. Luksch, M. Malec, E. Polska, M. Wolzt, and L. Schmetterer, "Role of endothelin-1 in choroidal blood flow regulation during isometric exercise in healthy humans," *Investigative Ophthalmology & Visual Science*, vol. 44, no. 2, pp. 728–733, 2003.

[49] M. E. Källberg, D. E. Brooks, K. N. Gelatt, G. A. Garcia-Sanchez, N. J. Szabo, and G. N. Lambrou, "Endothelin-1, nitric oxide, and glutamate in the normal and glaucomatous dog eye," *Veterinary Ophthalmology*, vol. 10, supplement 1, pp. 46–52, 2007.

[50] L. Wang, B. Fortune, G. Cull, J. Dong, and G. A. Cioffi, "Endothelin B receptor in human glaucoma and experimentally induced optic nerve damage," *Archives of Ophthalmology*, vol. 124, no. 5, pp. 717–724, 2006.

[51] K. Polak, V. Petternel, A. Luksch et al., "Effect of endothelin and BQ123 on ocular blood flow parameters in healthy subjects," *Investigative Ophthalmology and Visual Science*, vol. 42, no. 12, pp. 2949–2956, 2001.

[52] J. Flammer, K. Konieczka, and A. J. Flammer, "The primary vascular dysregulation syndrome: implications for eye diseases," *The EPMA Journal*, vol. 4, no. 1, article 14, 2013.

[53] Y. Delaney, T. E. Walshe, and C. O'Brien, "Vasospasm in glaucoma: clinical and laboratory aspects," *Optometry and Vision Science*, vol. 83, no. 7, pp. 406–414, 2006.

[54] Y. Shoshani, A. Harris, M. M. Shoja et al., "Impaired ocular blood flow regulation in patients with open-angle glaucoma and diabetes," *Clinical and Experimental Ophthalmology*, vol. 40, no. 7, pp. 697–705, 2012.

[55] J. Weiss, S. A. Fränkl, J. Flammer et al., "No difference in genotype frequencies of polymorphisms of the nitric oxide pathway between Caucasian normal and high tension glaucoma patients," *Molecular Vision*, vol. 18, pp. 2174–2181, 2012.

[56] D. Schmidl, L. Schmetterer, G. Garhöfer, and A. Popa-Cherecheanu, "Gender differences in ocular blood flow," *Current Eye Research*, vol. 40, no. 2, pp. 201–212, 2015.

[57] T. Iwase, K. Yamamoto, E. Ra, K. Murotani, S. Matsui, and H. Terasaki, "Diurnal variations in blood flow at optic nerve head and choroid in healthy eyes: diurnal variations in blood flow," *Medicine*, vol. 94, no. 6, article e519, 2015.

[58] E. Polska, P. Ehrlich, A. Luksch, G. Fuchsjäger-Mayrl, and L. Schmetterer, "Effects of adenosine on intraocular pressure, optic nerve head blood flow, and choroidal blood flow in healthy humans," *Investigative Ophthalmology and Visual Science*, vol. 44, no. 7, pp. 3110–3114, 2003.

[59] E. Polska, A. Luksch, J. Schering et al., "Propranolol and atropine do not alter choroidal blood flow regulation during isometric exercise in healthy humans," *Microvascular Research*, vol. 65, no. 1, pp. 39–44, 2003.

[60] M. Portellos, C. E. Riva, S. D. Cranstoun, B. L. Petrig, and A. J. Brucker, "Effects of adenosine on ocular blood flow," *Investigative Ophthalmology and Visual Science*, vol. 36, no. 9, pp. 1904–1909, 1995.

[61] B. Siesky, A. Harris, E. Brizendine et al., "Literature review and meta-analysis of topical carbonic anhydrase inhibitors and ocular blood flow," *Survey of Ophthalmology*, vol. 54, no. 1, pp. 33–46, 2009.

[62] J. W. Kiel, "Choroidal myogenic autoregulation and intraocular pressure," *Experimental Eye Research*, vol. 58, no. 5, pp. 529–543, 1994.

[63] M. C. Leske, A. Heijl, L. Hyman, B. Bengtsson, L. Dong, and Z. Yang, "Predictors of long-term progression in the early manifest glaucoma trial," *Ophthalmology*, vol. 114, no. 11, pp. 1965–1972, 2007.

[64] G. Fuchsjäger-Mayrl, B. Wally, M. Georgopoulos et al., "Ocular blood flow and systemic blood pressure in patients with primary open-angle glaucoma and ocular hypertension," *Investigative Ophthalmology and Visual Science*, vol. 45, no. 3, pp. 834–839, 2004.

[65] G. Garhöfer, G. Fuchsjäger-Mayrl, C. Vass, B. Pemp, A. Hommer, and L. Schmetterer, "Retrobulbar blood flow velocities in open angle glaucoma and their association with mean arterial blood pressure," *Investigative Ophthalmology and Visual Science*, vol. 51, no. 12, pp. 6652–6657, 2010.

[66] J. Caprioli and T. Zeyen, "A critical discussion of the rates of progression and causes of optic nerve damage in glaucoma: international glaucoma think tank II: July 25-26, 2008, Florence, Italy," *Journal of Glaucoma*, vol. 18, no. 6, supplement, pp. S1–S21, 2009.

[67] L. Wagenfeld, S. Weiss, M. Klemm, G. Richard, and O. Zeitz, "Vascular dysfunction in ocular blood flow regulation: impact of reactive oxygen species in an experimental setup," *Investigative Ophthalmology & Visual Science*, vol. 55, no. 9, pp. 5531–5536, 2014.

[68] Y. C. Chin, S. A. Perera, T. A. Tun et al., "Structural differences in the optic nerve head of glaucoma patients with and without disc hemorrhages," *Journal of Glaucoma*, 2015.

[69] D. R. Anderson, "Introductory comments on blood flow autoregulation in the optic nerve head and vascular risk factors in glaucoma," *Survey of Ophthalmology*, vol. 43, supplement 1, pp. S5–S9, 1999.

[70] M. C. Grieshaber, M. Mozaffarieh, and J. Flammer, "What is the link between vascular dysregulation and glaucoma?" *Survey of Ophthalmology*, vol. 52, supplement 2, pp. S144–S154, 2007.

[71] I. Januleviciene, I. Sliesoraityte, B. Siesky, and A. Harris, "Diagnostic compatibility of structural and haemodynamic parameters in open-angle glaucoma patients," *Acta Ophthalmologica*, vol. 86, no. 5, pp. 552–557, 2008.

[72] C. J. Pournaras, C. E. Riva, H. Bresson-Dumont, P. de Gottrau, and A. Bechetoille, "Regulation of optic nerve head blood flow in normal tension glaucoma patients," *European Journal of Ophthalmology*, vol. 14, no. 3, pp. 226–235, 2004.

[73] L. E. Pillunat, R. Stodtmeister, and I. Wilmanns, "Pressure compliance of the optic nerve head in low tension glaucoma," *British Journal of Ophthalmology*, vol. 71, no. 3, pp. 181–187, 1987.

[74] P. Gasser and J. Flammer, "Blood-cell velocity in the nailfold capillaries of patients with normal-tension and high-tension glaucoma," *American Journal of Ophthalmology*, vol. 111, no. 5, pp. 585–588, 1991.

[75] H. Ates, O. Uretmen, R. Killi, C. Akkin, and K. Andac, "Relationship between ocular perfusion pressure and retrobulbar blood flow in patients with glaucoma with progressive damage," *American Journal of Ophthalmology*, vol. 132, no. 4, pp. 598–599, 2001.

[76] T. S. Kern, J. Tang, and B. A. Berkowitz, "Validation of structural and functional lesions of diabetic retinopathy in mice," *Molecular Vision*, vol. 16, pp. 2121–2131, 2010.

[77] A. N. Kollias and M. W. Ulbig, "Diabetic retinopathy: early diagnosis and effective treatment," *Deutsches Ärzteblatt International*, vol. 107, no. 5, pp. 75–84, 2010.

[78] M. Karami, M. Janghorbani, A. Dehghani, K. Khaksar, and A. Kaviani, "Orbital Doppler evaluation of blood flow velocities in patients with diabetic retinopathy," *The Review of Diabetic Studies*, vol. 9, no. 2-3, pp. 104–111, 2012.

[79] T. T. Nguyen and R. Guymer, "Conbercept (KH-902) for the treatment of neovascular age-related macular degeneration," *Expert Review of Clinical Pharmacology*, vol. 8, no. 5, pp. 541–548, 2015.

[80] M. C. Leske, "Ocular perfusion pressure and glaucoma: clinical trial and epidemiologic findings," *Current Opinion in Ophthalmology*, vol. 20, no. 2, pp. 73–78, 2009.

Hindawi Publishing Corporation
Journal of Ophthalmology
Volume 2015, Article ID 161869, 8 pages
http://dx.doi.org/10.1155/2015/161869

Research Article

Corneal Biomechanical Properties in Myopic Eyes Measured by a Dynamic Scheimpflug Analyzer

Jingyi Wang, Ying Li, Yumei Jin, Xue Yang, Chan Zhao, and Qin Long

Department of Ophthalmology, Peking Union Medical College Hospital, Chinese Academy of Medical Sciences and Peking Union Medical College, Beijing 100730, China

Correspondence should be addressed to Qin Long; longqinbj@hotmail.com

Received 28 June 2015; Revised 22 August 2015; Accepted 9 September 2015

Academic Editor: Vishal Jhanji

Copyright © 2015 Jingyi Wang et al. This is an open access article distributed under the Creative Commons Attribution License, which permits unrestricted use, distribution, and reproduction in any medium, provided the original work is properly cited.

Purpose. To evaluate the corneal biomechanical parameters in myopic and emmetropic eyes using Corneal Visualization Scheimpflug Technology (CorVis ST). *Methods*. 103 myopic and emmetropic eyes of 103 patients were examined. Corneal biomechanical parameters, axial length, and mean keratometry were measured using CorVis ST, IOL Master, and topography, respectively. Corneal biomechanical properties were compared within four groups. Bivariate correlation analysis was used to assess the relationship between corneal biomechanical parameters and ocular characteristics. *Results*. Four of ten corneal biomechanical parameters, namely, deformation amplitude (DA), first- and second-applanation time (A1-time, A2-time), and radius at highest concavity (HC radius), were significantly different within the four groups ($P < 0.05$). In correlation analysis, DA was positively correlated with axial length ($r = 0.20$, $P = 0.04$); A2-time was positively correlated with spherical equivalent (SE) ($r = 0.24$, $P = 0.02$); HC radius was positively correlated with SE ($r = 0.24$, $P = 0.02$) and was negatively correlated with mean keratometry ($r = -0.20$, $P = 0.046$) and axial length ($r = -0.21$, $P = 0.03$). *Conclusions*. The corneal refraction-related biomechanical alterations were associated with ocular characteristics. Highly myopic eyes exhibited longer DA and smaller HC radius than do moderately myopic eyes; the eyes with longer axial length tend to have less corneal stiffness and are easier to deform under stress.

1. Introduction

Myopia is a most common ocular disorder and has become a global public health problem. Its worldwide prevalence is over 22% of the current world population and is rising dramatically yearly, reaching 80% in certain Asian countries [1, 2]. Several studies have revealed the correlation between the corneal biomechanical characteristics and myopic degree in children [3] and adult population [4]; nevertheless, the results are still lacking consistence in terms of the biomechanical parameters investigated [3–5]. Although axial length and corneal curvature have been shown to associate with refractive error, the relationship between the two parameters and corneal biomechanical behavior has not been clarified yet [3, 6, 7].

Although it is not an easy task to fulfill a precise evaluation of corneal biomechanical behavior, there are presently two clinical devices, the Ocular Response Analyzer (ORA) (Reichert, Buffalo, New York, USA) and Corneal Visualization Scheimpflug Technology (CorVis ST) (Oculus Optikgeräte GmbH, Wetzlar, Germany), which are commercially available for measuring the corneal biomechanical properties. Corneal hysteresis (CH) and corneal resistance factor (CRF) are the main biomechanical parameters for evaluating the corneal viscoelasticity [8]. Several studies have reported that CH was significantly lower in patients with high myopia, and a relationship between the refractive error and corneal biomechanical properties has also been addressed in adult Spanish and Caucasian population [4, 9]. However, this association failed to show in the study on Singaporean children [6]. CorVis ST is a recently developed noncontact tonometry system integrated with an ultra-high-speed Scheimpflug camera, with 4330 frames per second, which enables recording more biomechanical parameters in response to an air-jet induced deformation. Till now, CorVis ST has been used in the evaluation of healthy eyes [10] and several clinical conditions, such as glaucoma [11] and keratoconus [12, 13], and after refractive procedures [14, 15].

However, the evaluation of corneal biomechanical properties in myopic eyes measured by CorVis ST is limited.

Herein, the aims of this study are twofold: (1) to compare the corneal biomechanical parameters of patients with myopia and normal subjects by CorVis ST and (2) to assess the potential factors which can affect corneal biomechanical behavior, such as refractive error, corneal curvature, and axial length.

2. Methods

Unrelated Chinese patients with or without myopia were recruited from the Department of Ophthalmology, Peking Union Medical College Hospital. The study was performed according to the Declaration of Helsinki. Informed consent was obtained from all patients.

All subjects received a complete ophthalmic examination including measurement of best-corrected visual acuity (BCVA), axial length using IOL Master (Carl Zeiss Meditec AG, Jena, Germany), mean keratometry using Topographic Modeling System (TMS-4, TOMEY, Nagoya, Japan), slit-lamp anterior segment biomicroscopy, and fundus examination. Spherical equivalent (SE) was determined by 1 masked and experienced optometrist with noncycloplegic (age $\geq$ 40 years) or cycloplegic (age $<$ 40 years) refraction using the same Topcon Auto Kerato-Refractometer (KR-8900, Topcon Corporation, Tokyo, Japan). For cycloplegic measurements, 4 drops of Tropicamide Phenylephrine Eye Drops (Santen Pharmaceutical Co., Ltd., Japan) were instilled 10 minutes apart in each eye. The differences of sphere and cylinder value under autorefraction within 3 measurements less than 0.25 D were considered evidence of adequate cycloplegia. Autorefraction measurements were made at least 30 minutes after the last instillation. Subjects were divided into four groups according to their refractive status: Emmetropia group ($-0.50 \leq$ SE ≤ 0.50), Low myopia group ($-0.75 \leq$ SE ≤ -3.00 D), Moderate myopia group ($-3.25 \leq$ SE ≤ -6.00 D), and High myopia group (SE > -6.00 D).

Patients were excluded from the study if they had previous eye surgery, concurrent ocular infectious disease, ocular or systemic diseases (e.g., corneal scars, corneal dystrophy, corneal degradation, keratoconus, glaucoma, uveitis, systemic autoimmune diseases, and diabetes mellitus), or topical eye medication or were corticosteroid users; contact lens wearer and eyes with cylinder greater than 3.0 D were also excluded. Visual acuity was not an exclusion criterion in the current study.

Corneal biomechanical parameters were obtained using CorVis ST (Type 72100, Oculus Optikgeräte GmbH, Wetzlar, Germany) by the same investigator in every case to eliminate the possible interobserver variability. A high speed Scheimpflug camera (4330 frames/s) covering 8.0 mm horizontally was applied, which enabled recording 140 Scheimpflug images of the cornea during the deformation in response to a puff of air. Due to the air puff, the cornea underwent three distinct phases, first applanation, highest concavity, and second applanation, respectively (Figure 1). Ten phase-specific parameters generated automatically during the process were as follows: A1-time and A2-time (time from starting until the first and second applanation), A1-length and A2-length (length of the first and second applanation), A1-velocity (A1-V) and A2-velocity (A2-V) (corneal speed during the first- and second-applanation moment), highest concavity-time (HC-time) (time from starting until HC is reached), peak distance (PD) (distance between the two peaks of the cornea at HC), HC radius (central concave curvature at HC), and deformation amplitude (DA) (maximum amplitude at HC) [16]. Intraocular pressure (IOP) and central corneal thickness (CCT) were also obtained during one measurement procedure. CCT was determined by the illustrating snapshot obtained with CorVis ST; IOP was calculated based on the first applanation. To reduce the potential diurnal variations of measured parameters, all the measurements were fulfilled between 8:00 and 11:00 AM.

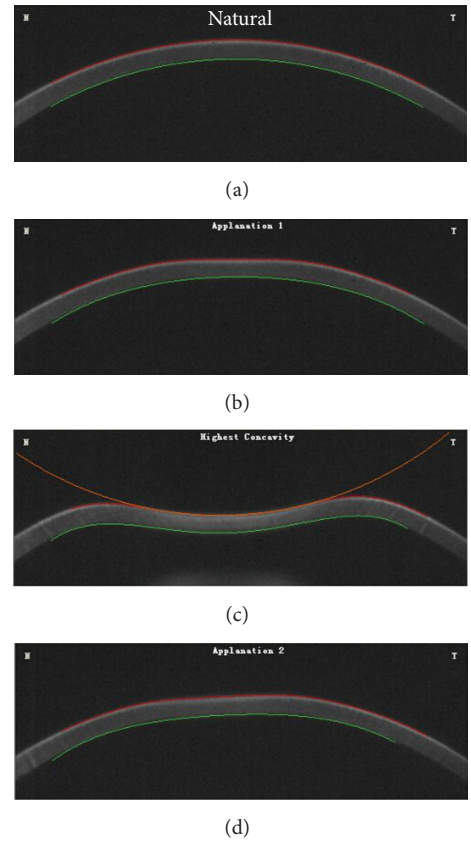

(a)
(b)
(c)
(d)

Figure 1: The corneal deformation processes during air puff from CorVis ST. Due to the air puff, the cornea starts with a natural convex shape and undergoes three distinct phases, first applanation, highest concavity, and second applanation, respectively.

3. Data Analysis

Data were analyzed using IBM SPSS 19.0 for Windows statistical software (SPSS, Chicago, IL) and GraphPad Prism 5 (GraphPad Software, Inc.). Numerical variables were presented as mean ± SD. Kolmogorov-Smirnov (K-S) test was used for testing normal distribution. One-way analysis of variance (ANOVA) and Tukey post hoc tests were used

Table 1: The demographic data of the study population.

Parameter	Emmetropia ($n = 21$)	Low myopia ($n = 21$)	Moderate myopia ($n = 28$)	High myopia ($n = 33$)	P value
Age (years)	34.00 ± 7.85	30.43 ± 6.43	29.54 ± 6.77	29.29 ± 6.97	0.09[a]
Sex (M/F)	17/4	13/8	23/5	24/9	0.37[b]
SE (D)	−0.07 ± 0.28	−1.71 ± 0.78	−4.41 ± 0.73	−8.98 ± 2.66	<0.001[a]
AL (mm)	23.21 ± 0.94	24.34 ± 1.08	25.28 ± 0.82	26.69 ± 1.27	<0.001[a]
MK (D)	43.85 ± 0.99	43.44 ± 1.23	43.40 ± 1.36	43.84 ± 1.02	0.32[a]

M: male; F: female; D: diopters; SE: spherical equivalent; AL: axial length; MK: mean keratometry.
[a]One-way analysis of variance.
[b]χ-test.
Significant differences in SE and AL were present among the four groups (post hoc test, $P < 0.05$).

for comparing the parameters of four groups. Pearson's correlation coefficient (r) was used to assess the relationship between corneal biomechanical parameters and age, IOP, CCT, SE, axial length, and mean keratometry; Spearman's correlation coefficient (rho) was utilized for determining the relationship between corneal biomechanical parameters and gender. The level of statistical significance was set to $P < 0.05$. Due to the significant correlation for the values between right and left eye, only one randomly selected eye from each subject was analyzed.

4. Results

A total of 103 eyes (103 patients) were included in this study. The SE of all included eyes ranged from 0 to −14.00 D. The Emmetropia group (21 eyes of 21 patients) included 17 female and 4 male patients, with a mean age of 34.00 years (range, 21 to 50 years), the Low myopia group (21 eyes of 21 patients) included 13 female and 8 male patients, with a mean age of 30.43 years (range, 21 to 45 years), the Moderate myopia group (28 eyes of 28 patients) included 23 female and 5 male patients, with a mean age of 29.54 years (range, 18 to 44 years), and finally the High myopia group (33 eyes of 33 patients) included 24 female and 9 male patients, with a mean age of 29.29 years (range, 18 to 44 years). Significant differences in SE and axial length were found within the four groups ($F = 160.1$, $P < 0.001$ and $F = 51.16$, $P < 0.001$, resp.). There were no differences within the four groups in terms of age ($F = 2.21$, $P = 0.09$), gender (Kruskal-Wallis test statistic = 3.116, $P = 0.37$), and mean keratometry ($F = 1.19$, $P = 0.32$) (Table 1).

Four of ten biomechanical parameters, which were deformation amplitude (DA), first- and second-applanation time (A1-time, A2-time), and radius at highest concavity (HC radius), were significantly different within the four groups. In post hoc tests, DA in the High myopia group was significantly higher than in the Moderate myopia group ($q = 3.86$, $P = 0.008$); A1-time in Moderate myopia group was significantly longer than in the Emmetropia group ($q = 3.99$, $P = 0.006$); A2-time of Moderate and High myopia group was significantly longer than that in the Emmetropia group ($q = 4.03$, $P = 0.005$ and $q = 4.04$, $P = 0.005$, resp.); HC radius was significantly smaller in the High myopia group than in the Moderate myopia group ($q = 6.65$, $P = 0.004$). No statistical significance was found within the four groups in terms of A1-length, A2-length, A1-velocity (A1-V), A2-velocity (A2-V), highest concavity-time (HC-time), and peak distance (PD) (all $P > 0.05$). Statistical comparisons for the four groups of the parameters obtained by CorVis ST are shown in Table 2 and Figure 2.

Bivariate correlation analysis was performed to investigate the correlations between the above four significantly different biomechanical parameters of the cornea with potential impact factors, such as age, gender, IOP, CCT, SE, axial length, and mean keratometry. In correlation analysis, DA was positively correlated with age ($r = 0.33$, $P < 0.001$) and axial length ($r = 0.20$, $P = 0.04$) (Figure 3(a)) and negatively correlated with CCT ($r = -0.35$, $P < 0.001$) and IOP ($r = -0.73$, $P < 0.001$); A1-time was positively correlated with CCT ($r = 0.40$, $P < 0.001$) and IOP ($r = 0.94$, $P < 0.001$) and negatively correlated with age ($r = -0.26$, $P < 0.001$); A2-time was positively correlated with age ($r = 0.31$, $P < 0.001$) and SE ($r = 0.24$, $P = 0.02$) and was negatively correlated with IOP ($r = -0.75$, $P < 0.001$); HC radius was positively correlated with SE ($r = 0.24$, $P = 0.02$) (Figure 3(b)), CCT ($r = 0.27$, $P < 0.001$), and IOP ($r = 0.24$, $P = 0.02$) and was negatively correlated with mean keratometry ($r = -0.20$, $P = 0.046$) and axial length ($r = -0.21$, $P = 0.03$) (Figure 3(c)). None of the above four biomechanical parameters was found to be significantly correlated to gender (all $P > 0.05$). The correlation coefficients and P values are shown in Table 3.

5. Discussion

The cornea is a complex tissue with both viscous and elastic properties; elasticity refers to the deformation of the cornea in response to an external stress, and viscosity refers to the resistance of the cornea in regaining the original shape when the stress is removed [17]. The corneal biomechanical behavior can be affected by a number of factors, such as age, IOP, CCT, hydration, connective tissue composition, and some other factors which are still under investigation [18]. Increased knowledge of corneal biomechanical characteristics in myopic population is of great importance, especially for the preoperative evaluation before refractive surgery. Although several studies have used ORA to identify the corneal biomechanical characteristics of myopic eyes and tried to find the association with certain ocular characteristics, such as refractive error, axial length, and corneal curvature, the results were not consistent with each other. For

Table 2: All the parameters obtained by CorVis ST for the 4 groups, mean ± SD.

Parameters	Emmetropia ($n = 21$)	Low myopia ($n = 21$)	Moderate myopia ($n = 28$)	High myopia ($n = 33$)	P value
A1-time (ms)	7.30 ± 0.23	7.37 ± 0.22	7.50 ± 0.28$^{\#}$	7.42 ± 0.20	0.04
A2-time (ms)	21.88 ± 0.33	21.84 ± 0.37	21.68 ± 0.38$^{\#}$	21.69 ± 0.39†	0.02
A1-length (mm)	1.76 ± 0.05	1.77 ± 0.03	1.76 ± 0.08	1.78 ± 0.04	0.68
A2-length (mm)	1.67 ± 0.34	1.75 ± 0.21	1.70 ± 0.24	1.74 ± 0.25	0.71
A1-velocity (m/s)	0.15 ± 0.01	0.14 ± 0.01	0.14 ± 0.02	0.15 ± 0.01	0.10
A2-velocity (m/s)	−0.32 ± 0.05	−0.31 ± 0.08	−0.30 ± 0.05	−0.33 ± 0.07	0.37
HC-time (ms)	17.18 ± 0.47	17.06 ± 0.57	17.07 ± 1.10	17.87 ± 0.49	0.46
PD (mm)	3.80 ± 1.17	3.78 ± 1.17	4.15 ± 1.13	3.69 ± 1.22	0.47
HC radius (mm)	7.09 ± 1.08	7.12 ± 0.91	7.32 ± 0.89	6.65 ± 0.66*	0.03
DA (mm)	1.03 ± 0.08	1.01 ± 0.09	0.98 ± 0.09	1.05 ± 0.10*	0.048
IOP (mmHg)	13.69 ± 2.04	13.93 ± 2.11	15.03 ± 2.67	14.33 ± 1.98	0.17
CCT (μm)	537.3 ± 34.6	546.4 ± 30.0	541.7 ± 21.7	533.6 ± 32.2	0.49

A1- and A2-time: time reaching the first and second applanation; A1- and A2-length: length of the first and second applanation; A1- and A2-velocity: velocity at the first- and second-applanation moment; HC-time: highest concavity- (HC-) time; PD: peak distance; HC radius: radius at HC; DA: deformation amplitude; IOP: intraocular pressure; CCT: central corneal thickness.

$^{*}P < 0.05$ versus Moderate myopia group.

$^{\#}P < 0.05$ versus Emmetropia group.

$^{\dagger}P < 0.05$ versus Emmetropia group.

Table 3: Factors associated with corneal parameters with bivariate correlation analysis.

Parameters	A1-time ($n = 103$)		A2-time ($n = 103$)		HC radius ($n = 103$)		DA ($n = 103$)	
	Coeff.	P	Coeff.	P	Coeff.	P	Coeff.	P
Age	−0.26	0.01	0.31	0.002	−0.05	0.66	0.33	<0.001
Sex	0.01	0.96	0.04	0.67	0.05	0.61	0.05	0.64
SE (D)	−0.15	0.13	0.24	0.02	0.24	0.02	−0.13	0.18
AL (mm)	0.07	0.46	−0.15	0.15	−0.21	0.03	0.20	0.04
MK (D)	0.07	0.49	−0.18	0.08	−0.20	0.046	−0.003	0.97
IOP (mmHg)	0.94	<0.001	−0.75	<0.001	0.24	0.02	−0.73	<0.001
CCT (μm)	0.40	<0.001	−0.17	0.09	0.27	0.01	−0.35	<0.001

D: diopters; SE: spherical equivalent; AL: axial length; MK: mean keratometry; A1- and A2-time: time reaching the first and second applanation; HC radius: radius at highest concavity; DA: deformation amplitude; IOP: intraocular pressure; CCT: central corneal thickness; Coeff.: the correlation coefficient.

example, lower CH was significantly associated with longer axial length in 293 Spanish children [3] and 872 Chinese children [5] but not in 271 Singaporean children [6]. And lower CRF was significantly correlated to flatter corneal curvature in a Singapore children study [6] but not in a Chinese children population [7]. To our knowledge, this is the first study to investigate the corneal biomechanics in myopic eyes using CorVis ST, a newly developed dynamic Scheimpflug analyzer, and correlated to ocular characteristics, not only refractive error, but also axial length and corneal curvature.

We found that corneal biomechanical properties, at least some of the parameters achieved by CorVis ST, were significantly altered within different diagnostic groups based on the degree of myopia. Four of ten biomechanical parameters, which were DA, A1-time, A2-time, and HC radius, were significantly different within the four groups in our study. Regarding the factors that affected these parameters, we found that DA was positively correlated to axial length. Since DA is measured from the start of the deformation to the highest concavity, a stiffer cornea would probably be expected to yield lower DA value [12, 19]. For some myopic eyes, the remodeling of the posterior scleral tissue leads to the elongation of the axial length, which in turn contributes to the progression of myopia [20]. Given that the posterior eye is a complex biomechanical structure, the surrounding sclera serves to create a stable biomechanical environment for the ocular tissues [21, 22]. Chang et al. found that lower corneal stiffness was associated with longer axial length [7]; our results consisted with it and suggested that the expansion of the sclera may result in the instability of ocular tissue which consequently reduced the corneal stiffness and caused higher DA value. Since we failed to find the correlation between DA and SE, this hypothesis needs to be confirmed in the future study.

In terms of the HC radius, it showed significant difference within the four groups; in correlation study, the HC radius was positively correlated with SE and negatively correlated with axial length. Since HC radius tends to change in contrast to DA [23], therefore, this result confirmed the finding of DA and suggested that higher myopia and longer axial length result in smaller central concave curvature at the highest concavity.

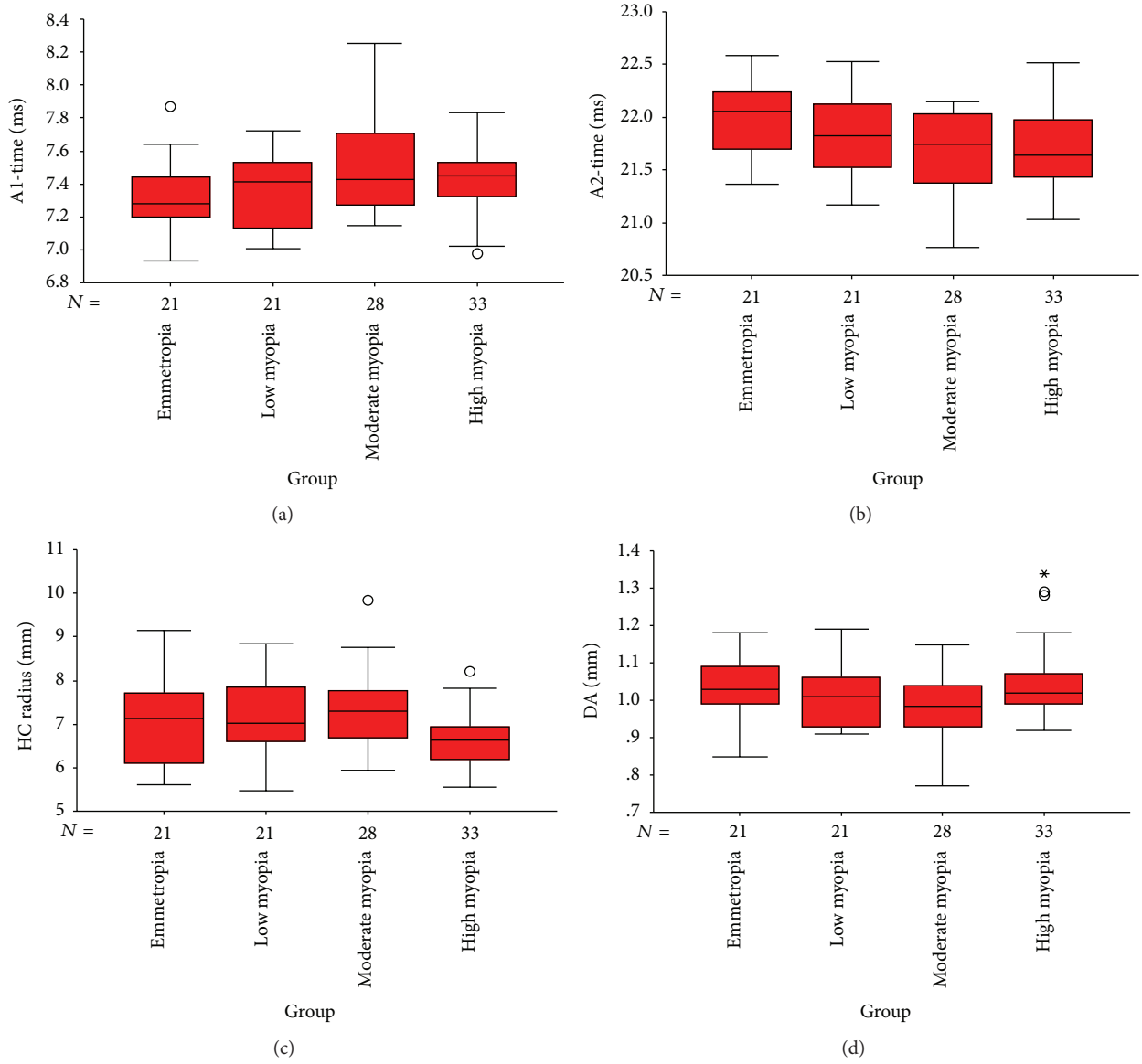

Figure 2: Box plots showing the distribution percentage difference between 4 groups for the A1-time, A2-time, HC radius, and deformation amplitude (DA) levels. The median for each data set is indicated by the center line, and the first and third quartiles are represented by the edges of the area, which is known as the interquartile range (IQR). The 95%/5% confidence intervals are represented by the ends of the lines extending from the IQR. Circles denote outliers with values more than 1.5 IQR from the upper or lower edge of the box.

Increasing evidences show that the corneal biomechanical properties are correlated with IOP and CCT. A lower IOP and thinner central cornea were associated with less stiffness of the cornea and lead to a larger DA and smaller HC radius [24, 25]. It has also been proved in the eyes that underwent corneal refractive surgery, with the weakness of the corneal collagen fibres, which are the main contributors to corneal stiffness, that the cornea tends to have increased indentation during deformation and reduced radius at highest concavity [14, 26]. Our study, as expected, identified that IOP and CCT were negatively correlated with DA and positively correlated with HC radius.

Age is also a potential factor for the corneal biomechanical alterations; age related changes in corneal biomechanical properties have been reported and demonstrated corneal stiffness with age due to the more cross-links of collagen fibrils within the cornea in elderly individuals [27, 28]. Surprisingly, we found a conflicting result which showed a positive instead of theoretically negative correlation between age and DA; however, this is concordant with some other studies, which showed a higher DA value in older individuals [25]. Since most of the elder individuals were excluded from our study because of their systemic diseases, such as coronary heart disease, diabetes mellitus, or the systemic medicine intervention, which could interfere with the interpretation of the study results, the range of age in our study was relatively narrow; further study needs to be conducted to clarify the influence of age on corneal biomechanical properties.

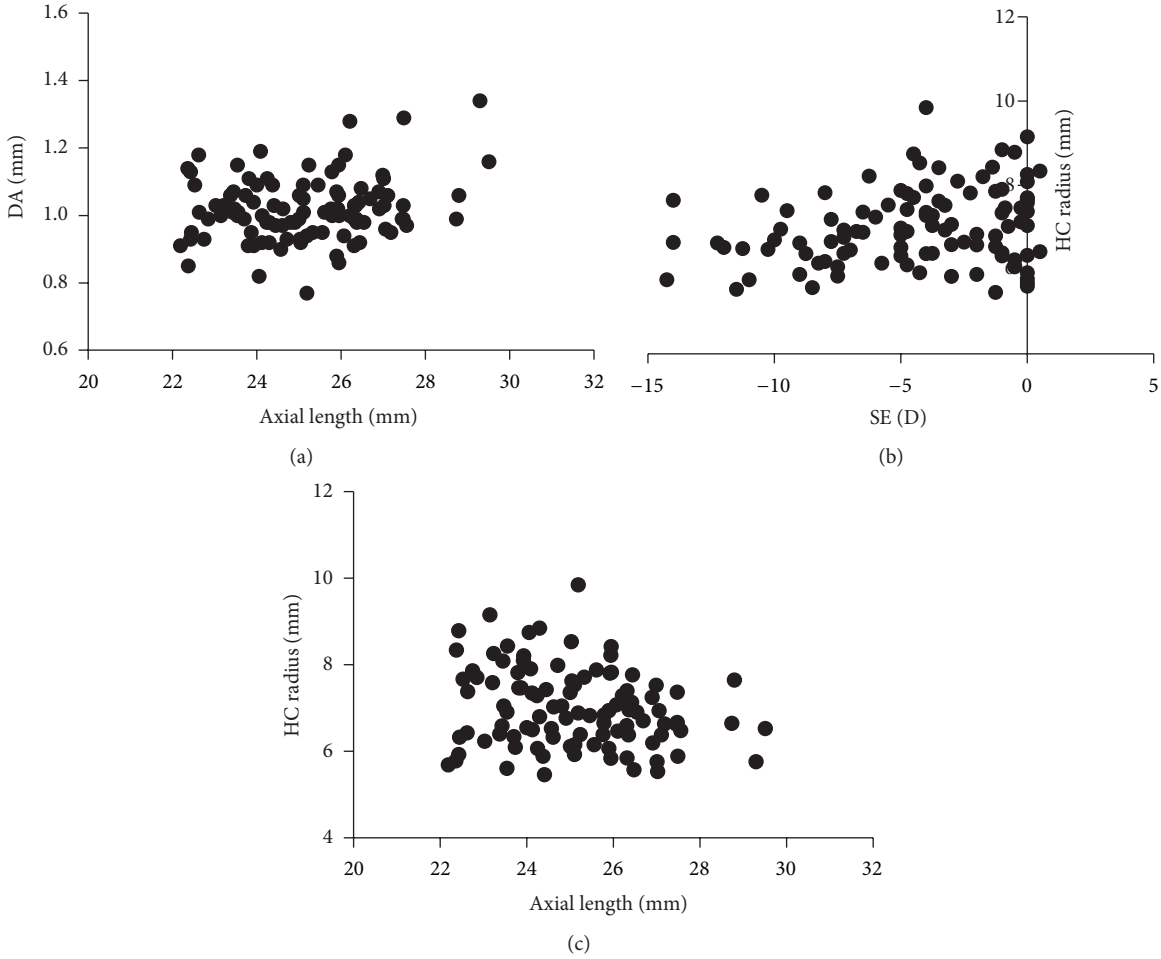

Figure 3: Scatter diagrams of bivariate correlation analysis. (a) Positive correlation between the deformation amplitude (DA) and axial length; (b) positive correlation between the HC radius and spherical equivalent (SE); (c) negative correlation between the HC radius and axial length.

A1-time and A2-time also exhibited significant differences within groups; A1-time and A2-time were the times from starting until the first and second applanation. Both of the parameters are determined not only by the distance from the starting to the first and second applanation, but also by the velocity during the two applanation processes. We found A2-time was positively correlated with SE, which suggested that a higher SE resulted in a longer time to reach the second applanation. This phenomenon needs to be better interpreted in our future studies.

The main limitations of our study are as follows. (1) The sample size in each diagnostic group is relatively small. (2) The age range of the subjects studied was limited. (3) The mean keratometry of the posterior corneal surface was not measured, so the importance of this factor to the corneal biomechanical behavior in myopic population is unknown. (4) Not all the subjects had a general examination and we excluded systemic diseases only by the history; therefore, the potential confounders were not fully excluded. (5) According to the literature, not all of the CorVis ST parameters have ideal repeatability in adults studies, except for IOP, CCT, DA, and A1-time [29, 30], while HC-time, A2-time, and HC radius had low coefficient of variation values [31], so our results still need to be confirmed in the future studies along with the improvement of the equipment design.

In summary, our data showed that there did exist refraction-related biomechanical alterations of the cornea which were associated with ocular characteristics. Highly myopic eyes exhibited longer DA and smaller HC radius than do moderately myopic eyes. The eyes with longer axial length tend to have less corneal stiffness and are easier to deform under stress. This study provided evidences for the application of corneal biomechanical parameters in clinical experience. For example, it has been reported that large DA may induce the underestimation of the IOP measurement [32]; thus, the positive association between DA and myopic degree reminds us of carefully considering IOP value in highly myopic eyes. However, these are our preliminary findings; further large, controlled studies are needed to illustrate highly consistent clinical criteria of corneal biomechanical properties in myopic population, especially for the purpose of ophthalmologic intervention, such as refractive surgery.

Finally, there is one thing which needs to be highlighted, as addressed by Piñero and Alcón [33]; a lack of enough

scientific evidence demonstrating the relationship between biomechanical parameters provided by CorVis ST and the standard mechanical properties limits the ensuring of these parameters in clinical application; therefore, great efforts need to be made to achieve the challenge of developing more accurate devices with which to generate biomechanical parameters closer to the real biomechanical properties of the cornea; thus clear-cut conclusions may be drawn.

Conflict of Interests

The authors have neither a conflict of interests nor commercial interest in the devices mentioned in the paper.

Acknowledgment

This work was supported by grants from the National Natural Science Foundation of China (30600692, 81070755).

References

[1] L. J. Wu, Q. S. You, J. L. Duan et al., "Prevalence and associated factors of myopia in high-school students in Beijing," *PloS ONE*, vol. 10, no. 3, Article ID e0120764, 2015.

[2] V. Koh, A. Yang, S. M. Saw et al., "Differences in prevalence of refractive errors in young asian males in singapore between 1996-1997 and 2009-2010," *Ophthalmic Epidemiology*, vol. 21, no. 4, pp. 247–255, 2014.

[3] I. Bueno-Gimeno, E. España-Gregori, A. Gene-Sampedro, A. Lanzagorta-Aresti, and D. P. Piñero-Llorens, "Relationship among corneal biomechanics, refractive error, and axial length," *Optometry and Vision Science*, vol. 91, no. 5, pp. 507–513, 2014.

[4] M. A. del Buey, L. Lavilla, F. J. Ascaso, E. Lanchares, V. Huerva, and J. A. Cristóbal, "Assessment of corneal biomechanical properties and intraocular pressure in myopic Spanish healthy population," *Journal of Ophthalmology*, vol. 2014, Article ID 905129, 6 pages, 2014.

[5] Y. Huang, C. Huang, L. Li et al., "Corneal biomechanics, refractive error, and axial length in Chinese primary school children," *Investigative Ophthalmology and Visual Science*, vol. 52, no. 7, pp. 4923–4928, 2011.

[6] L. Lim, G. Gazzard, Y.-H. Chan et al., "Cornea biomechanical characteristics and their correlates with refractive error in Singaporean children," *Investigative Ophthalmology & Visual Science*, vol. 49, no. 9, pp. 3852–3857, 2008.

[7] P.-Y. Chang, S.-W. Chang, and J.-Y. Wang, "Assessment of corneal biomechanical properties and intraocular pressure with the Ocular Response Analyzer in childhood myopia," *The British Journal of Ophthalmology*, vol. 94, no. 7, pp. 877–881, 2010.

[8] N. Terai, F. Raiskup, M. Haustein, L. E. Pillunat, and E. Spoerl, "Identification of biomechanical properties of the cornea: the ocular response analyzer," *Current Eye Research*, vol. 37, no. 7, pp. 553–562, 2012.

[9] A. Plakitsi, C. O'Donnell, M. A. Miranda, W. N. Charman, and H. Radhakrishnan, "Corneal biomechanical properties measured with the Ocular Response Analyser in a myopic population," *Ophthalmic & Physiological Optics*, vol. 31, no. 4, pp. 404–412, 2011.

[10] M. Lanza, S. Iaccarino, M. Cennamo, A. Lanza, and G. Coen, "New Scheimpflug camera device in measuring corneal power changes after myopic laser refractive surgery," *Contact Lens & Anterior Eye*, vol. 38, no. 2, pp. 115–119, 2013.

[11] W. Wang, S. Du, and X. Zhang, "Corneal deformation response in patients with primary open-angle glaucoma and in healthy subjects analyzed by corvis ST," *Investigative Opthalmology & Visual Science*, vol. 56, no. 9, pp. 5557–5565, 2015.

[12] C. Ye, M. Yu, G. Lai, and V. Jhanji, "Variability of corneal deformation response in normal and keratoconic eyes," *Optometry and Vision Science*, vol. 92, no. 7, pp. e149–e153, 2015.

[13] H. R. Vellara and D. V. Patel, "Biomechanical properties of the keratoconic cornea: a review," *Clinical & Experimental Optometry*, vol. 98, no. 1, pp. 31–38, 2015.

[14] A. Frings, S. J. Linke, E. L. Bauer, V. Druchkiv, T. Katz, and J. Steinberg, "Effects of laser in situ keratomileusis (LASIK) on corneal biomechanical measurements with the Corvis ST tonometer," *Clinical Ophthalmology*, vol. 9, pp. 305–311, 2015.

[15] J. Hong, Z. Yu, C. Jiang et al., "Corvis st tonometer for measuring postoperative IOP in lasik patients," *Optometry and Vision Science*, vol. 92, no. 5, pp. 589–595, 2015.

[16] B. F. Valbon, R. Ambrósio, B. M. Fontes, and M. R. Alves, "Effects of age on corneal deformation by non-contact tonometry integrated with an ultra-high-speed (UHS) scheimpflug camera," *Arquivos Brasileiros de Oftalmologia*, vol. 76, no. 4, pp. 229–232, 2013.

[17] D. P. Piñero and N. Alcón, "*In vivo* characterization of corneal biomechanics," *Journal of Cataract & Refractive Surgery*, vol. 40, no. 6, pp. 870–887, 2014.

[18] C. J. Roberts, "Concepts and misconceptions in corneal biomechanics," *Journal of Cataract & Refractive Surgery*, vol. 40, no. 6, pp. 862–869, 2014.

[19] Y. Shen, Z. Chen, M. C. Knorz, M. Li, J. Zhao, and X. Zhou, "Comparison of corneal deformation parameters after SMILE, LASEK, and femtosecond laser-assisted LASIK," *Journal of Refractive Surgery*, vol. 30, no. 5, pp. 310–318, 2014.

[20] A. R. Harper and J. A. Summers, "The dynamic sclera: extracellular matrix remodeling in normal ocular growth and myopia development," *Experimental Eye Research*, vol. 133, pp. 100–111, 2015.

[21] I. C. Campbell, B. Coudrillier, and C. R. Ethier, "Biomechanics of the posterior eye: a critical role in health and disease," *Journal of Biomechanical Engineering*, vol. 136, no. 2, Article ID 021005, 2014.

[22] J. A. Summers Rada, S. Shelton, and T. T. Norton, "The sclera and myopia," *Experimental Eye Research*, vol. 82, no. 2, pp. 185–200, 2006.

[23] F. Bao, M. Deng, Q. Wang et al., "Evaluation of the relationship of corneal biomechanical metrics with physical intraocular pressure and central corneal thickness in *ex vivo* rabbit eye globes," *Experimental Eye Research*, vol. 137, pp. 11–17, 2015.

[24] R. Lee, R. T. Chang, I. Y. Wong, J. S. Lai, J. W. Lee, and K. Singh, "Novel parameter of corneal biomechanics that differentiate normals from glaucoma," *Journal of Glaucoma*, 2015.

[25] L. Tian, D. Wang, Y. Wu et al., "Corneal biomechanical characteristics measured by the CorVis Scheimpflug technology in eyes with primary open-angle glaucoma and normal eyes," *Acta Ophthalmologica*, 2015.

[26] Z. Hassan, L. Modis Jr., E. Szalai, A. Berta, and G. Nemeth, "Examination of ocular biomechanics with a new Scheimpflug technology after corneal refractive surgery," *Contact Lens & Anterior Eye*, vol. 37, no. 5, pp. 337–341, 2014.

[27] N. S. Malik, S. J. Moss, N. Ahmed, A. J. Furth, R. S. Wall, and K. M. Meek, "Ageing of the human corneal stroma: structural and biochemical changes," *Biochimica et Biophysica Acta*, vol. 1138, no. 3, pp. 222–228, 1992.

[28] A. Elsheikh, B. Geraghty, P. Rama, M. Campanelli, and K. M. Meek, "Characterization of age-related variation in corneal biomechanical properties," *Journal of the Royal Society Interface*, vol. 7, no. 51, pp. 1475–1485, 2010.

[29] Y. Hon and A. K. C. Lam, "Corneal deformation measurement using Scheimpflug noncontact tonometry," *Optometry and Vision Science*, vol. 90, no. 1, pp. e1–e8, 2013.

[30] G. Nemeth, Z. Hassan, A. Csutak, E. Szalai, A. Berta, and L. Modis Jr., "Repeatability of ocular biomechanical data measurements with a Scheimpflug-based noncontact device on normal corneas," *Journal of Refractive Surgery*, vol. 29, no. 8, pp. 558–563, 2013.

[31] I. B. Pedersen, S. Bak-Nielsen, A. H. Vestergaard, A. Ivarsen, and J. Hjortdal, "Corneal biomechanical properties after LASIK, ReLEx flex, and ReLEx smile by scheimpflug-based dynamic tonometry," *Graefe's Archive for Clinical and Experimental Ophthalmology*, vol. 252, no. 8, pp. 1329–1335, 2014.

[32] T. Huseynova, G. O. Waring IV, C. Roberts, R. R. Krueger, and M. Tomita, "Corneal biomechanics as a function of intraocular pressure and pachymetry by dynamic infrared signal and scheimpflug imaging analysis in normal eyes," *American Journal of Ophthalmology*, vol. 157, no. 4, pp. 885–893, 2014.

[33] D. P. Piñero and N. Alcón, "Corneal biomechanics: a review," *Clinical & Experimental Optometry*, vol. 98, no. 2, pp. 107–116, 2015.

Hindawi Publishing Corporation
Journal of Ophthalmology
Volume 2015, Article ID 171564, 7 pages
http://dx.doi.org/10.1155/2015/171564

Research Article

The Ocular Biometry of Adult Cataract Patients on Lifeline Express Hospital Eye-Train in Rural China

Xiaoguang Cao, Xianru Hou, and Yongzhen Bao

Peking University People's Hospital, Ophthalmology Department, Key Laboratory of Vision Loss and Restoration, Ministry of Education, Beijing Key Laboratory for the Diagnosis and Treatment of Retinal and Choroid Diseases, Beijing 100044, China

Correspondence should be addressed to Yongzhen Bao; drbaoyz@sina.com

Received 23 May 2015; Accepted 5 August 2015

Academic Editor: Qin Long

Copyright © 2015 Xiaoguang Cao et al. This is an open access article distributed under the Creative Commons Attribution License, which permits unrestricted use, distribution, and reproduction in any medium, provided the original work is properly cited.

Aims. To describe and explore the distribution of ocular biometric parameters of adult cataract patients in rural China. *Methods*. Three Lifeline Express Hospital Eye-Train missions of Peking University People's Hospital in China were chosen. 3828 adult cataract patients aged 29 to 88 years with axial length (AL) less than 27.0 mm were enrolled. The ocular biometry including visual acuity (VA), intraocular pressure, AL, corneal power ($K1$ and $K2$), and corneal endothelial counting (CEC) were collected and analysis. Corneal radius (CR) was calculated from the corneal power. *Results*. The participants in Zhoukou of these three missions had the worse preoperative VA ($p < 0.001$), the lowest $K1$ ($p < 0.001$), $K2$ ($p < 0.001$), and K ($p < 0.001$) and the highest $|K1 - K2|$ ($p < 0.001$), moreover AL/CR more closely to 3.0. The AL, $|K1 - K2|$, and AL/CR were normally distributed. But the $K1$, $K2$, K, and CEC were not normal distributions. Except $K1$, all parameters were positively skewed and peaked. *Conclusion*. Our study provides normative ocular biometry in a large, representative rural Chinese population. The AL is normally distributed with a positive skew and big kurtosis. The corneal powers are not normal distribution. The corneal astigmatism might have a significant effect on the visual acuity.

1. Introduction

According to China's Ministry of Health, China has approximately 4 million cataract victims, with 500,000 new cases being diagnosed each year [1]. As a developing country, especially in rural China, poverty and limited access to health care, due to the uneven distribution of health care sources, can make it very difficult for these people to obtain proper treatment [2]. Cataract surgical rate (CSR) is still very low in rural China. Moreover, a lot of these cataract surgeries were charge-free. Lifeline Express Hospital Eye-Train (LEHET), the first charge-free cataract surgery project founded in 1997, is a quite important way to restore vision for the low-income rural people in China.

Independent of cost or other factors, the first expectation from surgeons and patients is good postoperative visual outcomes. To meet these expectations, attention to accurate biometry measurements is critical [3]. The biometry is indispensable to the surgeons and patients as it might indicate the prognosis and safety of the coming operation. In the biometric parameters, axial length (AL) and corneal curvature are the most important. However, the distribution and determinants of AL have been assessed in only a few population-based studies of older persons [4–10], of which there is still no study of rural Chinese population, especially in Middle China, having cities with extremely long history.

In 2011 and 2012, our hospital (Peking University People's Hospital, PUPH) had three missions of LEHET in Middle China. In this study, we explored the biometric parameters of adult cataract patients who had cataract surgeries on LEHET in these missions and all were rural people.

2. Methods

2.1. Recruitment of Patients, Preoperative Assessment, and Exclusion Criteria. Our hospital, PUPH, had four missions of LEHET, Zhoukou in Henan province and Songyuan in Jilin province in 2011, Yuncheng in Shanxi province and Sanmenxia in Henan province in 2012. The sites were selected by the office of LEHET, and they were blind to our hospital

Table 1: CSR of China 2010.

Province	Population	Cataract surgeries	Charge-free cataract surgeries for low-income people	CSR	Charge-free CSR	Ratio of charge-free cataract surgeries for low-income people
Beijing	19,612,368	11961	1402	610	71	11.72%
Shanxi	35,712,101	15902	4929	445	138	31.00%
Henan	94,029,939	36935	9915	393	105	26.84%

CSR: cataract surgical rate.

Table 2: Demographic characteristics of the three groups.

	Zhoukou (n = 991)	Yuncheng (n = 1240)	Sanmenxia (n = 1497)	p
Age (years)	69.20 ± 8.10	69.73 ± 7.84	69.49 ± 8.20	0.293
Sex Male/female	355/636	502/838	562/935	0.640
Eye operated on Right/left	538/453	697/643	749/748	0.113

p values were calculated with ANOVA.

before the mission start. Songyuan in Jilin province was excluded from this study as the incompleted data. Yuncheng (N 35.03; E 111.01; altitude: 369.53 m) in Shanxi province and Zhoukou (N 33.62; E 114.66; altitude: 50.50 m) in Henan province have thousands of years of history. Most residents in these two cities are rural people and live there since birth. Sanmenxia (N 34.77; E 111.20; altitude: 376.08 m) in Henan province was built in the 1950s and also is a rural city. Residents in this new city partly immigrated from the whole of China, such as Northeast China and West China. In 2011, the pure annual income of rural people was 5601.40 CNY (about 889.11 USD) in Shanxi province and 6604.03 CNY (1048.26 USD) in Henan province, much lower than Beijing 14735.68 CNY (about 2339.00 USD) cited from China Statistical Yearbook 2012 [2]. Based on the Sixth National Census of China 2010 (http://www.stats.gov.cn/) [11] and the 2010 annual survey data of China Disabled Persons' Federation (http://www.cdpf.org.cn) [12], cataract surgical rate (CSR) was calculated as in Table 1.

Any patients who wanted to have the charge-free cataract operations on LEHET registered at the base hospital (a local hospital selected by the office of LEHET). After the systemic and ocular examinations and signing the informed consent at the base hospital, the patients were sent to LEHET. Preoperatively on LEHET, all patients underwent a complete ophthalmological examination, that is, measurement of presenting visual acuity (VA) by means of Snellen charts (performed by the nurses from the base hospital), intraocular pressure evaluation (IOP) by noncontact tonometer (Canon TX-10/TX-F, Tokyo, Japan) by the trained nurses from PUPH, slit lamp examination (Topcon SL-1E, Tokyo, Japan), and fundus examination (90 Dioptre, Volk Optical, Mentor, OH) with dilated pupil by the ophthalmologists from PUPH. Corneal curvature by Auto-Keratometer (Nikon Speedy-K, Tokyo, Japan), axial length (AL) and B-scan by ultrasonic system (ODM-2100, MEDA, Tianjing, China), and corneal endothelial counting (CEC) by Specular Microscope (Topcon SP-3000P, Tokyo, Japan) were performed by the trained technicians from PUPH on the patients suitable for operation. The flatter ($K1$) and steeper corneal curvature ($K2$) were read directly from the Auto-Keratometer, and K was calculated as the average of $K1$ and $K2$. Corneal radius (CR) was calculated from the formula CR (millimeter, mm) = $1000 \times 0.3375/K$ (Diopter, D). The SRK/T formula for normal or long axial length (AL more than 25.00 mm) and Hoffer Q formula for short axial length (AL less than 22.00 mm) were used to calculate the power of intraocular lens (IOL) and the estimated postoperative refractive errors were less than ±0.25 D except patients with high myopia. LEHET was equipped with Specular Microscope, SP-3000P, in the first half of year 2012; the patients of Zhoukou and part of Yuncheng had no CEC measurement.

Exclusion criteria for this study are as follows: age less than 20 years, AL equal to or more than 27.00 mm, and history of intraocular surgery.

The study was in accordance with the tenets of the Declaration of Helsinki and has been approved by the institutional review board of PUPH. Written informed consent was obtained from all patients.

2.2. Statistical Analysis. The Student t-test was used to compare age and chi-square test was used to compare the female ratio between the groups. A p value less than 0.05 was considered to be statistically significant. Statistical analysis was performed using Statistical Product and Service Solutions software (SPSS version 20.0, Armonk, New York, USA).

3. Results

The demographic characteristics of the three missions are shown in Table 2. Totally, 3828 cataract patients (3828 eyes) were enrolled in this study, including 1419 males and 2409

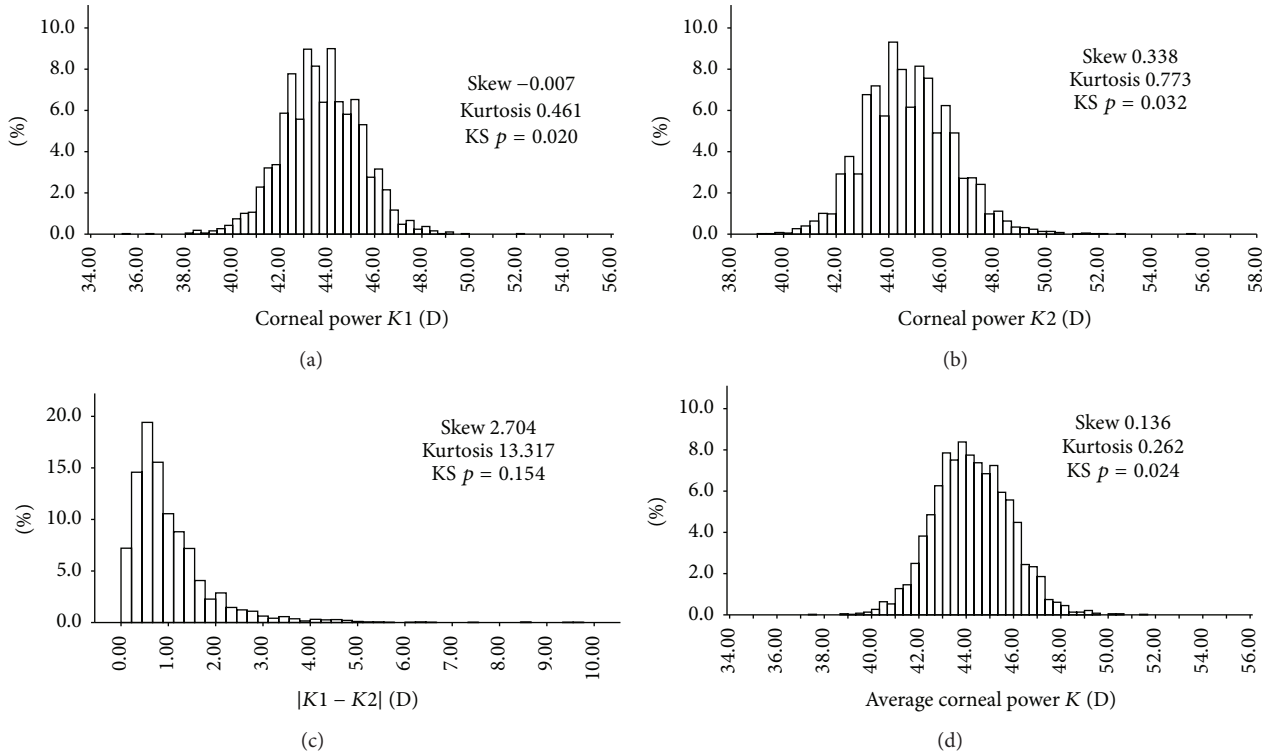

Figure 1: The distributions of corneal power in rural China. $K1$ (a), $K2$ (b), $|K1 - K2|$ (c), and average corneal power (K) (d).

females (male : female = 1 : 1.70) and 1984 right eyes and 1844 left eyes. There were no statistically significant differences between missions preoperatively in age, gender, and eye operated on.

As in Table 2, average age of these cataract patients was 69.50 ± 8.05, which was 69.10 ± 8.41 for males and 69.74 ± 7.82 for females (p = 0.019), respectively. In detail, the average age was 68.55 ± 8.12 for males and 69.57 ± 8.07 for females in Zhoukou (p = 0.056), 69.02 ± 8.33 for males and 70.16 ± 7.50 for females in Yuncheng (p = 0.010), and 69.52 ± 8.64 for males and 69.48 ± 7.92 for females in Sanmenxia (p = 0.933). Although the average age of females is older than males totally, that of males and females was of no difference for Zhoukou and Sanmenxia, except that of females which was older than that of males in Yuncheng.

As shown in Tables 3, 4, and 5, not only for males or females, but also for total patients, the preoperative VA (LogMAR) of these three groups is as follows: Zhoukou > Yuncheng > Sanmenxia. The patients in Sanmenxia had the best preoperative VA, even in each gender, significantly.

As shown in Tables 3, 4, and 5, there was a statistically significant difference in preoperative IOP between the patients of Yuncheng and Zhoukou, Yuncheng and Sanmenxia. The males, females, and total patients of Yuncheng had lower preoperative IOP compared with those in Zhoukou or Sanmenxia.

As shown in Figure 1 and Tables 3, 4, and 5, the patients of Zhoukou had lower $K1$ and $K2$, significantly. There was no statistically significant difference in $K1$ between those of Yuncheng and Sanmenxia, but $K2$ of Yuncheng was higher than Sanmenxia significantly. Respectively, both the males and females in Zhoukou had lower $K1$ and $K2$. However, for either the males or the females, there was no difference of $K1$ and $K2$ between those in Yuncheng and Sanmenxia.

Average corneal power (K) is an important parameter to calculate the power of IOL. In Figure 1 and Tables 3, 4, and 5, the patients in Zhoukou had lower average corneal power (K) significantly compared with the other two groups, the same for male and female patients in Zhoukou. But there was no significant difference in average corneal power (K) between those in Yuncheng and Sanmenxia, for either the males or the females.

The difference between $K1$ and $K2$ could be used to indicate the corneal astigmatism, which has the effect on the postoperative visual acuity. In Figure 1 and Tables 3, 4, and 5, the difference of $K1$ and $K2$ for the patients was as follows: Zhoukou > Yuncheng > Sanmenxia. That was the same for the females. But for the males except that $|K1-K2|$ of Zhoukou was higher than Sanmenxia significantly, there was no significant difference between Zhoukou and Yuncheng or between Yuncheng and Sanmenxia.

AL is another important parameter to calculate the power of IOL. As seen in Figure 2 and Tables 3, 4, and 5, AL for the patients was as follows: Zhoukou < Sanmenxia < Yuncheng. For the males, AL of Zhoukou was shorter than the other two cities. For the females, AL of Yuncheng was longer than the other two sites. There was no significant difference in AL between Yuncheng and Sanmenxia for males or between Zhoukou and Sanmenxia for females.

The AL/CR ratio is highly correlated with the spherical equivalent as a previous study. As seen in Figure 2 and Tables 3, 4, and 5, the patients in Zhoukou had the smallest AL/CR

Table 3: Biological parameters of the three groups.

		Zhoukou	Yuncheng	Sanmenxia	Total	p
Preoperative visual acuity	LogMAR	1.20 ± 0.38	0.95 ± 0.37	0.63 ± 0.43	0.87 ± 0.46	0.000
	Less than 6/60 n (%)	763 (76.99%)	653 (48.73%)	636 (42.48%)	2052 (53.61%)	0.000
	Equal to or better than 6/60 and less than 6/18 n (%)	218 (22.00%)	565 (42.16%)	710 (47.43%)	1493 (39.00%)	0.000
	Equal to or better than 6/18 n (%)	10 (1.01%)	122 (9.10%)	151 (10.09%)	283 (7.39%)	0.000
Preoperative IOP (mmHg)		14.53 ± 3.44	13.98 ± 2.92	14.78 ± 3.11	14.44 ± 3.15	0.000
Corneal curvature (D)	$K1$	43.40 ± 1.65	43.89 ± 1.68	43.82 ± 1.56	43.74 ± 1.64	0.000
	$K2$	44.59 ± 1.79	44.88 ± 1.70	44.75 ± 1.57	44.75 ± 1.68	0.000
	$\lvert K1 - K2 \rvert$	1.20 ± 1.03	0.98 ± 0.81	0.93 ± 0.76	1.02 ± 0.86	0.000
	Average corneal power (K)	44.00 ± 1.64	44.38 ± 1.64	44.29 ± 1.52	44.24 ± 1.60	0.000
Axial length (AL) (mm)		22.95 ± 1.05	23.17 ± 0.95	23.12 ± 0.92	23.04 ± 1.49	0.000
AL/CR		2.99 ± 0.14	3.04 ± 0.12	3.03 ± 0.11	3.03 ± 0.12	0.000
CEC (n/mm^2)		*	2505.63 ± 431.98*	2445.24 ± 419.23	2462.36 ± 423.65*	0.003

p values were calculated with ANOVA or chi-square test.

*LEHET was equipped with Specular Microscope, SP-3000P, in the first half of year 2012; the patients of Zhoukou and part of Yuncheng had no CEC measurement.

Table 4: Biological parameters for males of the three groups.

	Zhoukou	Yuncheng	Sanmenxia	Total	p
Preoperative visual acuity (LogMAR)	1.21 ± 0.38	0.98 ± 0.36	0.66 ± 0.44	0.89 ± 0.46	0.000
Preoperative IOL (mmHg)	14.28 ± 3.46	13.69 ± 2.87	14.50 ± 3.18	14.16 ± 3.17	0.000
Corneal curvature (D)					
$K1$	42.80 ± 1.52	43.37 ± 1.64	43.31 ± 1.44	43.20 ± 1.55	0.000
$K2$	43.86 ± 1.50	44.27 ± 1.64	44.19 ± 1.45	44.13 ± 1.54	0.000
$\lvert K1 - K2\rvert$	1.07 ± 0.85	0.91 ± 0.80	0.87 ± 0.66	0.94 ± 0.77	0.001
Average corneal power (K)	43.33 ± 1.45	43.82 ± 1.59	43.75 ± 1.41	43.67 ± 1.49	0.000
Axial length (AL) (mm)	23.12 ± 0.90	23.44 ± 0.89	23.46 ± 0.88	23.37 ± 0.90	0.000
AL/CR	2.97 ± 0.12	3.04 ± 0.11	3.04 ± 0.11	3.02 ± 0.11	0.000
CEC (n/mm^2)	*	2537.49 ± 450.38*	2437.86 ± 439.39	2467.32 ± 444.71*	0.004

p values were calculated with ANOVA.
*LEHET was equipped with Specular Microscope, SP-3000P, in the first half of year 2012; the patients of Zhoukou and part of Yuncheng had no CEC measurement.

Table 5: Biological parameters for females of the three groups.

	Zhoukou	Yuncheng	Sanmenxia	Total	p
Preoperative visual acuity (LogMAR)	1.19 ± 0.38	0.93 ± 0.37	0.61 ± 0.42	0.85 ± 0.46	0.000
Preoperative IOL (mmHg)	14.67 ± 3.43	14.17 ± 2.93	14.95 ± 3.06	14.60 ± 3.13	0.000
Corneal curvature (D)					
$K1$	43.74 ± 1.63	44.20 ± 1.63	44.13 ± 1.54	44.05 ± 1.61	0.000
$K2$	45.00 ± 1.81	45.24 ± 1.63	45.09 ± 1.54	45.12 ± 1.65	0.016
$\lvert K1 - K2\rvert$	1.27 ± 1.11	1.02 ± 0.82	0.96 ± 0.81	1.06 ± 0.91	0.000
Average corneal power (K)	44.37 ± 1.63	44.72 ± 1.58	44.61 ± 1.49	44.58 ± 1.56	0.000
Axial length (AL) (mm)	22.86 ± 1.11	23.01 ± 0.96	22.91 ± 0.88	22.93 ± 0.97	0.008
AL/CR	3.00 ± 0.15	3.05 ± 0.12	3.03 ± 0.11	3.03 ± 1.29	0.000
CEC (n/mm^2)	*	2484.59 ± 418.72*	2449.66 ± 406.84	2459.30 ± 410.29*	0.174

p values were calculated with ANOVA.
*LEHET was equipped with Specular Microscope, SP-3000P, in the first half of year 2012; the patients of Zhoukou and part of Yuncheng had no CEC measurement.

ratio closer to 3.0, and Yuncheng and Sanmenxia had similar ratio. That is the same for the males and females.

CEC is a very important factor to decide the operation scheme and to predict prognosis. As there was no machine in Zhoukou at that time, we only could compare CEC between those in Yuncheng and Sanmenxia. As shown in Figure 2 and Tables 3, 4, and 5, CEC of Yuncheng was higher than Sanmenxia, which was same result for the males. But for the females, there was no significant difference in CEC between Yuncheng and Sanmenxia.

4. Discussion

This study explored the data of cataract patient, who had the free surgeries on LEHET, on ocular biometry of Chinese population in rural China. And our study provided the normative data on $K1$, $K2$, $|K1 - K2|$, average corneal power (K), AL, AL/CR, and CEC of this population; those were 43.74 ± 1.64 D, 44.75 ± 1.68 D, 1.02 ± 0.86 D, 44.24 ± 1.60 D, 23.04 ± 1.49 mm, 3.03 ± 0.12, and 2462.36 ± 423.65/mm^2, respectively.

Our study showed AL in rural Chinese population was normally distributed with a positive skew and a big kurtosis (1.417). Skew and kurtosis have been reported in the distribution of AL in the Reykjavik Eye study [13], the Singapore Malay Eye study [7], the Singapore Indian Eye study [10], and Fotedar et al.'s study [14]. Hence, this is the first report of the appearance of big kurtosis in the distribution of AL in rural Chinese population.

It is worthwhile comparing our findings with those of the Tanjong Pagar study on adult Chinese population in Singapore, which also used A-scan. The mean AL in that study (23.23 ± 1.17 mm) was a little longer than in our study (23.04 ± 1.49 mm). Moreover, AL in our study is shorter than Latinos (23.38 mm) in Los Angeles with A-scan [8], Malay people (23.55 mm) [7] in Singapore, Indian people (23.45 mm) [10] in Singapore, and Caucasian people (23.44) [14] in the Blue Mountains area in Australia with IOLMaster, longer than another Asian population (22.76 mm) in Myanmar with Ocuscan [9]. The similarity of AL in those studies with A-scan and ours is likely to be explained by the same method of AL measurement. The difference in AL of these studies might be explained by a greater degree of urbanization in Singapore and subsequently a higher rate of axial myopia [10]. Those three studies with IOLMaster indicated that the race might have significant effect on AL compared with region as the similarity of Indian and Caucasian people.

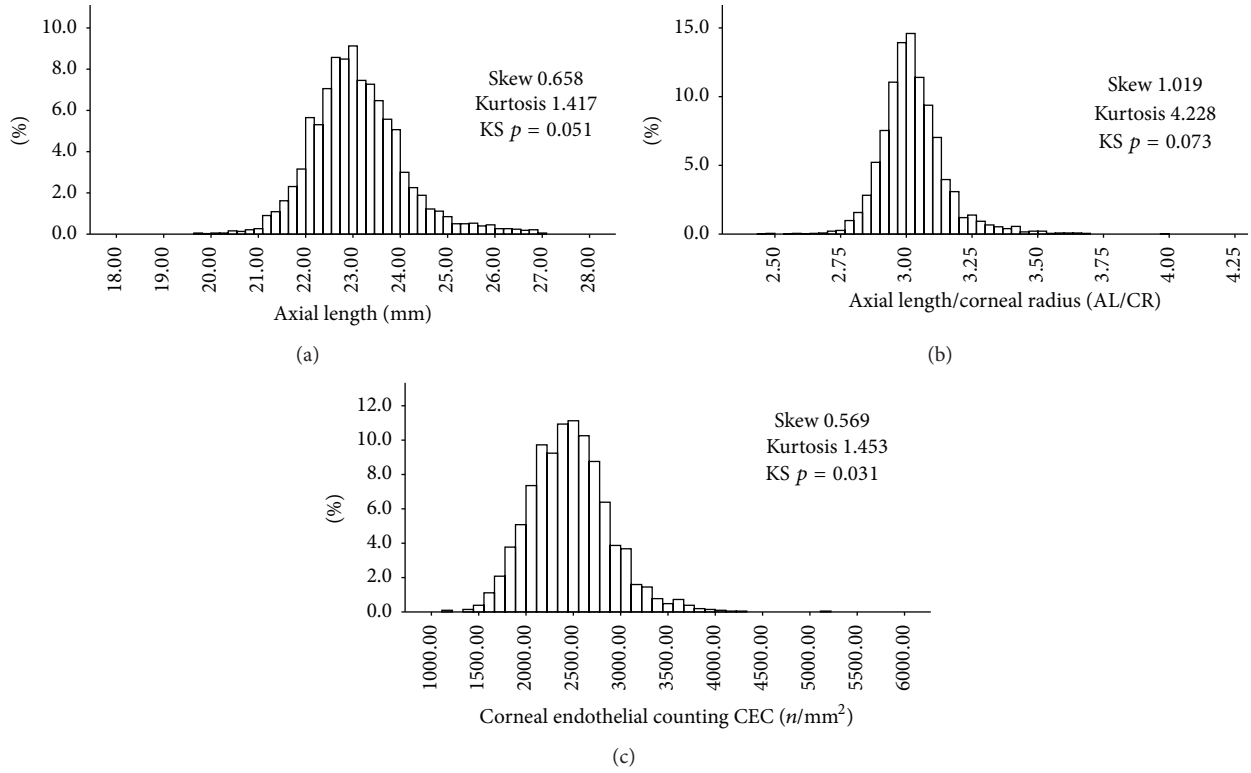

Figure 2: The distributions of axial length (AL), axial length/corneal curvature (AL/CR), and corneal endothelial counting (CEC) in rural China. Axial length (AL) (a), axial length/corneal curvature (AL/CR) (b), and corneal endothelial counting (CEC) (c).

The corneal power $K1$, corneal power $K2$, and K (average corneal power) in our study were not normally distributed with different skews and kurtosis. That is similar to the Singapore Malay Eye study [7] and Fotedar et al.'s study [14]. On the contrary, $|K1 - K2|$ in our study was normally distributed with a positive skew (2.704) and a significant kurtosis (13.317). Moreover, the preoperative visual acuities in the three missions of our study had the same trend as $|K1 - K2|$, both of that of males and females are the same. It indicated that the corneal astigmatism might have obvious effect on the visual acuity.

There is evidence that the AL/CR ratio of an emmetropic eye is usually very close to 3.0, and a higher AL/CR ratio was reported to be a risk factor in myopia [15, 16]. However, few studies have reported the AL/CR ratio [10]. Compared with Zhoukou, the patients in Yuncheng and Sanmenxia had similar AL/CR ratio, also in males and in females. The Singapore Indian Eye study [10] showed that the AL/CR ratio correlated more highly with the spherical equivalent than AL alone. This correlation indicated that longer eyes are not necessarily myopic and worse presenting visual acuity, including those that are long because of overall body stature. The patients in Zhoukou, who had shorter AL and AL/CR closer to 3.0, had the worst preoperative visual acuities. This indicated that in rural Chinese population at least in the cataract patients the AL/CR ratio, in other words, the spherical equivalent, had less effect on the visual acuity than $|K1 - K2|$, the corneal astigmatism.

In conclusion, this study provides normative ocular biometry in a large, representative rural Chinese population. The AL is normally distributed with a positive skew and a big kurtosis. The corneal power $K1$, corneal power $K2$, and K (average corneal power) are not with normal distribution. The corneal astigmatism might have a significant effect on the visual acuity.

Conflict of Interests

The authors declare that there is no conflict of interests and that they have no proprietary or commercial interest in any materials discussed in this paper.

Authors' Contribution

Xiaoguang Cao and Xianru Hou contributed to the work equally and should be regarded as co-first authors.

References

[1] Lifeline Express Hospital Eye-Train, Lifeline Express: A Mission of Sight, 2013, http://lxenglish.com/article.php?id=171fb2589f73f2e5b4a6ca52db5737f7_136.

[2] National Bureau of Statistics of China, *China Statistical Yearbook 2012*, 2012, http://www.stats.gov.cn/tjsj/ndsj/2012/indexch.htm.

[3] A. B. Bhatt, A. C. Schefler, W. J. Feuer, S. H. Yoo, and T. G. Murray, "Comparison of predictions made by the intraocular lens master and ultrasound biometry," *Archives of Ophthalmology*, vol. 126, no. 7, pp. 929–933, 2008.

[4] T. Y. Wong, P. J. Foster, T. P. Ng et al., "Variations in ocular biometry in an adult Chinese population in Singapore: the Tanjong Pagar survey," *Investigative Ophthalmology and Visual Science*, vol. 42, no. 1, pp. 73–80, 2001.

[5] J. Francois and F. Goes, "Ultrasonographic study of 100 emmetropic eyes," *Ophthalmologica*, vol. 175, no. 6, pp. 321–327, 1977.

[6] M. G. Villarreal, J. Ohlsson, M. Abrahamsson, A. Sjöström, and J. Sjöstrand, "Myopisation: the refractive tendency in teenagers. Prevalence of myopia among young teenagers in Sweden," *Acta Ophthalmologica Scandinavica*, vol. 78, no. 2, pp. 177–181, 2000.

[7] L. S. Lim, S.-M. Saw, V. S. E. Jeganathan et al., "Distribution and determinants of ocular biometric parameters in an asian population: the Singapore malay eye study," *Investigative Ophthalmology and Visual Science*, vol. 51, no. 1, pp. 103–109, 2010.

[8] C. Shufelt, S. Fraser-Bell, M. Ying-Lai, M. Torres, and R. Varma, "Refractive error, ocular biometry, and lens opalescence in an adult population: the Los Angeles Latino Eye Study," *Investigative Ophthalmology and Visual Science*, vol. 46, no. 12, pp. 4450–4460, 2005.

[9] S. Warrier, H. M. Wu, H. S. Newland et al., "Ocular biometry and determinants of refractive error in rural Myanmar: the Meiktila eye study," *The British Journal of Ophthalmology*, vol. 92, no. 12, pp. 1591–1594, 2008.

[10] C.-W. Pan, T.-Y. Wong, L. Chang et al., "Ocular biometry in an Urban Indian population: the Singapore Indian Eye study (SINDI)," *Investigative Ophthalmology and Visual Science*, vol. 52, no. 9, pp. 6636–6642, 2011.

[11] National Bureau of Statistics of China, *Sixth National Census of China*, National Bureau of Statistics of China, Beijing, China, 2010, http://www.stats.gov.cn/tjsj/pcsj/rkpc/6rp/indexch.htm.

[12] China Disabled Persons' Federation, *Comprehensive Statistical Data—Rehabilitation*, 2010, http://www.cdpf.org.cn/tjsj/ndsj/2010/indexch.htm.

[13] T. Olsen, A. Arnarsson, H. Sasaki, K. Sasaki, and F. Jonasson, "On the ocular refractive components: the Reykjavik Eye Study," *Acta Ophthalmologica Scandinavica*, vol. 85, no. 4, pp. 361–366, 2007.

[14] R. Fotedar, J. J. Wang, G. Burlutsky et al., "Distribution of axial length and ocular biometry measured using partial coherence laser interferometry (IOL Master) in an older white population," *Ophthalmology*, vol. 117, no. 3, pp. 417–423, 2010.

[15] D. A. Goss and P. Erickson, "Meridional corneal components of myopia progression in young adults and children," *American Journal of Optometry and Physiological Optics*, vol. 64, no. 7, pp. 475–481, 1987.

[16] T. Grosvenor and R. Scott, "Comparison of refractive components in youth-onset and early adult-onset myopia," *Optometry and Vision Science*, vol. 68, no. 3, pp. 204–209, 1991.

Hindawi Publishing Corporation
Journal of Ophthalmology
Volume 2015, Article ID 579695, 8 pages
http://dx.doi.org/10.1155/2015/579695

Research Article

Epigenetic Regulation of Werner Syndrome Gene in Age-Related Cataract

Xi Zhu, Guowei Zhang, Lihua Kang, and Huaijin Guan

Eye Institute, Affiliated Hospital of Nantong University, Nantong, Jiangsu 226001, China

Correspondence should be addressed to Huaijin Guan; gtnantongeye@gmail.com

Received 31 December 2014; Revised 11 March 2015; Accepted 13 March 2015

Academic Editor: Jun Zhang

Copyright © 2015 Xi Zhu et al. This is an open access article distributed under the Creative Commons Attribution License, which permits unrestricted use, distribution, and reproduction in any medium, provided the original work is properly cited.

Purpose. To examine the promoter methylation and histone modification of WRN (Werner syndrome gene), a DNA repair gene, and their relationship with the gene expression in age-related cataract (ARC) lens. *Methods*. We collected the lenses after cataract surgery from 117 ARC patients and 39 age-matched non-ARC. WRN expression, DNA methylation and histone modification around the CpG island were assessed. The methylation status of Human-lens-epithelium cell (HLEB-3) was chemically altered to observe the relationship between methylation and expression of WRN. *Results*. The WRN expression was significantly decreased in the ARC anterior lens capsules comparing with the control. The CpG island of WRN promoter in the ARC anterior lens capsules displayed hypermethylation comparing with the controls. The WRN promoter was almost fully methylated in the cortex of ARC and control lens. Acetylated H3 was lower while methylated H3-K9 was higher in ARC anterior lens capsules than that of the controls. The expression of WRN in HLEB-3 increased after demethylation of the cells. *Conclusions*. A hypermethylation in WRN promoter and altered histone modification in anterior lens capsules might contribute to the ARC mechanism. The data suggest an association of altered DNA repair capability in lens with ARC pathogenesis.

1. Introduction

Age-related cataract (ARC) is one of the dominant causes of visual impairment in the elderly [1]. The disease can be classified as cortical, nuclear, and posterior subcapsular according to the location of the opacity within the lens [2]. ARC is a complex disease with multiple genetic and environmental risk components, including UV light, sun exposure, vitamin C deficiency, and hypertension [3], but its etiology is not fully understood [4, 5].

Oxidative stress has long been recognized as an important mediator of pathophysiology in lens epithelial cells (LECs) and also plays a vital role in the pathogenesis of cataract [6–8]. Recent studies have reported the association between reactive oxygen species- (ROS-) induced DNA damage of LECs and the development of cataract [8–10]. In our previous studies, we have also found that oxidative DNA damage marker, 8-oxoG, was significantly increased in ARC group compared with control group [11, 12]. Oxidative DNA lesions are repaired by nucleotide excision repair, double-strand break (DSB) repair, and base excision repair [13, 14]. The WRN gene plays an important role in aging [15] and is known to function in repair of damaged DNA, particularly in repairing double-strand breaks [16]. The WRN protein belongs to RecQ family and has 1432 amino acids possessing both $3' \rightarrow 5'$ DNA helicase and $3' \rightarrow 5'$ DNA exonuclease activities. These biochemical functions are known to have roles in DNA replication, repair of DNA damage, gene transcription, and telomere maintenance [17]. WRN disruption causes Werner's syndrome (WS), an autosomal recessive segmental progeroid syndrome that results in accelerated aging and affects multiple organs and tissues [17]. Most WS patients develop bilateral ocular cataract when they are 20 years old and beyond [18, 19]. Previously, we reported that polymorphisms and copy number variations of WRN are associated with ARC [20, 21].

Epigenetics pertains to heritable alterations in gene expression that do not involve modification of the underlying genomic DNA sequence [22]. DNA methylation and histone modifications (including methylation, acetylation, sumoylation, and phosphorylation) are the major epigenetic mechanisms for gene expression [23]. Hypermethylation of

Table 1: Demographic information of study participants.

	Control	ARC
N	39	117
Age (mean ± SD)	69.66 ± 4.51	70.38 ± 7.72
Female *N* (%)	21 (54.8)	70 (60.1)
Male *N* (%)	18 (45.2)	47 (39.9)
Cortical *N* (%)	0	39 (33.3)
Nuclear *N* (%)	0	39 (33.3)
PSC *N* (%)	0	39 (33.3)

promoter CpG islands and histone H3 methylated at lysine 9 have been linked to heterochromatin and gene silencing, whereas histone H3 acetylated is enriched in euchromatic domains and correlates with active gene expressions [24–26]. DNA methylation is a critical regulator of gene expression in the eye and is necessary for the proper development and postmitotic survival of retinal neurons [27]. Aberrant methylation patterns have been associated with age-related macular degeneration, cataract, pterygium, and retinoblastoma [28–32]. Changes in histone modifications have also been observed in experimental models of diabetic retinopathy and glaucoma [22]. A decreased expression of WRN is related to aberrant DNA hypermethylation in various tumors; epigenetic inactivation of this gene may be a biomarker for selection of drugs for the treatment of cancer [33–37].

In this study, we investigated WRN expression in anterior lens capsules and lens cortex of ARC and age-matched controls and analyzed the correlation between epigenetic modification and expression profiles of WRN gene to explore the possible effect of epigenetics on the development of ARC.

2. Materials and Methods

2.1. Study Participants. The research followed the tenets of the Declaration of Helsinki. All participants signed the informed consent forms. The study was approved by the Ethics Committee of Affiliated Hospital of Nantong University.

We enrolled 117 ARC patients that consisted of three subgroups: age-related cortical cataract (ARC-C), age-related nuclear cataract (ARC-N), and age-related posterior subcapsular cataract (ARC-P). The criteria for ARC group included (1) opaque ocular lenses, (2) ≥50 years of age, and (3) $C \geq 4$, $N \geq 4$, and $P \geq 4$ according to the lens opacity classification system III (LOCSIII) [38] and excluded (1) complicated cataract due to high myopia, uveitis, ocular trauma, or other known causes and (2) hypertension, diabetes, or other systemic diseases. We enrolled 39 patients with vitreoretinal diseases who received transparent lens extraction as control group. The criteria for the control included (1) transparent ocular lenses and (2) ≥50 years of age and excluded (1) other major eye diseases such as glaucoma, myopia, diabetic retinopathy, and uveitis and (2) hypertension, diabetes, or other systemic diseases. The demographic information for all participants was listed in Table 1.

2.2. Anterior Lens Capsules and Lens Cortex Preparation. Anterior lens capsules that included lens epithelium (LE) and peripheral cortex were obtained through small incision extra capsular cataract surgery. The tissue was dissected and rapidly frozen in liquid nitrogen and then stored at −80°C for protein, RNA, and genomic DNA extraction.

2.3. RNA Isolation and cDNA Preparation. Total RNA from anterior lens capsules and lens cortex was isolated from the frozen tissues using TRIzol reagent (Invitrogen, Carlsbad, CA), and cDNAs were synthesized using PrimeScript RT reagent Kit (TaKaRa, Dalian, China).

2.4. Quantification of WRN mRNA. TaqMan gene expression assay probe (Applied Biosystems, Foster City, CA) was used for WRN mRNA quantification (Applied Biosystems assay ID: Hs01087915_m1). The results were normalized against the expression of housekeeping gene GAPDH from the same sample. RT-PCR was performed using ABI 7500 real time PCR system (Applied Biosystems, Foster City, CA). The fold change of WRN expression was determined using the comparative CT ($2^{-\Delta\Delta CT}$) method.

2.5. Western Blot Assay. The protein of anterior lens capsules and lens cortex was extracted in lysis buffer (1 M Tris-HCl at pH 7.5, 1% Triton X-100, 1% Nonidet p-40, 10% SDS, 0.5% sodium deoxycholate, 0.5 M EDTA, 10 mg/mL leupeptin, 10 mg/mL aprotinin, and 1 mM phenylmethylsulfonyl fluoride). Proteins were size-fractionated by sodium dodecyl sulfate-polyacrylamide gel electrophoresis and transferred onto polyvinylidene difluoride filter membranes (Millipore, Bedford, MA). Nonspecific protein binding to the membrane was blocked with blocking buffer (5% nonfat milk, 200 mM NaCl, 50 mM Tris, and 0.05% Tween 20). The blocked membrane was then incubated with mouse anti-human-WRN (1 : 800; Abcam, Cambridge, UK) and anti-GAPDH (1 : 1000; Santa Cruz, CA, USA) at 4°C for 18 h. The membrane was washed three times with TBST (20 mM Tris, 500 mM NaCl, and 0.1% Tween 20) for 5 min each time, followed by incubating with an alkaline phosphatase-conjugated goat anti-mouse IgG antibody (1 : 2000; Santa Cruz, CA, USA) for 2 h. Detection was performed using an ECL chemiluminescence kit (Pierce, Rockford, IL) and the signal was exposed to an X-ray film that was scanned using Image Quant software (Molecular Dynamics, Sunnyvale, CA, USA).

2.6. DNA Methylation Detection. DNA sequence of WRN from the NCBI genome database was used for the bioinformatic analysis. Transcription start site (TSS) of the gene was predicted by the online database (http://dbtss.hgc.jp/). CpG islands of WRN were predicted by using online software (http://www.urogene.org/methprimer/).

Genomic DNA from the frozen tissues and HLEB-3 was isolated by phenol/chloroform and ethanol extraction. Two micrograms of genomic DNA was treated with sodium bisulfite using the EpiTect Bisulfite Kit (Qiagen, Inc., Frederick, MD). EpiTect Control DNA (Qiagen, Inc.) was used as the positive controls in all experiments.

The bisulfite-sequencing PCR (BSP) primer was designed by web-based Meth Primer software (http://www.urogene.org/methprimer/) to cover a CpG island near WRN. The

primers used for region 1 were 5′-TTATTTTGAAAGAAG-TTTTTTTTGG-3′ (forward) and 5′-AAACAAACTATT-ATCCTCCCAACAC-3′ (reverse). The primers used for region 2 were 5′-TTTTTTGTGTTGGGAGGATAATAGT-3′ (forward) and 5′-AACAAAAAACAAAACTCCAAA-AAAA-3′ (reverse). The primers used for region 3 were 5′-AGGTCTCCAGCCGGCGGGCACTCA-3′ (forward) and 5′-TGAGGGGAAGAGGGGGTC-3′ (reverse). The primers used for region 4 were 5′-TTTAGTGTATTTTTTGAT-TGAAGTT-3′ (forward) and 5′-CTAAACAACTAAAAT-CCTACATCCC-3′ (reverse). The PCR products were gel-extracted and cloned into the pMD-20-T vector (Takara, Japan). Plasmid-transformed bacteria DH5a were grown for 14 h and the plasmid DNA was isolated. At least 10 clones were chosen for sequence analysis. The degree of methylation was presented as mC/CpG.

2.7. Chromatin Immunoprecipitation (ChIP) Assay. Chromatin immunoprecipitation (ChIP) assay was performed using Tissue Acetyl-Histone H3 ChIP kit and Tri-Methyl-Histone H3K9 ChIP kit (Epigentek, Farmingdale, NY, USA) according to the manufacturer's instructions. Briefly, the anterior lens capsules and cortex were cross-linked with 1% formaldehyde for 8 min and then homogenized. The homogenate was sonicated for 4 pulses of 15 sec each at level 2 using the microtip probe of a Branson Digital Sonifier (Model 450, Branson Ultrasonics Corporation, Connecticut, USA), followed by a 40 sec interval on ice between each pulse, to generate fragments of genomic DNA ranging from 200 to 800 bp in length. For the ChIP assays, equal amounts of treated chromatin were added to microwells containing immobilized antibody for the targeted protein or a negative control normal mouse IgG antibody. In addition, a small portion of treated chromatin, which was equal to 5% of the extracted genomic DNA, was used as the Input DNA to calculate the enrichment of the leptin promoter DNA after immunoprecipitation of the targeted proteins. After incubation for 90 min at 65°C to reverse the cross-links and elute the DNA, Fast-Spin columns were used for DNA purification. The primers for WRN promoter were 5′-CCGCCGCCTGACTTCGGACACC-3′ (forward) and 5′-TCGCACTCCCGCTGCACCCCAC-3′ (reverse).

2.8. Cell Culture and Demethylation Treatment. To test the relationship between the methylation and the expression of the WRN, an in vitro study of demethylation was performed. Human lens epithelium cell line (HLEB-3) was obtained from American Type Culture Collection (ATCC; Rockville, MD) and cultured in Eagle's minimum essential medium (Invitrogen-GIBCO, Carlsbad, CA) with 10% fetal bovine serum at 37°C in a humidified 5% CO_2 atmosphere. After reaching 80–90% confluency, the cells were demethylated by incubation in medium containing 3 mM of 5-aza-2-deoxycytidine (5-aza-dC) (Sigma, CA, USA) for 72 h. Whole cell protein extracts of HLEB-3 were isolated for Western blotting.

2.9. Statistical Analysis. One-way ANOVA analysis was used to determine the difference in averages between the four groups. P value <0.05 was considered statistically significant. Statistical analyses were performed with SPSS software (SPSS 17.0; SPSS, Inc., Chicago, IL).

3. Results

3.1. Expression of WRN in Anterior Lens Capsules and Lens Cortex. RT-PCR analysis was performed to investigate WRN mRNA content in anterior lens capsules and context of the ARC and the controls. Lower WRN mRNA (Figure 1(a)) expression in anterior lens capsules was detected in all three subtypes of ARC cases compared with the controls ($P < 0.01$).

To confirm the change of WRN in protein level between ARC and controls, Western blot analysis was performed. As shown in Figure 1(b), the expression pattern of WRN protein in anterior lens capsules was lower in all three subtypes of ARC cases compared with the controls ($P < 0.01$). However, WRN was undetected in lens cortex in both the ARC cases and the controls (data not shown).

3.2. Methylation Status of WRN. To analyze the relationship between methylation status and expression of WRN, we detected the methylation rate of WRN promoter in the DNA extracted from the anterior lens capsules and cortex of ARC and control group using BSP. Bioinformatic analysis indicated four CpG islands in the promoter of WRN (Figure 2(a)) (R1: −1287 to −1133, R2: −875 to −620, R3: −209 to 164, and R4: 173 to 324, relative to the TSS). Figures 2(b) and 2(c) showed a representative result of bisulfite genomic sequencing of the R3 fragment. Each row stands for a single plasmid clone, and each circle represents a CpG site. The unmethylated and methylated CpGs were represented by unfilled and filled cycles, respectively. As shown in Figure 2(b), the methylation rate of all three subtypes of ARC was higher than that of the control group at region 3 of WRN promoter. As shown in Figure 2(c), the methylation rate of lens cortex at region 3 was almost 100% in both ARC group and control group. The methylation rates at regions 1, 2, and 4 in WRN promoter were almost 100% in both ARC group and control group (data not shown).

3.3. Histone Modifications around the CpG Islands of the WRN Gene in ARC. In general, hypermethylation of H3-K9 exhibits the silencing of gene expression, whereas acetylation of H3 is associated with activation of gene expression. We performed ChIP to analyze the correlation between the histone modification and the expression profiles of WRN gene. ChIP analysis depicted that acetylated H3 levels were lower in all three subtypes of ARC than the control in anterior lens capsules while methylated H3-K9 was increased in all three subtypes of ARC (Figure 3). The histone modification of cortex was undetectable (data not shown).

3.4. Methylation Status and Protein Expression of WRN in HLEB-3 after Treatment with 5-Aza-dC. To test the relationship between the methylation and the expression of the WRN, an in vitro study of demethylation was performed. 5-Aza-dC

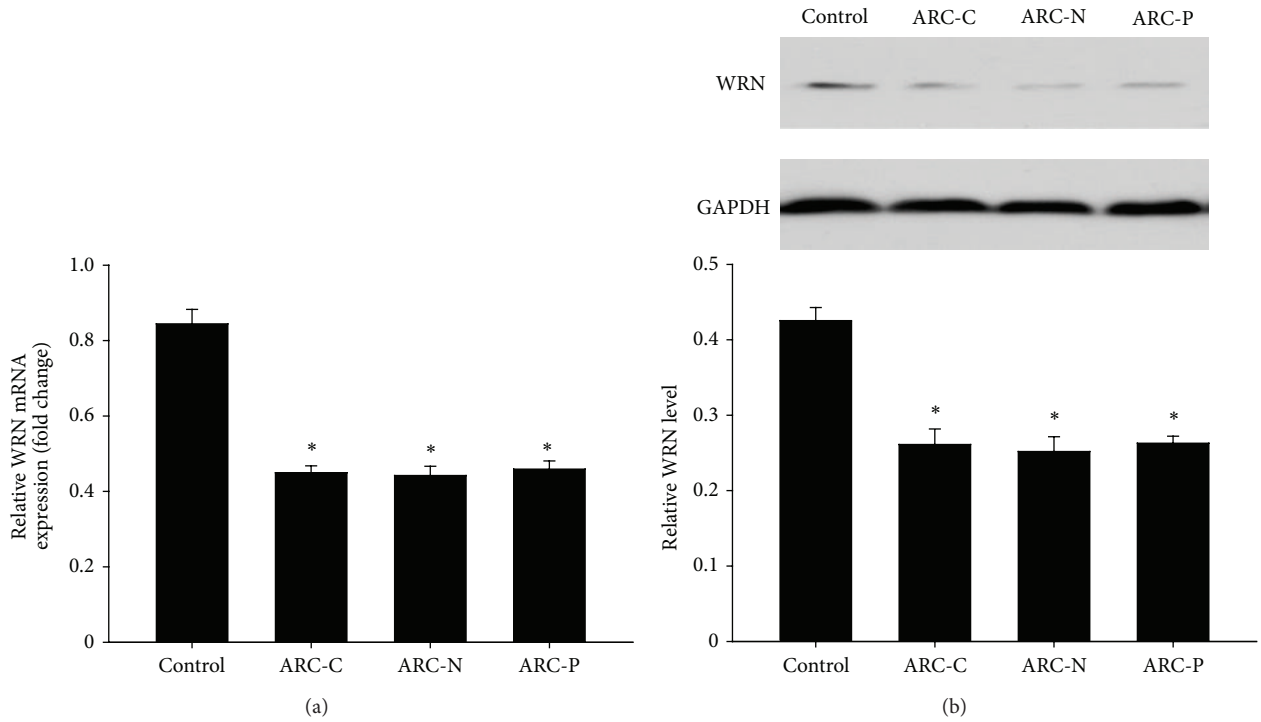

Figure 1: Relative expression of mRNA and protein levels of WRN in anterior lens capsules of control and ARC. (a) RT-PCR analysis of the expression of WRN in control ($n = 20$) and ARC-C ($n = 20$), ARC-N ($n = 20$), and ARC-P ($n = 20$). Values represent mean ± SD. $^{*}P < 0.01$. (b) WRN protein levels in control ($n = 9$) and ARC-C ($n = 9$), ARC-N ($n = 9$), and ARC-P ($n = 9$) anterior lens capsules were detected using Western blotting. Relative WRN protein level to GAPDH is presented as mean ± SD. $^{*}P < 0.01$.

is a DNA methyltransferase inhibitor which is used to inhibit DNA methylation. As shown in Figure 4(a), after treatment with 5-aza-dC, the methylation rate of WRN promoter in HLEB-3 was decreased in comparison with the untreated control. In contrast, the protein expression of WRN in HLEB-3 after treatment with 5-aza-dC was increased in comparison with the untreated control (Figure 4(b)).

4. Discussion

Although the pathophysiology of ARC is far from being clearly understood, it is well accepted that oxidative stress plays an important role in the disease pathogenesis. When reactive oxygen species (ROS) production exceeds the capacity of its removal by various mechanisms, they may cause oxidative damage to DNA [6–10]. In a normal physiologic condition, most oxidative DNA lesions are rapidly repaired by base excision repair (BER), nucleotide excision repair (NER), and double-strand break repair (DSBR) pathways [13, 14]. WRN is a protein functioning in the DSBR pathway and is also required for cellular DNA replication and mismatch repair [33]. Both mRNA and protein expression of WRN are downregulated in anterior lens capsules in ARC, implying a reduced DNA repair capability in the ARC lens from all included subtypes. The results have provided an additional evidence of DNA repair mechanism in ARC development by using patients' lens tissue.

We demonstrated that WRN undergoes epigenetic alterations in ARC lens tissue from all included subtypes and this alteration is associated with the mRNA and protein expression of the gene. The treatment with a demethylating agent restored the WRN expression in HLEB-3. The results linked the epigenetic changes with the target gene expression and are consistent with the current knowledge on the effect of epigenetic modification on human genome.

It is of interest that the ARC-associated epigenetic changes of WRN gene only occur in anterior lens capsules but not in lens cortex in which both ARC cases and control had an undetectable or very weak expression of WRN and a very high degree of WRN methylation. Lens cortex is made up of lens fibers which are differentiated from LECs. The results suggest that the strategies to intervene epigenetic alteration in ARC should aim at anterior lens capsules.

We analyzed methylation status at four regions of WRN promoter in both ARC and control groups; only region 3 showed significant changes between the cases and the controls. This sequence-specific change is reasonable because this region contains the most abundant CpG islands among the four selected regions and spans the translation starting site.

5. Conclusions

Overall, our study found that aberrant epigenetic methylation in WRN DNA and the associated histone linked to low expression of WRN and lens opacity. This is the first report to show a relationship between the epigenetic modification of WRN gene and ARC by directly studying the lens tissue from human subjects. This study provided a deeper insight

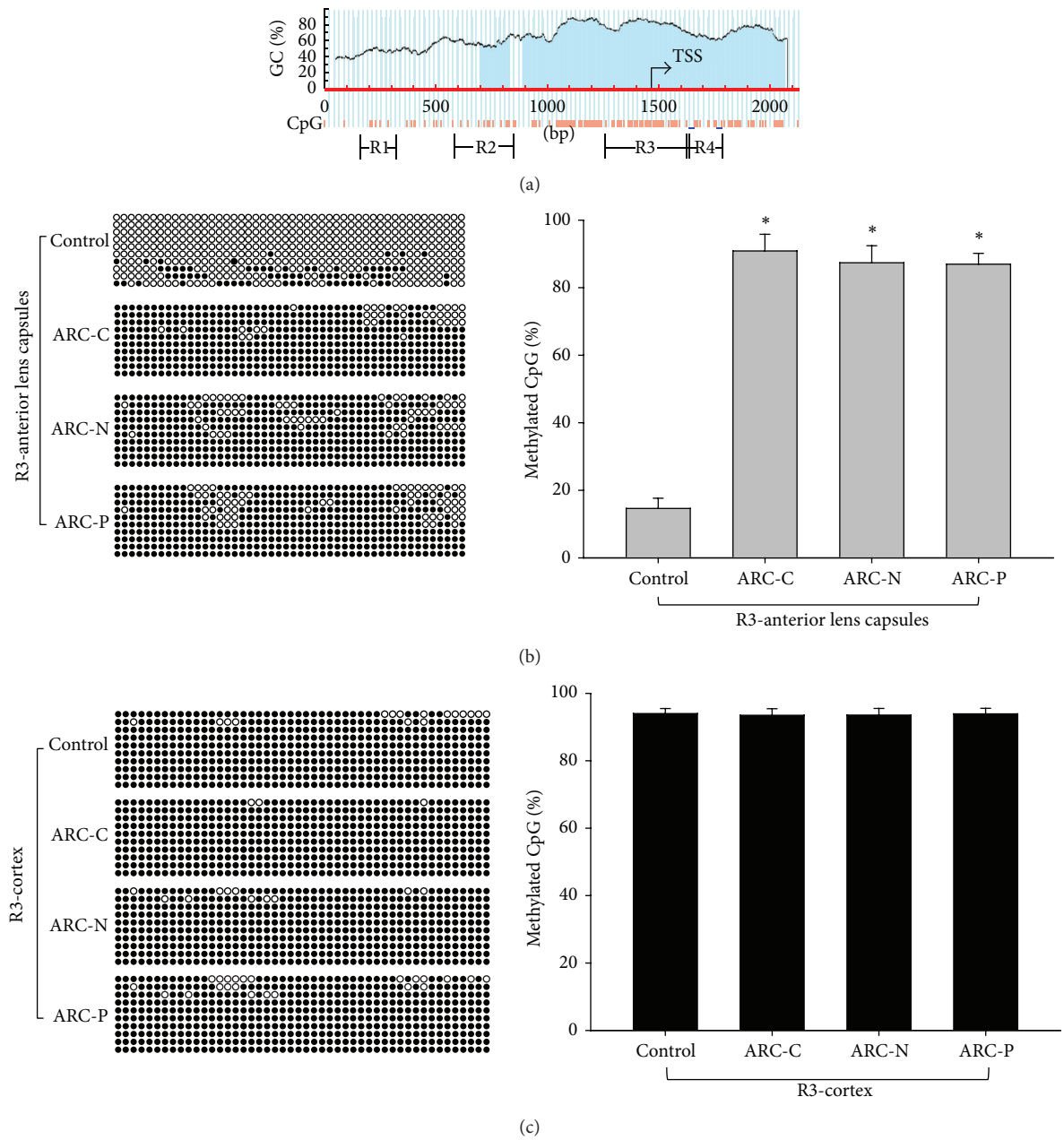

Figure 2: Methylation status at region 3 in WRN promoter in anterior lens capsules and cortex of control and ARC. (a) The positions of CpG islands within WRN promoter. In the following panels, each row of circles represents a single clone. Open and close circles represent unmethylated and methylated CpG sites, respectively. (b) Methylation status of region 3 in WRN promoter in anterior lens capsules of control ($n = 20$) and ARC-C ($n = 20$), ARC-N ($n = 20$), and ARC-P ($n = 20$). The ARC group displayed hypermethylation compared to the control group. $^{*}P < 0.01$. (c) Methylation status of region 3 in WRN promoter in lens cortex of control and ARC lens. There were no significant statistical differences between the ARC group and the control group. $P > 0.05$.

on the DNA repair mechanism in the pathogenesis of ARC, and the knowledge can be used to identify novel options for the prevention and therapy for ARC.

Disclaimer

The authors are responsible for the content and writing of the paper.

Conflict of Interests

The authors declare no conflict of interests.

Acknowledgments

This study was supported by the National Natural Science Foundation of China (no. 81270987 and no. 81070718), the 333

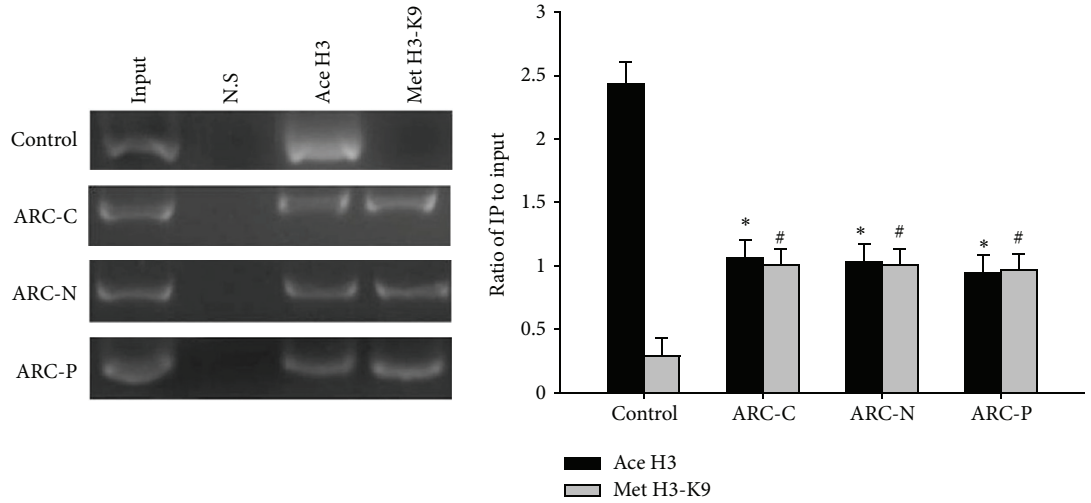

Figure 3: Histone modifications of the WRN promoter in anterior lens capsules of control and ARC. In anterior lens capsules, compared with the control group ($n = 10$), ChIP analysis revealed that acetylated H3 levels were lower in ARC-C ($n = 10$), ARC-N ($n = 10$), and ARC-P ($n = 10$). At the same time, methylated H3-K9 was increased. $^{*}P < 0.01$.

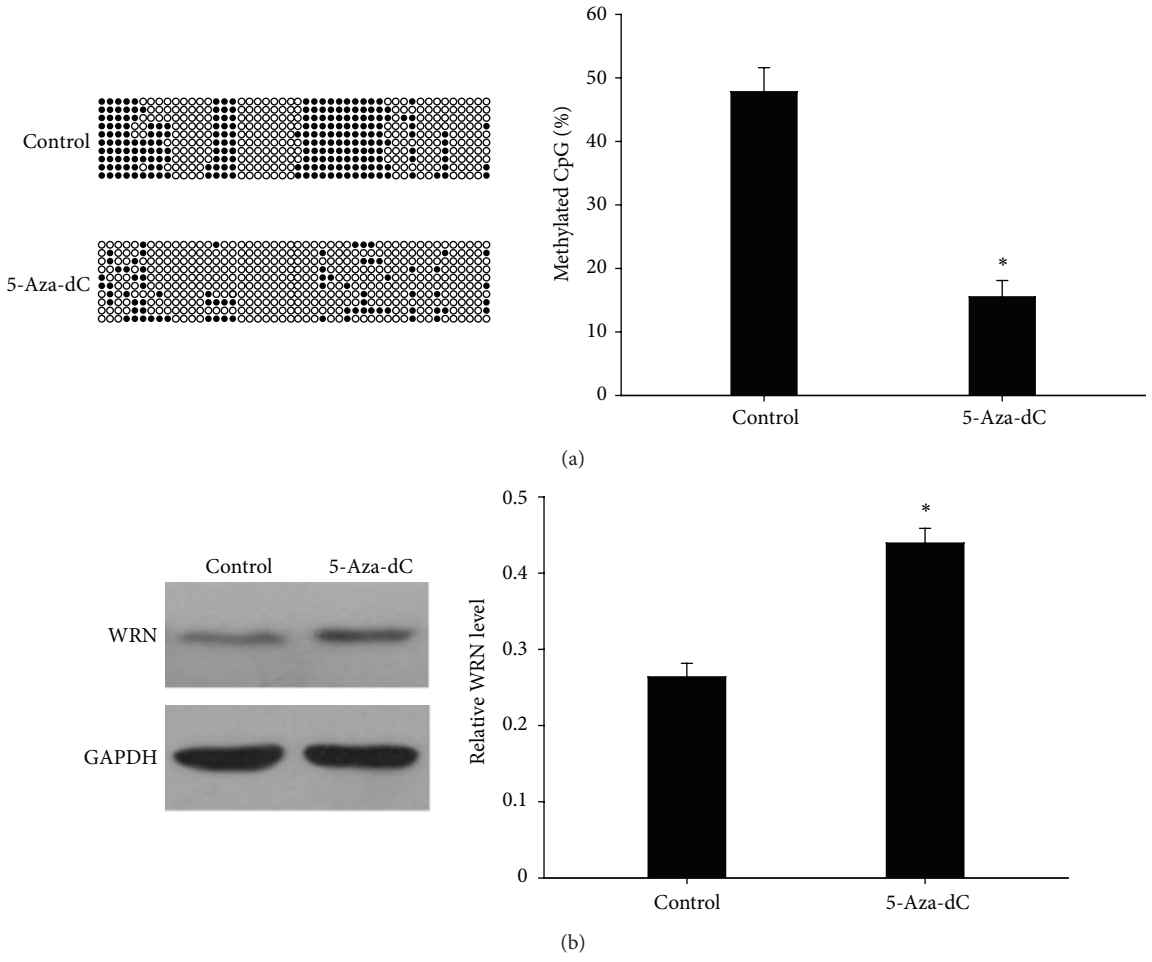

Figure 4: Relative methylation status and expression of protein levels of WRN in HLEB-3 after treatment with 5-aza-dC. In the following panels, each row of circles represents a single clone. Open and close circles represent unmethylated and methylated CpG sites, respectively. (a) After treatment with 5-aza-dC, the methylation rate of WRN in HLEB-3 was decreased. (b) Protein expression of WRN in the untreated control cells and in cells after treatment with 5-aza-dC. Relative WRN protein level to GAPDH is presented as mean ± SD. $^{*}P < 0.01$.

Project of Jiangsu Province, China (no. BRA2010173), and the Ordinary University Graduate Student Research Innovation project of Jiangsu Province, China (no. 03050487).

References

[1] B. Thylefors, "A global initiative for the elimination of avoidable blindness," *The American Journal of Ophthalmology*, vol. 125, no. 1, pp. 90–93, 1998.

[2] B. E. K. Klein, R. Klein, and K. L. P. Linton, "Prevalence of age-related lens opacities in a population: the Beaver Dam Eye Study," *Ophthalmology*, vol. 99, no. 4, pp. 546–552, 1992.

[3] J. Zuercher, J. Neidhardt, I. Magyar et al., "Alterations of the 5′untranslated region of *SLC16A12* lead to age-related cataract," *Investigative Ophthalmology & Visual Science*, vol. 51, no. 7, pp. 3354–3361, 2010.

[4] A. Shiels and J. F. Hejtmancik, "Genetic origins of cataract," *Archives of Ophthalmology*, vol. 125, no. 2, pp. 165–173, 2007.

[5] C. J. Hammond, H. Snieder, T. D. Spector, and C. E. Gilbert, "Genetic and environmental factors in age-related nuclear cataracts in monozygotic and dizygotic twins," *The New England Journal of Medicine*, vol. 342, no. 24, pp. 1786–1790, 2000.

[6] S. Ottonello, C. Foroni, A. Carta, S. Petrucco, and G. Maraini, "Oxidative stress and age-related cataract," *Ophthalmologica*, vol. 214, no. 1, pp. 78–85, 2000.

[7] O. Ates, H. H. Alp, I. Kocer, O. Baykal, and I. A. Salman, "Oxidative DNA damage in patients with cataract," *Acta Ophthalmologica*, vol. 88, no. 8, pp. 891–895, 2010.

[8] R. J. W. Truscott, "Age-related nuclear cataract—oxidation is the key," *Experimental Eye Research*, vol. 80, no. 5, pp. 709–725, 2005.

[9] W. Pendergrass, P. Penn, D. Possin, and N. Wolf, "Accumulation of DNA, nuclear and mitochondrial debris, and ROS at sites of age-related cortical cataract in mice," *Investigative Ophthalmology and Visual Science*, vol. 46, no. 12, pp. 4661–4670, 2005.

[10] Y. Zhang, L. Zhang, L. Zhang, J. Bai, H. Y. Ge, and P. Liu, "Expression changes in DNA repair enzymes and mitochondrial DNA damage in aging rat lens," *Molecular Vision*, vol. 16, pp. 1754–1763, 2010.

[11] L. Kang, W. Zhao, G. Zhang, and H. Guan, "Acetylated 8-oxoguanine DNA glycosylase 1 and its relationship with p300 and SIRT1 in lens epithelium cells from age-related cataract," *Experimental Eye Research*, 2015.

[12] B. Xu, L. Kang, G. Zhang et al., "The changes of 8-OHdG, hOGG1, APE1 and Pol beta in lenses of patients with age-related cataract," *Current Eye Research*, vol. 40, no. 4, pp. 378–385, 2015.

[13] R. D. Wood, M. Mitchell, J. Sgouros, and T. Lindahl, "Human DNA repair genes," *Science*, vol. 291, no. 5507, pp. 1284–1289, 2001.

[14] D. M. Wilson III, T. M. Sofinowski, and D. R. McNeill, "Repair mechanisms for oxidative DNA damage," *Frontiers in Bioscience*, vol. 8, pp. D963–D981, 2003.

[15] D. K. Singh, B. Ahn, and V. A. Bohr, "Roles of RECQ helicases in recombination based DNA repair, genomic stability and aging," *Biogerontology*, vol. 10, no. 3, pp. 235–252, 2009.

[16] H. Yan, J. McCane, T. Toczylowski, and C. Y. Chen, "Analysis of the Xenopus Werner syndrome protein in DNA double-strand break repair," *The Journal of Cell Biology*, vol. 171, no. 2, pp. 217–227, 2005.

[17] J. Gee, Q. X. Ding, and J. N. Keller, "Analysis of Werner's expression within the brain and primary neuronal culture," *Brain Research*, vol. 940, no. 1-2, pp. 44–48, 2002.

[18] L. H. Camacho, A. Mora-Bowen, R. Munden, W. R. Smythe, and N. G. Ordoñez, "Malignant mesothelioma: natural history, pathologic features and future therapies," *American Journal of Medicine*, vol. 120, no. 7, pp. E7–E9, 2007.

[19] M. Goto, "Hierarchical deterioration of body systems in Werner's syndrome: implications for normal ageing," *Mechanisms of Ageing and Development*, vol. 98, no. 3, pp. 239–254, 1997.

[20] S. Su, Y. Yao, R. R. Zhu et al., "The associations between single nucleotide polymorphisms of DNA repair genes, DNA damage, and age-related cataract: Jiangsu eye study," *Investigative Ophthalmology and Visual Science*, vol. 54, no. 2, pp. 1201–1207, 2013.

[21] J. Jiang, J. Zhou, Y. Yao et al., "Copy number variations of DNA repair genes and the age-related cataract: jiangsu eye study," *Investigative Ophthalmology & Visual Science*, vol. 54, no. 2, pp. 932–938, 2013.

[22] M. M. Liu, C. C. Chan, and J. S. Tuo, "Epigenetics in ocular diseases," *Current Genomics*, vol. 14, no. 3, pp. 166–172, 2013.

[23] T. Jenuwein and C. D. Allis, "Translating the histone code," *Science*, vol. 293, no. 5532, pp. 1074–1080, 2001.

[24] J. C. Rice and B. W. Futscher, "Transcriptional repression of BRCA1 by aberrant cytosine methylation, histone hypoacetylation and chromatin condensation of the BRCA1 promoter," *Nucleic Acids Research*, vol. 28, no. 17, pp. 3233–3239, 2000.

[25] J. A. Fahrner, S. Eguchi, J. G. Herman, and S. B. Baylin, "Dependence of histone modifications and gene expression on DNA hypermethylation in cancer," *Cancer Research*, vol. 62, no. 24, pp. 7213–7218, 2002.

[26] S. Fujii, R. Z. Luo, J. Yuan et al., "Reactivation of the silenced and imprinted alleles of ARHI is associated with increased histone H3 acetylation and decreased histone H3 lysine 9 methylation," *Human Molecular Genetics*, vol. 12, no. 15, pp. 1791–1800, 2003.

[27] I. O. Nasonkin, K. Lazo, D. Hambright, M. Brooks, R. Fariss, and A. Swaroop, "Distinct nuclear localization patterns of DNA methyltransferases in developing and mature mammalian retina," *The Journal of Comparative Neurology*, vol. 519, no. 10, pp. 1914–1930, 2011.

[28] Y. Wang, F. Li, G. Zhang, L. Kang, B. Qin, and H. Guan, "Altered DNA methylation and expression profiles of 8-oxoguanine DNA glycosylase 1 in lens tissue from age-related cataract patients," *Current Eye Research*, 2014.

[29] M. Gemenetzi and A. J. Lotery, "The role of epigenetics in age-related macular degeneration," *Eye*, vol. 28, no. 12, pp. 1407–1417, 2014.

[30] M. Beta, S. Chitipothu, V. Khetan, J. Biswas, and S. Krishnakumar, "Hypermethylation of adenomatosis polyposis coli-2 and its tumor suppressor role in retinoblastoma," *Current Eye Research*, pp. 1–10, 2014.

[31] R. A. Kowluru, J. M. Santos, and M. Mishra, "Epigenetic modifications and diabetic retinopathy," *BioMed Research International*, vol. 2013, Article ID 635284, 9 pages, 2013.

[32] L. Wei, B. Liu, J. Tuo et al., "Hypomethylation of the IL17RC promoter associates with age-related macular degeneration," *Cell Reports*, vol. 2, no. 5, pp. 1151–1158, 2012.

[33] R. Agrelo, W. H. Cheng, F. Setien et al., "Epigenetic inactivation of the premature aging Werner syndrome gene in human cancer," *Proceedings of the National Academy of Sciences of the United States of America*, vol. 103, no. 23, pp. 8822–8827, 2006.

[34] K. Futami, M. Takagi, A. Shimamoto, M. Sugimoto, and Y. Furuichi, "Increased chemotherapeutic activity of camptothecin in cancer cells by siRNA-induced silencing of WRN

helicase," *Biological and Pharmaceutical Bulletin*, vol. 30, no. 10, pp. 1958–1961, 2007.

[35] K. Masuda, K. Banno, M. Yanokura et al., "Association of epigenetic inactivation of the WRN gene with anticancer drug sensitivity in cervical cancer cells," *Oncology Reports*, vol. 28, no. 4, pp. 1146–1152, 2012.

[36] L. Wang, L. Xie, J. Wang, J. Shen, and B. Liu, "Correlation between the methylation of SULF2 and WRN promoter and the irinotecan chemosensitivity in gastric cancer," *BMC Gastroenterology*, vol. 13, no. 1, article 173, 2013.

[37] G. Supic, R. Kozomara, M. Brankovic-Magic, N. Jovic, and Z. Magic, "Gene hypermethylation in tumor tissue of advanced oral squamous cell carcinoma patients," *Oral Oncology*, vol. 45, no. 12, pp. 1051–1057, 2009.

[38] L. T. Chylack Jr., J. K. Wolfe, D. M. Singer et al., "The lens opacities classification system III," *Archives of Ophthalmology*, vol. 111, no. 6, pp. 831–836, 1993.

Hindawi Publishing Corporation
Journal of Ophthalmology
Volume 2015, Article ID 429251, 8 pages
http://dx.doi.org/10.1155/2015/429251

Clinical Study

Acute-Onset Vitreous Hemorrhage of Unknown Origin before Vitrectomy: Causes and Prognosis

Dong Yoon Kim,[1] Soo Geun Joe,[2] Seunghee Baek,[3] June-Gone Kim,[4] Young Hee Yoon,[4] and Joo Yong Lee[4]

[1]*Department of Ophthalmology, College of Medicine, Chungbuk National University, Cheongju, Republic of Korea*
[2]*Department of Ophthalmology, Gangneung Asan Hospital, University of Ulsan, College of Medicine, Gangneung, Republic of Korea*
[3]*Department of Clinical Epidemiology and Biostatistics, Asan Medical Center, University of Ulsan, College of Medicine, Seoul, Republic of Korea*
[4]*Department of Ophthalmology, Asan Medical Center, University of Ulsan, College of Medicine, 88 Olympic-ro 43-gil, Songpa-gu, Seoul 138-736, Republic of Korea*

Correspondence should be addressed to Joo Yong Lee; ophthalmo@amc.seoul.kr

Received 17 April 2015; Accepted 7 June 2015

Academic Editor: Zhongfeng Wang

Copyright © 2015 Dong Yoon Kim et al. This is an open access article distributed under the Creative Commons Attribution License, which permits unrestricted use, distribution, and reproduction in any medium, provided the original work is properly cited.

Purpose. To analyze causes and prognosis of acute-onset preoperatively unknown origin vitreous hemorrhage (VH). *Methods*. This study included patients who underwent vitrectomy for acute-onset preoperatively unknown origin VH. The underlying causes of VH, which were identified after vitrectomy, were analyzed. And overall visual prognosis of unknown origin VH was analyzed. Risk scoring system was developed to predict visual prognosis after vitrectomy. *Results*. 169 eyes were included. Among these, retinal vein occlusion (RVO), retinal break, and age-related macular degeneration (AMD) were identified in 74 (43.8%), 50 (29.6%), and 21 (12.4%) patients, respectively. After vitrectomy, logMAR BCVA significantly improved from 1.93 ± 0.59 to 0.47 ± 0.71. However, postoperative BCVA in AMD eyes were significantly poorer than others. Poor visual prognosis after vitrectomy was associated with old age, poor preoperative vision in both eyes, and drusen in the fellow eye. *Conclusions*. RVO, retinal break, and AMD are the most common causes of acute-onset preoperatively unknown origin VH and the most common causes of VH change with age. The visual prognosis of unknown origin VH is relatively good, except among AMD patients. Older patients with poor preoperative BCVA in both eyes and patients with AMD in the fellow eye are at a higher risk of poor visual prognosis following vitrectomy.

1. Introduction

The annual incidence of acute-onset vitreous hemorrhage (VH) in the general population is 7 cases per 100,000 persons [1]. The causes of VH include proliferative diabetic retinopathy (PDR), trauma, retinal break, proliferative retinopathy after retinal vein occlusion (RVO), and posterior vitreous detachment without retinal detachment [2–6]. It is important to determine the underlying cause of acute-onset VH because the natural history and visual prognosis depend on the underlying cause. The visual prognosis of VH caused by retinal break, posterior vitreous detachment, and branch RVO is relatively good [4, 6–10]. However, the visual prognosis of VH secondary to PDR and exudative age-related macular degeneration (AMD) is poor due to recurrent VH, tractional retinal detachment, and submacular hemorrhage [11–14].

VH caused by a retinal break may be less severe and resolve more rapidly. Therefore, upright head position and immobilization of the patient allow blood to settle down in the eye, eventually clearing VH [4, 10, 15]. In cases of VH caused by retinal neovascularization due to diabetic retinopathy or RVO, peripheral laser photocoagulation can regress the abnormal vessels, which may lead to VH.

However, in some cases, it is difficult to determine the underlying cause of acute-onset VH. Lean and Gregor reported that 14% of acute-onset VH eyes were diagnosed on

follow-up examination and 4% remained undiagnosed after 1 year [4]. Little is known about the causes and visual prognosis of acute-onset VH of preoperatively unknown origin. Here, we analyzed the causes and overall visual prognosis of acute-onset VH of preoperatively unknown origin. We also analyzed the characteristics of the fellow eye in all patients. In addition, we generated a risk scoring system (RSS) to predict visual prognosis of acute-onset preoperatively unknown origin VH.

2. Materials and Methods

2.1. Study Design and Participants. This retrospective review was conducted on patients who underwent vitrectomy for acute-onset VH of preoperatively unknown origin at Asan Medical Center, Seoul, Republic of Korea, between January 2007 and June 2013. The following inclusion criteria were applied: (1) a history of 3-port pars plana vitrectomy for acute-onset VH, with or without cataract surgery, and (2) the cause of acute-onset VH could not be preoperatively identified because of dense VH which prevented retinal examination. Exclusion criteria included eyes with other ocular diseases that might affect vision, active intraocular inflammation and/or infection, and VH caused by trauma. Patients with more than mild nonproliferative diabetic retinopathy in the fellow eye and those with grades III–IV AMD (AREDS (age-related eye disease study) classification) in the fellow eye were also excluded. This study was approved by the institutional review board of Asan Medical Center and followed the tenets of the Declaration of Helsinki (2014-0358).

2.2. Primary and Secondary Objectives. The primary objective of this study was to analyze the causes of acute-onset VH of preoperatively unknown origin. The secondary objectives of this study were to determine (1) the causes of acute-onset VH of preoperatively unknown origin according to age, (2) the visual prognosis of acute-onset VH of preoperatively unknown origin, (3) differences in the baseline characteristics according to postoperative diagnosis, and (4) characteristics of the fellow eye and (5) to devise an RSS for predicting the visual prognosis of acute-onset VH of preoperatively unknown origin.

2.3. Ophthalmic Examinations. All included patients underwent a complete bilateral ophthalmic examination, including determination of BCVA using the Snellen chart. BCVA results were converted to the logMAR scale. Patients who were only able to count fingers, were only able to detect hand motion, had light perception, or had no light perception were assigned logMAR values 2.0, 2.3, 2.7, and 3.0, respectively [16]. All patients also underwent biomicroscopic examination, dilated fundus examination, and fundus photography of both eyes. Ultrasonography was performed on all eyes with VH of preoperatively unknown origin.

2.4. Identification of Causes of Acute-Onset VH of Preoperatively Unknown Origin. The postoperative diagnosis of acute-onset VH of preoperatively unknown origin was identified by thorough review of each patient's medical records. We divided all included patients according to age (≤60, 60–70, and >70 years), and the causes of VH were analyzed according to age.

2.5. Surgical Procedures. Vitrectomy was performed by well-experienced retinal surgeons (Joo Yong Lee, June-Gone Kim, and Young Hee Yoon). A 20-gauge, 23-gauge, and 25-gauge vitrectomy system was used to perform 3-port vitrectomy. Cataracts were extracted by phacoemulsification if the crystalline lens had significant opacity. After resolving the VH, which obscured retinal inspection, we attempted to determine the cause of VH and recorded the underlying cause of VH as an operative note. After completing vitrectomy, eyes with retinal break received perfluoropropane (C_3F_8) gas tamponade. For complicated cases, such as those with severe tractional retinal detachment or multiple retinal breaks, silicone oil tamponade was performed. The silicone oil was removed 6 months later.

2.6. Statistical Analysis. One-way ANOVA and the Bonferroni post test were used to analyze the visual prognosis of VH according to the postoperative diagnosis. According to the postoperative diagnosis, the clinical characteristics were analyzed using one-way ANOVA with the Bonferroni post test and Pearson Chi-square test. Finally, to develop an RSS for predicting visual prognosis of acute-onset VH of preoperatively unknown origin, multivariate logistic regression modeling was performed. Risk factors were selected using backward elimination from the full logistic model. Model discrimination was estimated using *C*-tatistic (or AUC), and calibration was assessed by determining agreement between the predicted and recorded prognosis of acute-onset VH of preoperatively unknown origin. We ran an internal validation of discrimination (*C*-statistic) to produce optimism-corrected values of the *C*-statistic by using bootstrapping with 500 replications of individuals that were sampled with replacement [17]. After considering the internally validated variables, we developed a scoring system using the model parameter estimates described by Sullivan et al. [18]. ROC curves from the original model and scoring system are presented. SPSS (version 21.0; SPSS, Inc., Chicago, IL) and R 3.0.2 (free software that can be downloaded at http://www.r-project.org/) with package "boot" and "pROC" were used to perform the statistical analyses.

3. Results

In total, 2031 eyes in 2031 patients underwent vitrectomy for VH at Asan Medical Center between January 2007 and June 2013. Among these 2031 patients, the underlying cause of VH was not identified in 169 eyes in 169 patients (8.3%), and these patients therefore satisfied the inclusion criteria for enrollment.

3.1. Primary Objective. The postoperative diagnoses of acute-onset VH of preoperatively unknown origin are listed in Table 1. RVO (74 eyes, 43.8%) was the most common cause.

Table 1: Causes of acute-onset vitreous hemorrhage (VH) of preoperatively unknown origin.

Underlying causes of VH	Eyes, *n* (%)
Retinal vein occlusion	74 (43.8%)
Central retinal vein occlusion (CRVO)	0/74 (0.0%)
Branch retinal vein occlusion (BRVO)	74/74 (100.0%)
BRVO with foveal involvement	10/74 (13.5%)
Vitreous hemorrhage with retinal break	50 (29.6%)
Age-related macular degeneration	21 (12.4%)
Macroaneurysm	8 (4.7%)
Eales disease	3 (1.8%)
Coats' disease	1 (0.6%)
Idiopathic	12 (7.1%)
Total	169 (100%)

All RVO eyes had branch retinal vein occlusion (BRVO). There were no cases of central or hemiretinal vein occlusion. Among the 74 eyes with BRVO, foveal involvement was only found in 10 eyes (13.5%). Fifty (29.6%), 21 (12.4%), and 8 (4.7%) eyes were diagnosed with retinal break, wet age-related macular degeneration (wAMD), or retinal arterial macroaneurysm, respectively, as the cause of preoperatively unknown VH. In 12 eyes (7.1%), we could not identify any retinal pathology even after vitrectomy.

3.2. Secondary Objectives. The causes of acute-onset VH of preoperatively unknown origin according to age are shown in Figure 1. We divided all included patients according to age (≤60, 60–70, and >70 years). In patients aged ≤60 years, retinal break was the most common cause of acute-onset VH of preoperatively unknown origin; however, the proportion of patients with retinal break declined with age. By contrast, the proportion of patients with wAMD increased with age. Among patients aged >60 years, RVO was the most common cause of acute-onset VH of preoperatively unknown origin. Visual prognoses according to postoperative diagnosis are shown in Figure 2. After vitrectomy, logMAR BCVA improved from 1.93 ± 0.59 to 0.47 ± 0.71. Preoperative logMAR BCVA significantly differed according to the postoperative diagnosis. The preoperative logMAR BCVA values of the wAMD patients were significantly poorer than those of other patients (wAMD, 2.37 ± 0.36; RVO, 1.87 ± 0.58; retinal break, 1.97 ± 0.57; $p = 0.001$). The postoperative logMAR BCVA values of the wAMD patients were also significantly worse than those of other patients (wAMD, 1.65 ± 0.88; RVO, 0.30 ± 0.43; retinal break, 0.21 ± 0.40; $p < 0.001$). Visual acuity changes after vitrectomy according to postoperative diagnosis are shown in Figure 2. BCVA significantly improved after vitrectomy among the RVO, retinal break, and idiopathic patients. However, vision did not improve after vitrectomy in wAMD patients.

The clinical characteristics of VH according to postoperative diagnoses are listed in Table 2. Mean age significantly differed according to the postoperative diagnosis. The mean age of the wAMD patients was significantly higher than that of the patients with RVO or retinal break (wAMD, 73.29 ± 8.30 years; RVO, 65.36 ± 9.82 years; retinal break, 58.50 ± 11.78 years; $p = 0.001$). Systemic hypertension was more frequently associated with RVO and wAMD patients. The characteristics of the fellow eyes among patients with acute-onset VH of preoperatively unknown origin are shown in Table 3. The logMAR BCVA values of the fellow eyes in wAMD patients were also significantly lower than in other patients (wAMD, 0.44 ± 0.45; RVO, 0.17 ± 0.38; retinal break, 0.05 ± 0.09; $p < 0.001$). Drusen was more significant in the fellow eyes of wAMD patients than in those of patients with RVO or retinal break (RVO, 6.8%; wAMD, 71.4%; retinal break, 2.0%; $p < 0.001$).

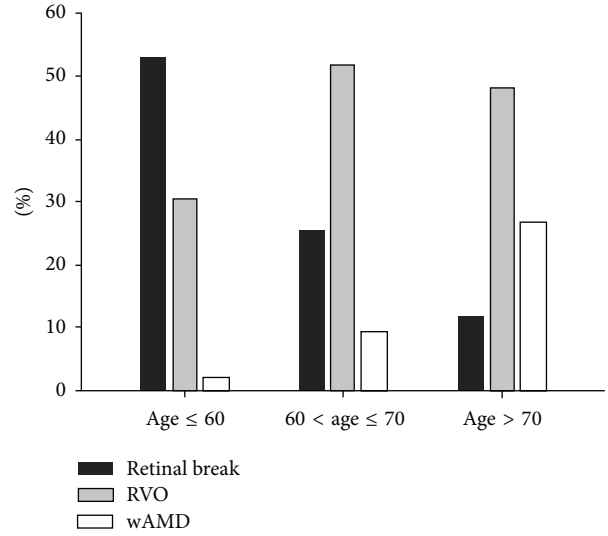

Figure 1: Causes of acute-onset vitreous hemorrhage of unknown origin according to age. Among patients aged ≤60 years, retinal break was the main cause of acute-onset VH of preoperatively unknown origin. Moreover, the proportion of cases of acute-onset VH of preoperatively unknown origin that was due to retinal break declined with age. In contrast to retinal break, the proportion of vitreous hemorrhage due to wAMD increased with age. Among patients aged >60 years, RVO was the most common cause of acute-onset VH of preoperatively unknown origin. RVO, retinal vein occlusion; wAMD, wet age-related macular degeneration.

The RSSs used to predict poor visual outcomes after vitrectomy among patients with acute-onset preoperatively unknown origin VH are shown in Table 4, and the risk scores of the included acute-onset VH of preoperatively unknown origin patients are shown in Table 5. The multivariate logistic regression model shows that old age, poor preoperative visual acuity in both the affected and fellow eyes, and drusen in the fellow eye were significantly associated with a poor visual prognosis after vitrectomy. The AUC of the scoring system was 0.907 (95% confidence interval [CI] = 0.853–0.948). Internal validation was investigated using the bootstrap validation algorithm. The optimism-corrected AUC was 0.898, which indicates the reliability of the RSS (Figure 3). In this RSS model, the maximal summation of risk score was −25. Therefore, to prevent obtaining a negative integer for the risk score, we added 25 to each estimated risk score.

Table 2: Clinical characteristics of acute-onset vitreous hemorrhage (VH) of preoperatively unknown origin.

	All	RVO	wAMD	Retinal break	Other	p
Number of eyes	169	77	21	50	24	0.001
Age (y)	63.64 ± 12.37	65.36 ± 9.82	73.29 ± 8.30	58.50 ± 11.78	60.63 ± 17.14	<0.001*
Sex (male/female)	83/86	33/41	11/10	31/19	8/16	0.216†
Right/left	88/81	38/36	9/12	29/21	12/12	0.093†
Follow-up duration (mo.)	13.24 ± 14.52	11.34 ± 11.59	15.62 ± 19.19	15.56 ± 17.00	12.21 ± 12.49	0.360*
Gauge of surgery						0.098†
20-gauge	19/169 (11.2%)	10/74 (13.5%)	5/21 (23.8%)	3/50 (6.0%)	1/24 (4.2%)	
23/25-gauge	150/169 (88.8%)	64/74 (86.5%)	16/21 (76.2%)	47/50 (94.0%)	23/24 (95.8%)	
Tamponade						<0.001†
No tamponade	56/169 (33.1%)	34/74 (45.9%)	4/21 (19.0%)	9/50 (18.0%)	9/24 (37.5%)	
Air	55/169 (32.5%)	32/74 (43.2%)	1/21 (4.8%)	13/50 (26.0%)	9/24 (37.5%)	
C_3F_8	24/169 (14.2%)	3/74 (4.1%)	1/21 (4.8%)	19/50 (38.0%)	1/24 (4.2%)	
Silicone oil	34/169 (20.1%)	5/74 (6.8%)	15/21 (71.4%)	9/50 (18.0%)	5/24 (20.8%)	
Systemic disease						
Hypertension	92/169 (54.4%)	48/74 (64.9%)	13/21 (61.9%)	17/50 (34.0%)	14/24 (54.4%)	0.006†
Duration (y)	8.44 ± 7.85	8.55 ± 8.46	6.92 ± 5.39	6.90 ± 5.52	11.57 ± 9.76	0.329*
Diabetes	20/169 (11.8%)	9/74 (12.2%)	2/21 (9.5%)	7/50 (14/0%)	2/24 (8.3%)	0.891†
Duration (y)	9.56 ± 8.46	7.56 ± 4.95	6.50 ± 4.95	12.71 ± 4.45	13.44 ± 9.50	0.658*
Anticoagulant	51/169 (30.2%)	34/74 (45.9%)	3/21 (14.3%)	8/50 (16.0%)	6/24 (25.0%)	0.001†

RVO, retinal vein occlusion; wAMD, wet age-related macular degeneration.
*According to one-way ANOVA with the Bonferroni post test.
†According to the Chi-square test.

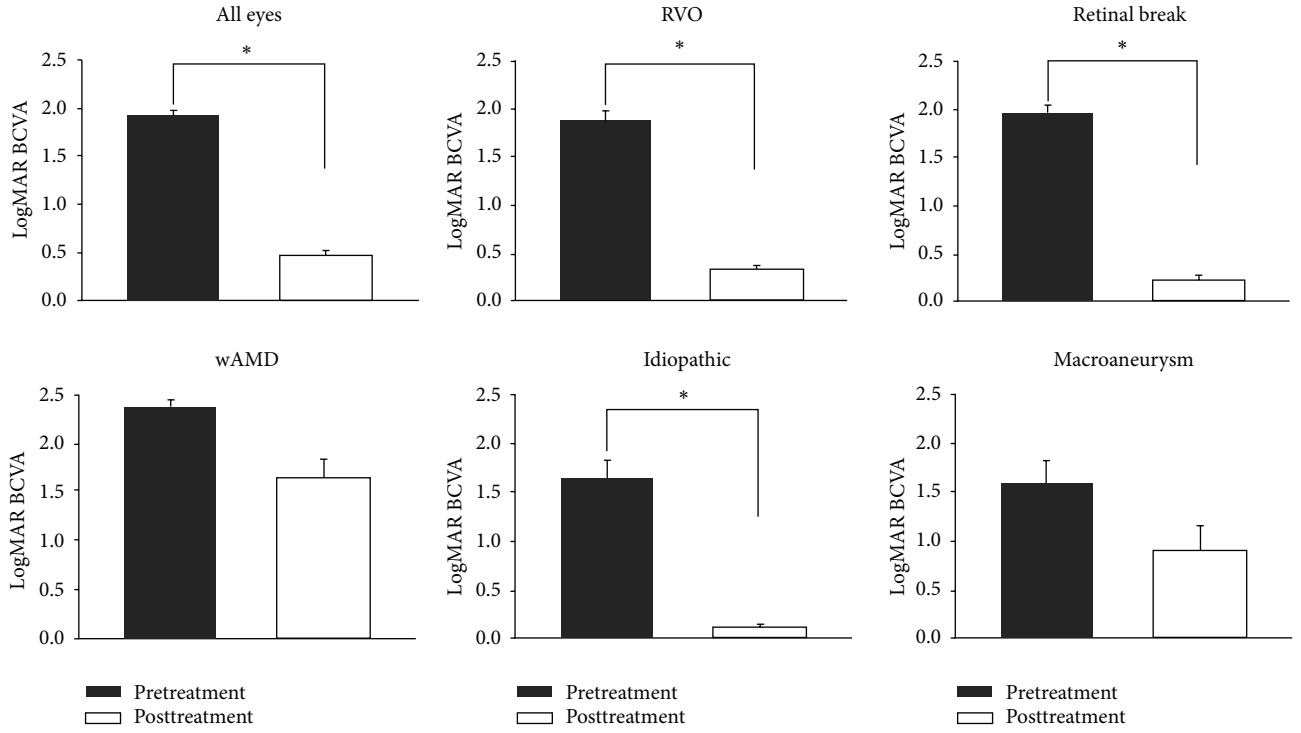

Figure 2: Changes in visual acuity after vitrectomy according to postoperative diagnosis. In the retinal vein occlusion, retinal break, and idiopathic groups, BCVA significantly improved after vitrectomy. However, visual improvement was not seen after vitrectomy among patients with wet age-related macular degeneration.

Table 3: Findings in the fellow eye of acute-onset vitreous hemorrhage (VH) of preoperatively unknown origin.

	All	RVO	wAMD	Retinal break	p
LogMAR BCVA	0.19 ± 0.46	0.17 ± 0.38	0.44 ± 0.45	0.05 ± 0.09	<0.001*
Fundus finding					
Normal	131/169 (77.5%)	61/74 (82.4%)	4/21 (19.0%)	45/50 (90.0%)	<0.001†
Drusen	21/169 (12.4%)	5/74 (6.8%)	15/21 (71.4%)	1/50 (2.0%)	<0.001†
Retinal break	5/169 (3.0%)	0/74 (0.0%)	0/21 (0.0%)	4/50 (8.0%)	0.020
RVO	1/169 (0.6%)	3/74 (4.1%)	1/21 (4.8%)	0/50 (0.0%)	0.334
Others	8/169 (4.7%)	5/74 (6.8%)	1/21 (4.8%)	0/50 (0.0%)	0.177

BCVA, best-corrected visual acuity; RVO, retinal vein occlusion; wAMD, wet age-related macular degeneration; AMD, age-related macular degeneration.
*According to one-way ANOVA with the Bonferroni post test.
†According to the Chi-square test.

Table 4: Risk scoring system used to predict poor visual outcomes after vitrectomy in patients with acute-onset vitreous hemorrhage (VH) of preoperatively unknown origin.

Categories	Reference value (W)	Beta	Beta($W - W_{ref}$)	Point = beta($W - W_{ref}$)/B [Clarify]	Score
Age					
24–40	33.5 (W_{ref})		0	0	0
40–49	44.5		−0.043	−1.0000854	−1
50–59	54.5	−0.004	−0.082	−1.9092539	−2
60–69	64.5		−0.121	−2.8184224	−3
>70	78.5		−0.176	−4.0912583	−4
Preoperative LogMAR BCVA in affected eye					
0–0.5	0.25 (W_{ref})		0	0	0
0.5–1.0	0.75		−0.056	−1.3076873	−1
1.0–1.5	1.25	−0.112	−0.112	−2.6153746	−3
1.5–2.0	1.75		−0.169	−3.9230619	−4
2.0–2.5	2.25		−0.225	−5.2307491	−5
2.5–3.0	2.75		−0.281	−6.5384364	−7
Preoperative LogMAR BCVA in the fellow eye					
0–0.5	0.25 (W_{ref})		0	0	0
0.5–1.0	0.75		−0.048101477	−1.118639	−1
1.0–1.5	1.25	−0.096	−0.096202955	−2.237278	−2
1.5–2.0	1.75		−0.144304432	−3.355917	−3
2.0–2.5	2.25		−0.19240591	−4.474556	−4
2.5–3.0	2.75		−0.240507387	−5.5931951	−6
Drusen in the fellow eye					
no	0 (W_{ref})	−0.358	0	0	0
yes	1		−0.358	−8.3255814	−8

BCVA, best-corrected visual acuity.
W: reference value.
Beta: beta coefficients used in the logistic regression model.
B: number of regression units that correspond to 1 point. We let $B = 0.043$ reflect the increase in risk associated with 10-year increases in age.

4. Discussion

The etiology of VH is diverse, and the cause of VH is identified at the initial visit in 32–79% of eyes with VH [4, 6]. Most cases of acute-onset VH are caused by PDR, trauma, retinal break, proliferative retinopathy after RVO, or posterior vitreous detachment without retinal detachment [2–6]. However, it is often difficult to determine the underlying causes of acute-onset VH because dense VH obscures retinal examination. Lean et al. reported that no diagnosis was made at initial presentation in 21.0% of VH eyes, and Lindgren et al. reported that the underlying disease could not be determined in 68% of VH eyes [2, 4, 6, 19, 20]. Little is known about the causes and visual prognosis of preoperatively unknown origin VH. Therefore, in this study, we analyzed the causes and visual prognosis of acute-onset VH of preoperatively unknown origin.

We excluded VH cases that were associated with PDR. Diabetic retinopathy was assumed to be the cause of acute-onset VH of preoperatively unknown origin if the patient

Table 5: Risk scores of study patients with acute-onset vitreous hemorrhage (VH) of preoperatively unknown origin.

Score*	Estimated chance having good vision	All included patients	
		Snellen visual acuity < 20/200 after vitrectomy (no.)	Snellen visual acuity ≥ 20/200 after vitrectomy (no.)
0	0.448		
1	0.459		
2	0.470	1	0
3	0.480		
4	0.491	1	0
5	0.502	1	0
6	0.512	2	2
7	0.523	1	1
8	0.534	3	4
9	0.545	1	2
10	0.555	2	1
11	0.566		
12	0.576	2	1
13	0.587	0	1
14	0.597	1	2
15	0.608	2	4
16	0.618	6	17
17	0.628	1	37
18	0.638	0	29
19	0.648	0	19
20	0.657	0	9
21	0.667	0	5
22	0.677	0	6
23	0.686	0	3
24	0.695	0	2
25	0.704		
Total		24	145

*Estimated risk score after 25 was added to prevent a negative integer as the risk score.

had a medical history of diabetes and fellow eye findings of PDR or severe nonproliferative diabetic retinopathy (NPDR). Therefore, patients with more than mild NPDR in the fellow eye were excluded. After excluding diabetic retinopathy, BRVO was the most common cause of acute-onset VH of preoperatively unknown origin VH (74 eyes [43.8%]).

According to previously published studies, except for PDR, retinal break is the most common cause of acute-onset VH [2, 4, 6, 19, 20]. Unlike previous studies, retinal break was the second most common cause of acute-onset VH of preoperatively unknown origin. This discrepancy between results can be explained by the characteristics of VH caused by retinal breaks. VH caused by a retinal break might be less severe and clear more rapidly [10]. Therefore, retinal breaks that lead to acute-onset VH can be found without vitrectomy. As a result, although retinal break may be the most common cause of acute-onset VH, the proportion of cases for which retinal break is the cause of acute-onset VH of preoperatively unknown origin was relatively small.

In the current study, we analyzed the visual prognosis after vitrectomy of acute-onset VH of preoperatively unknown origin. The overall visual prognosis of unknown origin VH was relatively good. Following vitrectomy, the logMAR BCVA improved from 1.93 ± 0.59 to 0.47 ± 0.71. However, the visual prognosis differed according to the underlying cause of preoperatively unknown origin VH. The preoperative and postoperative logMAR BCVA values of wAMD patients were significantly worse than those of patients with retinal break or RVO.

We believe that these differences in visual prognosis according to cause resulted from the different rates of foveal involvement. In our present study, only 10 cases (13.5%) of RVO involved the fovea and caused VH. In cases of RVO involving the fovea, patients were already diagnosed with RVO before the formation of retinal neovascularization, which eventually leads to VH. Therefore, the rate of foveal involvement was relatively small as a cause of acute-onset VH of preoperatively unknown origin. Because of the lower rate

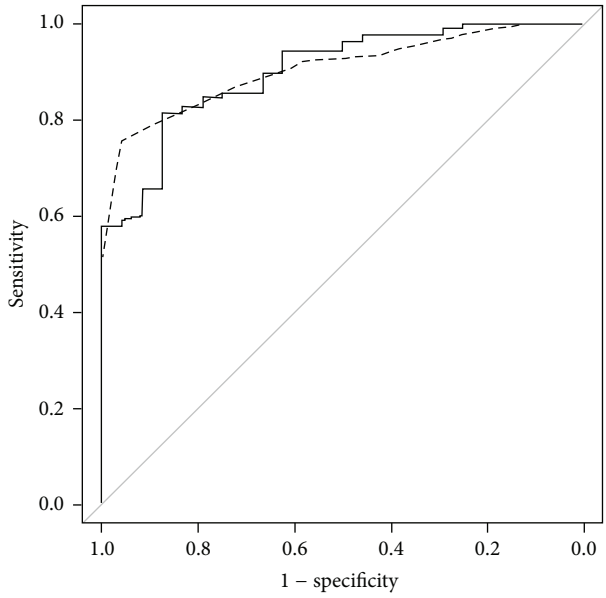

Figure 3: ROC curves of the scoring system used to predict the visual prognosis of acute-onset VH of preoperatively unknown origin. The solid line shows the ROC curves of four variables (age, baseline BCVA of the affected eye, baseline BCVA of the unaffected eye, and age-related macular changes in the fellow eyes), which were significantly associated with poor visual acuity following vitrectomy. The dashed line shows the ROC curve of the scoring system. The AUC of the scoring system was 0.907 (95% CI = 0.853–0.948).

of foveal involvement, the visual prognosis of RVO as cause of acute-onset VH of preoperatively unknown origin was relatively good. By contrast, among wAMD patients with acute-onset VH of preoperatively unknown origin, the visual prognosis was poor due to subretinal disciform scar formation.

We also developed an RSS to predict the visual prognosis of unknown origin VH. Our multivariate logistic regression model showed that (1) old age, (2) poor preoperative visual acuity in the affected eye, (3) poor preoperative visual acuity in the fellow eye, and (4) drusen in the fellow eye are significantly associated with poor visual prognosis after vitrectomy. The sensitivity and specificity values of this scoring system were 0.88 and 0.71, respectively. With this simple RSS, we could predict the visual prognosis of acute-onset preoperatively unknown origin VH following vitrectomy. Because of the retrospective nature of this study, we could not validate the accuracy of this RSS. We therefore plan to conduct a future prospective study to validate this system.

To the best of our knowledge, this is the first study to analyze the causes and visual prognosis of acute-onset VH of preoperatively unknown origin. However, our analyses had limitations that are inherent to its retrospective design. In addition, this study was conducted at a single tertiary referring center, which might have caused some selection bias. The sample size of this study was also relatively small, which may have limited the statistical strength of the analysis. Therefore, future studies that examine a larger number of patients are needed to confirm the causes and visual prognosis of acute-onset VH.

In conclusion, the first, second, and third most common causes of acute-onset VH of preoperatively unknown origin were RVO, retinal break, and wAMD, respectively. In addition, the most common cause of acute-onset VH of preoperatively unknown origin changed according to patient age. The visual prognosis of unknown origin VH was relatively good, except among AMD patients. After considering age, preoperative BCVA, and the characteristics of the fellow eye, we predicted visual prognosis of unknown VH. Furthermore, the characteristics of patients with poor visual outcomes following vitrectomy include (1) old age, (2) low preoperative visual acuity in the affected and fellow eyes, and (3) age-related macular changes in the fellow eye. Therefore, in these patients, we expect visual prognosis of acute-onset VH of preoperatively unknown origin to be poor.

Financial Disclosures

All authors certify that they have no affiliations with or involvement in any organization or entity with any financial interest (such as honoraria; educational grants; participation in speakers' bureaus; membership, employment, consultancies, stock ownership, or other equity interest; and expert testimony or patent-licensing arrangements), or nonfinancial interest (such as personal or professional relationships, affiliations, knowledge or beliefs) in the subject matter or materials discussed in this paper.

Conflict of Interests

The authors declare that there is no conflict of interests regarding the publication of this paper.

Authors' Contribution

Dong Yoon Kim, Joo Yong Lee, and June-Gone Kim designed the study. Dong Yoon Kim, Seunghee Baek, and Joo Yong Lee managed the data. Dong Yoon Kim, Joo Yong Lee, Soo Geun Joe, June-Gone Kim, and Joo Yong Lee analyzed, collected, and interpreted the data. Dong Yoon Kim, Seunghee Baek, Joo Yong Lee, Soo Geun Joe, June-Gone Kim, and Joo Yong Lee prepared the paper, performed the statistical analysis, and interpreted the data. Dong Yoon Kim, Joo Yong Lee, Soo Geun Joe, Seunghee Baek, June-Gone Kim, and Joo Yong Lee reviewed and approved the paper.

Acknowledgment

This study was supported by a grant (2014-7206) from the Asan Institute for Life Sciences, Seoul, Republic of Korea.

References

[1] C. W. Spraul and H. E. Grossniklaus, "Vitreous hemorrhage," *Survey of Ophthalmology*, vol. 42, no. 1, pp. 3–39, 1997.

[2] R. L. Winslow and B. C. Taylor, "Spontaneous vitreous hemorrhage: etiology and management," *Southern Medical Journal*, vol. 73, no. 11, pp. 1450–1452, 1980.

[3] M.-R. Dana, M. S. Werner, M. A. G. Viana, and M. J. Shapiro, "Spontaneous and traumatic vitreous hemorrhage," *Ophthalmology*, vol. 100, no. 9, pp. 1377–1383, 1993.

[4] J. S. Lean and Z. Gregor, "The acute vitreous haemorrhage," *British Journal of Ophthalmology*, vol. 64, no. 7, pp. 469–471, 1980.

[5] G. Lindgren and B. Lindblom, "Causes of vitreous hemorrhage," *Current Opinion in Ophthalmology*, vol. 7, no. 3, pp. 13–19, 1996.

[6] G. Lindgren, L. Sjodell, and B. Lindblom, "A prospective study of dense spontaneous vitreous hemorrhage," *American Journal of Ophthalmology*, vol. 119, no. 4, pp. 458–465, 1995.

[7] "Argon laser photocoagulation for macular edema in branch vein occlusion. The Branch Vein Occlusion Study Group," *The American Journal of Ophthalmology*, vol. 98, no. 3, pp. 271–282, 1984.

[8] "Argon laser scatter photocoagulation for prevention of neovascularization and vitreous hemorrhage in branch vein occlusion. A randomized clinical trial. Branch Vein Occlusion Study Group," *Archives of Ophthalmology*, vol. 104, no. 1, pp. 34–41, 1986.

[9] A. Yeshaya and G. Treister, "Pars plana vitrectomy for vitreous hemorrhage and retinal vein occlusion," *Annals of Ophthalmology*, vol. 15, no. 7, pp. 615–617, 1983.

[10] M. H. Seelenfreund, I. Sternberg, I. Hirsch, and B.-Z. Silverstone, "Retinal tears with total vitreous hemorrhage," *American Journal of Ophthalmology*, vol. 95, no. 5, pp. 659–662, 1983.

[11] "Early vitrectomy for severe proliferative diabetic retinopathy in eyes with useful vision. Results of a randomized trial—diabetic retinopathy vitrectomy study report 3. The Diabetic Retinopathy Vitrectomy Study Research Group," *Ophthalmology*, vol. 95, no. 10, pp. 1307–1320, 1988.

[12] "Early vitrectomy for severe vitreous hemorrhage in diabetic retinopathy. Two-year results of a randomized trial. Diabetic Retinopathy Vitrectomy Study report 2. The Diabetic Retinopathy Vitrectomy Study Research Group," *Archives of Ophthalmology*, vol. 103, no. 11, pp. 1644–1652, 1985.

[13] F. El Baba, W. H. Jarrett II, and T. S. Harbin Jr., "Massive hemorrhage complicating age-related macular degeneration. Clinicopathologic correlation and role of anticoagulants," *Ophthalmology*, vol. 93, no. 12, pp. 1581–1592, 1986.

[14] M. Cordido, J. Fernandez-Vigo, J. Fandino, and M. Sanchez-Salorio, "Natural evolution of massive vitreous hemorrhage in diabetic retinopathy," *Retina*, vol. 8, no. 2, pp. 96–101, 1988.

[15] H. Lincoff, I. Kreissig, and M. Wolkstein, "Acute vitreous haemorrhage: a clinical report," *British Journal of Ophthalmology*, vol. 60, no. 6, pp. 454–458, 1976.

[16] C. Lange, N. Feltgen, B. Junker, K. Schulze-Bonsel, and M. Bach, "Resolving the clinical acuity categories 'hand motion' and 'counting fingers' using the Freiburg Visual Acuity Test (FrACT)," *Graefe's Archive for Clinical and Experimental Ophthalmology*, vol. 247, no. 1, pp. 137–142, 2009.

[17] E. W. Steyerberg, F. E. Harrell Jr., G. J. J. M. Borsboom, M. J. C. Eijkemans, Y. Vergouwe, and J. D. F. Habbema, "Internal validation of predictive models: efficiency of some procedures for logistic regression analysis," *Journal of Clinical Epidemiology*, vol. 54, no. 8, pp. 774–781, 2001.

[18] L. M. Sullivan, J. M. Massaro, and R. B. D'Agostino Sr., "Presentation of multivariate data for clinical use: the Framingham Study risk score functions," *Statistics in Medicine*, vol. 23, no. 10, pp. 1631–1660, 2004.

[19] P. H. Morse, A. Aminlari, and H. G. Scheie, "Spontaneous vitreous hemorrhage," *Archives of Ophthalmology*, vol. 92, no. 4, pp. 297–298, 1974.

[20] R. W. Butner and A. R. McPherson, "Spontaneous vitreous hemorrhage," *Annals of Ophthalmology*, vol. 14, no. 3, pp. 268–270, 1982.

Hindawi Publishing Corporation
Journal of Ophthalmology
Volume 2015, Article ID 369312, 9 pages
http://dx.doi.org/10.1155/2015/369312

Research Article

Responses of Multipotent Retinal Stem Cells to IL-1β, IL-18, or IL-17

Shida Chen,[1,2] Defen Shen,[1] Nicholas A. Popp,[1] Alexander J. Ogilvy,[3] Jingsheng Tuo,[1] Mones Abu-Asab,[3] Ting Xie,[4,5] and Chi-Chao Chan[1]

[1]*Laboratory of Immunology, National Eye Institute, National Institutes of Health, Bethesda, MD 20892, USA*
[2]*Zhongshan Ophthalmic Center, Sun Yat-sen University, Guangzhou 510060, China*
[3]*Histology Core, National Eye Institute, National Institutes of Health, Bethesda, MD 20892, USA*
[4]*Stowers Institute for Medical Research, Kansas City, MO 64110, USA*
[5]*Department of Anatomy and Cell Biology, University of Kansas School of Medicine, Kansas City, KS 66160, USA*

Correspondence should be addressed to Chi-Chao Chan; chanc@nei.nih.gov

Received 29 March 2015; Accepted 14 July 2015

Academic Editor: Naoshi Kondo

Copyright © 2015 Shida Chen et al. This is an open access article distributed under the Creative Commons Attribution License, which permits unrestricted use, distribution, and reproduction in any medium, provided the original work is properly cited.

Purpose. To investigate how multipotent retinal stem cells (RSCs) isolated from mice respond to the proinflammatory signaling molecules, IL-1β, IL-18, and IL-17A. *Materials and Methods*. RSCs were cultured in a specific culture medium and were treated with these cytokines. Cell viability was detected by MTT assay; ultrastructure was evaluated by transmission electron microscopy; expression of IL-17rc and proapoptotic proteins was detected by immunocytochemistry and expression of *Il-6* and *Il-17a* was detected by quantitative RT-PCR. As a comparison, primary mouse retinal pigment epithelium (RPE) cells were also treated with IL-1β, IL-18, or IL-17A and analyzed for the expression of *Il-6* and *Il-17rc*. *Results*. Treatment with IL-1β, IL-18, or IL-17A decreased RSC viability in a dose-dependent fashion and led to damage in cellular ultrastructure including pyroptotic and/or necroptotic cells. IL-1β and IL-18 could induce proapoptotic protein expression. All treatments induced significantly higher expression of *Il-6* and *Il-17rc* in both cells. However, neither IL-1β nor IL-18 could induce *Il-17a* expression in RSCs. *Conclusions*. IL-1β, IL-18, and IL-17A induce retinal cell death via pyroptosis/necroptosis and apoptosis. They also provoke proinflammatory responses in RSCs. Though IL-1β and IL-18 could not induce *Il-17a* expression in RSCs, they both increase *Il-17rc* expression, which may mediate the effect of *Il-17a*.

1. Introduction

Age-related macular degeneration (AMD) is a progressive disease characterized by the degeneration of retinal pigment epithelium (RPE) and photoreceptor atrophy in the macula [1, 2]. Inflammation, particularly innate immunity, is implicated in AMD pathogenesis [3]. Recently, the inflammasome, a multimeric protein consisting of nod-like receptor (NLR), apoptosis-associated speck-like domain contains a caspase-recruitment domain (ASC), and pro-caspase-1 plays a central role in innate immunity and has been implicated in the pathogenesis of AMD [4, 5]. Activation of the NLRP3 inflammasome results in caspase-1 cleaving pro-IL-1β and pro-IL-18 into their mature proinflammatory forms in macrophages and RPE cells [5, 6]. However, the direct effect of IL-1β and IL-18 on other retinal cells has not been well studied.

In combination with IL-23, IL-1β or IL-18 can induce interleukin-17A (IL-17A) production by Th17 cells, $\gamma\delta$ T cells, and iNKT cells [7–10]. Growing evidence has implicated IL-17A involvement in AMD pathogenesis. Higher levels of IL-17A are found in the serum and macular tissues of the AMD patients when compared to age-matched controls [11, 12]. *In vitro*, IL-17A is cytotoxic to ARPE-19 cells, characterized by the accumulation of cytoplasmic lipids, autophagosome formation, and the presence of cleaved caspase-9 and cleaved caspase-3 [12]. IL-17RC, a member of IL-17R family and the primary receptor for IL-17A, is highly expressed in AMD macular tissues and in ARPE-19 cells [12]. In a study of

twins with discordant AMD status, hypomethylation of the IL-17RC promoter was found in those with AMD. This finding was correlated with elevated expression of IL-17RC in peripheral blood cells as well as the macular tissue of AMD patients [13]. However, the direct effect of IL-17A on other cell types remains to be explored.

To test the hypothesis that IL-18 and IL-1β could stimulate IL-17A secretion in retinal cells, we used a mouse-derived multipotent retinal stem cell line (RSCs) as a model. RSCs are cultured stem cells from the mouse retina and can be efficiently differentiated into photoreceptor cells and all major cell types of neural retina under optimized differentiation conditions [14]. Subretinal injection of these differentiated photoreceptors into slowly degenerating *rd7* mouse eyes can form new synapses with resident retinal neurons; in fast degenerating *rd1* mouse eyes, injection of these cells can restore light response. These findings suggest that human retinal or neuronal stem cells could be useful for treating retinal degeneration in AMD [14]. We stimulated RSCs with IL-1β, IL-18, or IL-17A and characterized the inflammatory and cytotoxic responses.

2. Materials and Methods

2.1. Cell Culture and Stimulation. The RSC line was obtained from primary culture of adult CD-1 mouse neuroretina and cultured as described previously [14]. Briefly, RSCs were cultured in medium for retinal stem cells (RCM) composed of DMEM/F12 (1 : 1, Sigma, St Louis, MO, USA), insulin-transferrin-selenium-A supplement (Invitrogen, Eugene, OR, USA), 1.0 g/L bovine serum albumin (BSA, Sigma), 1.0 g/L glucose (Sigma), 1.0 g/L lactose (Sigma), 0.045 g/L proline (Sigma), 11.25 μg/mL linoleic acid (Sigma), 5 mM glutamine (Invitrogen), 2 mM nicotinamide (Sigma), 5% knockout serum replacement (Life Technologies, NY, USA), 20 ng/mL epidermal growth factor (EGF, Millipore, Billerica, MA, USA), and 20 ng/mL basic fibroblast growth factor (bFGF, R&D Systems, Minneapolis, MN, USA). Cells were passaged at 90% confluence using Accutase (Sigma). RSCs grown to 70%–80% confluence were treated with 1–100 ng/mL recombinant mouse IL-1β (R&D Systems), recombinant mouse IL-18 (MBL, Woods Hole, MA, USA), or recombinant mouse IL-17 (R&D Systems) for 24 hours.

2.2. Culture of Primary RPE Cells. All procedures using animals adhered to the Association for Research in Vision and Ophthalmology statement for the use of animals and the NEI's Institutional Animal Care and Use Committee approved protocols. Mouse RPE was isolated from retinas of C57/B6J mice at 6–8 weeks of age as described previously [15]. Briefly, mice were euthanized, and their eyes were enucleated. The globes were washed with PBS containing 1% penicillin-streptomycin (Sigma) and then were dissected free of periocular connective tissue. Then, the globe was placed on 2% Dispase II (neutral protease, grade II, Roche, Indianapolis, IN, USA) and incubated at 37°C for 40 min. The globe was transferred to DMEM/F12 media, the anterior segment was removed, and the retina containing the RPE layer was dissected free. The loosely adherent RPE cell layer was gently separated from the retina and transferred to a 15 mL tube containing DMEM/F12, 20% FBS, and 1% L-glutamine-penicillin-streptomycin. Cells were then centrifuged at 1000 rpm for 5 min and resuspended. The RPE suspension was added to 6-well cell culture plates. The medium was changed after 5-6 days and every 2-3 days thereafter. The RPE cells between two and three passages were stimulated with 100 ng/mL recombinant mouse IL-1β (R&D Systems), 10 ng/mL recombinant mouse IL-18 (MBL), or 10 ng/mL recombinant mouse IL-17 (R&D Systems) for 24 hours.

2.3. MTT Assay. The assessment of cell viability was performed using a 3-(4,5-dimethylthiazol-2-yl)-2,5-diphenyl tetrazolium bromide (MTT) assay in RSCs as described previously [15]. Briefly, cells were seeded at 80% confluence to 96-well culture plates. After stimulation with IL-1β, IL-18, or IL-17A for 24 hours, cells were washed with PBS and incubated with 20 μL of 5 mg/mL MTT solution (Sigma) for 4 h at 37°C. The medium was aspirated and 200 μL DMSO was added to each well. Plates were then shaken for 15 min at room temperature. Cell viability was determined by measuring the optical density at 570 nm using an ELISA plate reader (BioTek, Burlington, VT, USA). Cell viability represented the optical density ratio of stimulated cells relative to that of unstimulated cells.

2.4. Transmission Electron Microscopy. For transmission electron microscopy (TEM), cells were fixed in glutaraldehyde (2.5%, PBS buffered) for 24 hours, then suspended in warm low-melting point agarose (1.5%), pelleted down, and refrigerated overnight at 4°C; solidified pellets were rinsed with PBS three times, doubly-fixed with osmium tetroxide, rinsed again three times with PBS, dehydrated in ethanol, and embedded in Spurr's epoxy resin. Ultrathin sections (100 nm) were mounted on 200 lines/inch copper grids, double-stained with uranyl acetate and lead citrate, and viewed with a JEOL JEM-1010 transmission electron microscope.

2.5. Immunocytochemistry. The cells were seeded into 2-well chamber slides, and stimulation was performed at 70% confluence. After stimulation, cells were fixed with acetone, blocked with 1% BSA, and incubated overnight with the following primary antibodies: rabbit anti-mouse FasL (1 : 100, Santa Cruz, Dallas, Texas, USA); rabbit anti-mouse Fas (1 : 100, Santa Cruz); rabbit anti-mouse cleaved caspase-3 (1 : 200, Cell Signaling Technology, Danvers, MA, USA); rabbit anti-mouse cleaved caspase-9 (1 : 200 Cell Signaling Technology). After washing with PBS, secondary antibodies conjugated to either Alexa-488 or Alexa-555 (1 : 500, Invitrogen) were added and incubated for 1 h. After rinsing with PBS, cells were counterstained with 40, 6-diamidino-2-phenylindole dihydrochloride (DAPI, 1 : 1000, Invitrogen) for 5 min. The stained cells were examined under Zeiss 700 Confocal microscope with Zen software.

2.6. RNA Isolation and Quantitative RT-PCR. Total RNA was extracted from RSCs by using an RNeasy Mini Kit (Qiagen, Hilden, Germany), and equal amounts of RNA were synthesized to cDNA with Superscript II RNase H Reverse Transcriptase (Invitrogen) according to the manufacturer's instructions. Quantitative RT-PCR (qRT-PCR) was performed using RT^2 SYBR Green ROX qPCR Mastermix (Qiagen). cDNA was amplified with primers *β-actin*, *Il-6*, *Il-17rc*, or *Il-17a* (Qiagen) separately for 50 cycles. All data were normalized to the *β-actin* mRNA level. Expression fold-changes were calculated by $2^{-\Delta\Delta CT}$.

2.7. Statistical Analysis. Statistical analyses were performed using SPSS version 17.0 (SPSS, Chicago, IL, USA). Unpaired *t*-tests or analysis of variance (ANOVA) were used to compare the difference among different groups. GraphPad Prism 6 software was used to make the figures. A p value <0.05 was considered statistically significant.

3. Results

3.1. Stimulation of the Expression of IL-17RC in RSCs. RSCs cultured in RCM medium maintained spindle-shaped morphology (Figure 1(a)). Because the inflammatory response in RSCs has not yet been characterized, we evaluated expression of Il-17rc, which has been implicated in AMD pathogenesis previously [12, 13]. Indeed, *Il-17rc* mRNA expression was significantly increased in a dose-dependent fashion after stimulation with each cytokine (Figure 1(b)). Further, increased expression of IL-17rc protein was detected after treatment with 100 ng/mL IL-1*β*, 10 ng/mL IL-18, or 10 ng/mL IL-17A, respectively (Figure 1(c)). Interestingly, *Il-17rc* mRNA expression was also significantly increased in primary cultured mouse RPE cells after stimulation with each cytokine (Figure 1(d)).

3.2. Proapoptotic Effect of IL-1β, IL-18, or IL-17A on RSCs. In order to test whether IL-1*β*, IL-18, or IL-17A could induce apoptosis in RSCs, cleaved caspase-3, cleaved caspase-9, Fas, and FasL were evaluated by immunohistochemistry. IL-1*β* (100 ng/mL) or IL-18 (10 ng/mL) induced the expression of all the tested proapoptotic proteins when compared to the untreated cells (Figure 2); however, IL-17A had minimal effect on the cells. Accordingly, the MTT assay results demonstrated lower RSC viability in a dose-dependent manner after the cells were treated with IL-1*β* and IL-18. Interestingly, RSCs were also less viable after treatment with IL-17A for 24 hours despite little increase in expression of any proapoptotic proteins (Figure 3).

3.3. Ultrastructural Damage in RSCs. To further elucidate the subcellular features of RSCs after treatment with IL-1*β*, IL-18, or IL-17A, cellular ultrastructure was examined. With treatment of IL-1*β* (100 ng/mL) or IL-18 (10 ng/mL), the RSCs showed autophagosome formation, mitochondrial degeneration, cytoplasmic vacuoles, and glycogen accumulation (Figure 4). The average number of autophagosomes per cell increased from 1.3 in untreated controls to 9.8, 14.3, and 11 when RSCs were stimulated with IL-1*β*, IL-18, and Il-17, respectively. A few necroptotic and pyroptotic cells with degradation of cytoplasmic contents and chromatin condensations were also noted. IL-17A (10 ng/mL) had a similar effect as IL-18, but to a lesser extent and without necroptosis (Figure 4).

3.4. Proinflammatory Effect of IL-1β, IL-18, or IL-17A on RSCs. Proinflammatory effects of IL-1*β*, IL-18, and IL-17A were also explored in RSCs. Surprisingly, only the highest concentration of IL-1*β* (100 ng/mL) induced significantly higher expression of *Il-6* transcripts in RSCs (Figure 5(a)). Both IL-18 and IL-17A induced high *Il-6* transcriptsin a dose-dependent manner (Figures 5(b)-5(c)). Consistent with these findings, IL-1*β* (100 ng/mL), IL-18 (10 ng/mL), and IL-17A (10 ng/mL) could induce higher expression of *Il-6* mRNA transcripts in primary cultured mouse RPE cells (Figure 5(d)). However, neither IL-1*β* nor IL-18 could induce detectable *Il-17a* expression from the RSCs (data not shown).

4. Discussion

RSCs can be differentiated into many types of retinal cells, including ganglion cells, bipolar cells, and photoreceptor cells. Differentiated photoreceptors from this stem cell line could effectively integrate into *rd1* or *rd7* mouse retinas, improving vision [14]. Recently, the potential for stem cell therapy in AMD has been highlighted [16, 17]. However, no extensive studies on the inflammatory response of RSCs have been performed previously. In our study, we found that RSCs indeed respond to inflammatory stimuli.

Our TEM finding of necroptosis and pyroptosis in the cells stimulated by the cytokines is unique. In contrast to apoptosis, necroptosis requires the function of RIPK3 [18, 19], which regulates the NLRP3 inflammasome [20, 21]. Pyroptosis is a caspase-dependent form of programmed cell death that differs from apoptosis. It depends on the activation of caspase-1 [22]. NLRP3, ASC, and pro-caspase-1 induce caspase-1 activation and can lead to maturation and secretion of IL-1*β* and IL-18. This suggests a link between these two cytokines and pyroptosis/necroptosis, which could be novel pathways for cell death in AMD in addition to apoptosis [23]. Further research on the role of RIPK3 and necroptosis in AMD pathogenesis is warranted.

Our findings of releasing proinflammatory cytokines are in parallel with previous studies [4, 12, 24]. We found that IL-1*β* could induce expression of IL-6 and IL-8 at both the transcript and the protein level in ARPE-19 and human RPE cells, yet this treatment had no effect on cell viability [24]. In our study, IL-1*β* could also induce *Il-6* expression in primary cultured mouse RPE cells and RSCs. However, IL-1*β* upregulated proapoptotic protein expression and decreased cell viability in RSCs, suggesting that IL-1*β* may be more destructive to these cells than to RPE cells. Indeed, the large number of autophagosomes in IL-1*β* treated RSCs supports this conclusion.

Tarallo and colleagues found that intravitreal injection of recombinant IL-18 could induce RPE degeneration in mice,

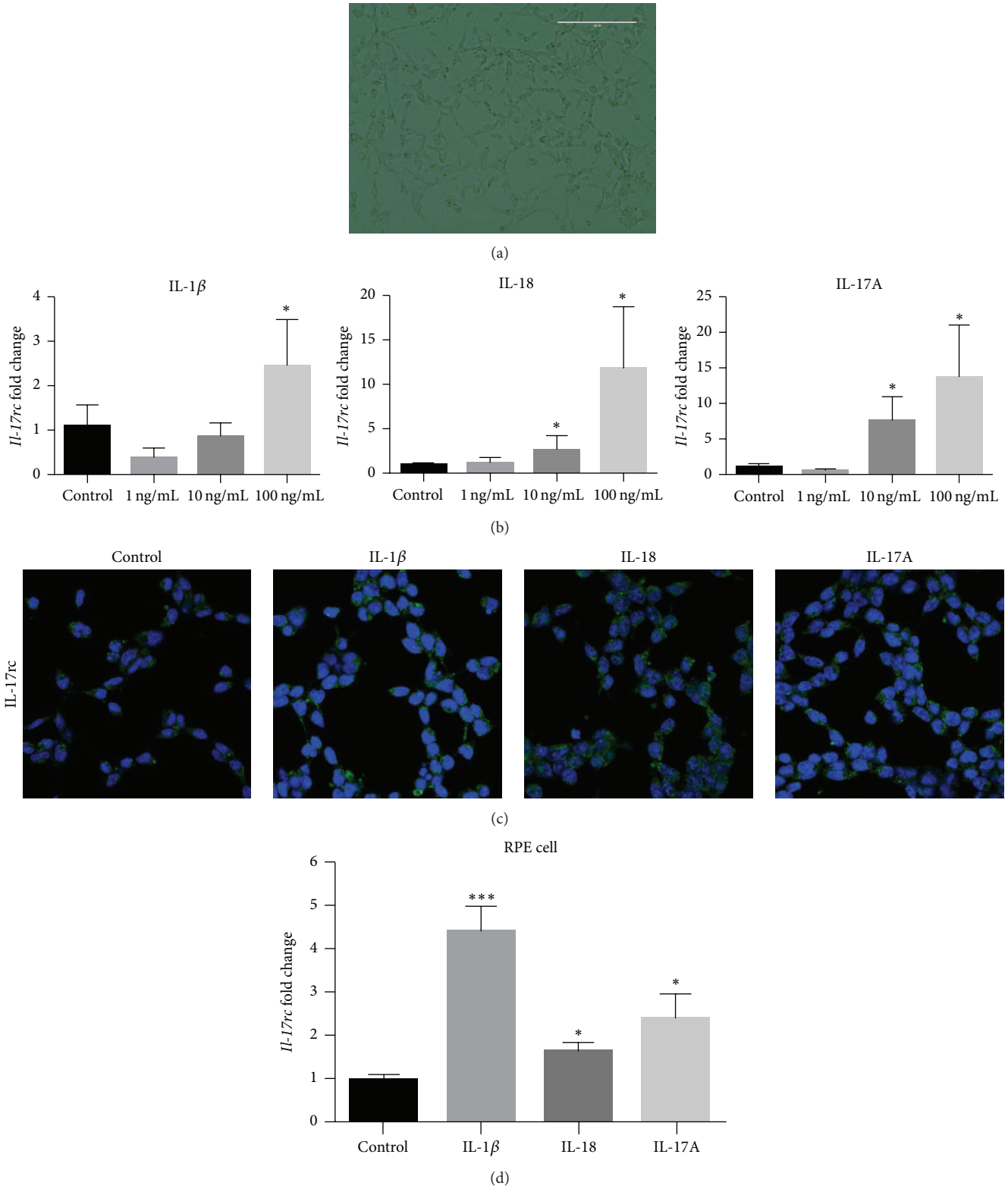

Figure 1: Morphology of the RSCs and Il-17rc expression. (a) RSCs are spindle-shaped even after passaging (scale bar: 200 μm). (b) *Il-17rc* mRNA was induced after the stimulation of IL-1β, IL18, or IL-17A in a dose-dependent manner. (c) IL-17rc protein (green) is weakly expressed in nonstimulated RSCs, but more highly expressed after stimulation with IL-1β (100 ng/mL), IL18 (10 ng/mL), or IL-17A (10 ng/mL). The nuclei were stained with DAPI (blue) (scale bar: 20 μm). (d) *Il-17rc* mRNA was induced after the stimulation of 100 ng/mL IL-1β, 10 ng/mL IL-18, or 10 ng/mL IL-17A in primary cultured mouse PRE cells. $^{*}p < 0.05$ compared to control. $^{***}p < 0.001$ compared to control.

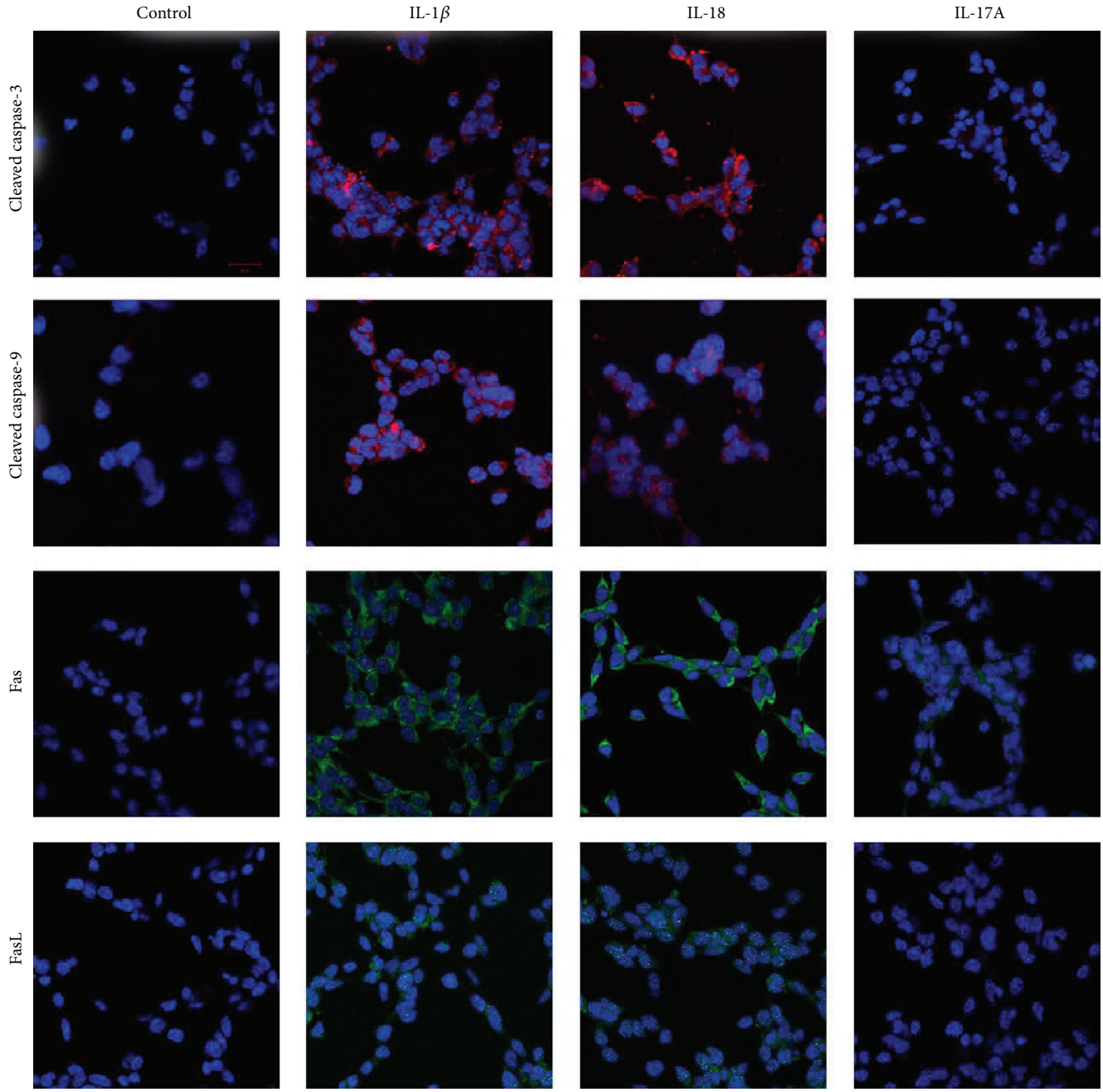

Figure 2: Proapoptotic protein expression in RSCs under stimulation. Immunofluorescence showed higher cleaved caspase-3 (red), cleaved caspase-9 (red), Fas (green), and FasL (green) expression in RSCs under stimulation with IL-1β (100 ng/mL) or IL18 (10 ng/mL). IL-17A (10 ng/mL) did not induce these proapoptotic proteins. The nuclei were stained with DAPI (blue) (scale bar: 20 μm).

and IL-18 neutralization protected against pAlu-induced RPE degeneration [4]; however, Doyle and her group reported that IL-18 has a protective role in laser induced choroid neovascularization (CNV), as intravitreally injected IL-18-neutralizing antibodies resulted in increased CNV development in mice [5]. These two seemingly conflicting studies may point to diverging roles of IL-18 in RPE versus the myeloid cells and vascular endothelium. Supporting the hypothesis that IL-18 is damaging to the neuroretina, we found that IL-18 decreased cell viability, induced necroptosis/pyroptosis by ultrastructure (Figure 4), and induced proinflammatory response (*Il-6* production) in RSCs. Furthermore, inflammatory response was similarly upregulated in primary cultured RPE cells. Interestingly, it was found that there are increased level of NLRP3 protein, *IL-1β* and *IL-18* mRNA in the RPE of donor eyes from individuals with geographic atrophy and neovascular AMD [4, 25]. Combined with our findings that both IL-1β and IL-18 could induce RSCs death *in vitro*, this mechanism may to some extent explain neuroretinal (photoreceptor) atrophy in AMD patients.

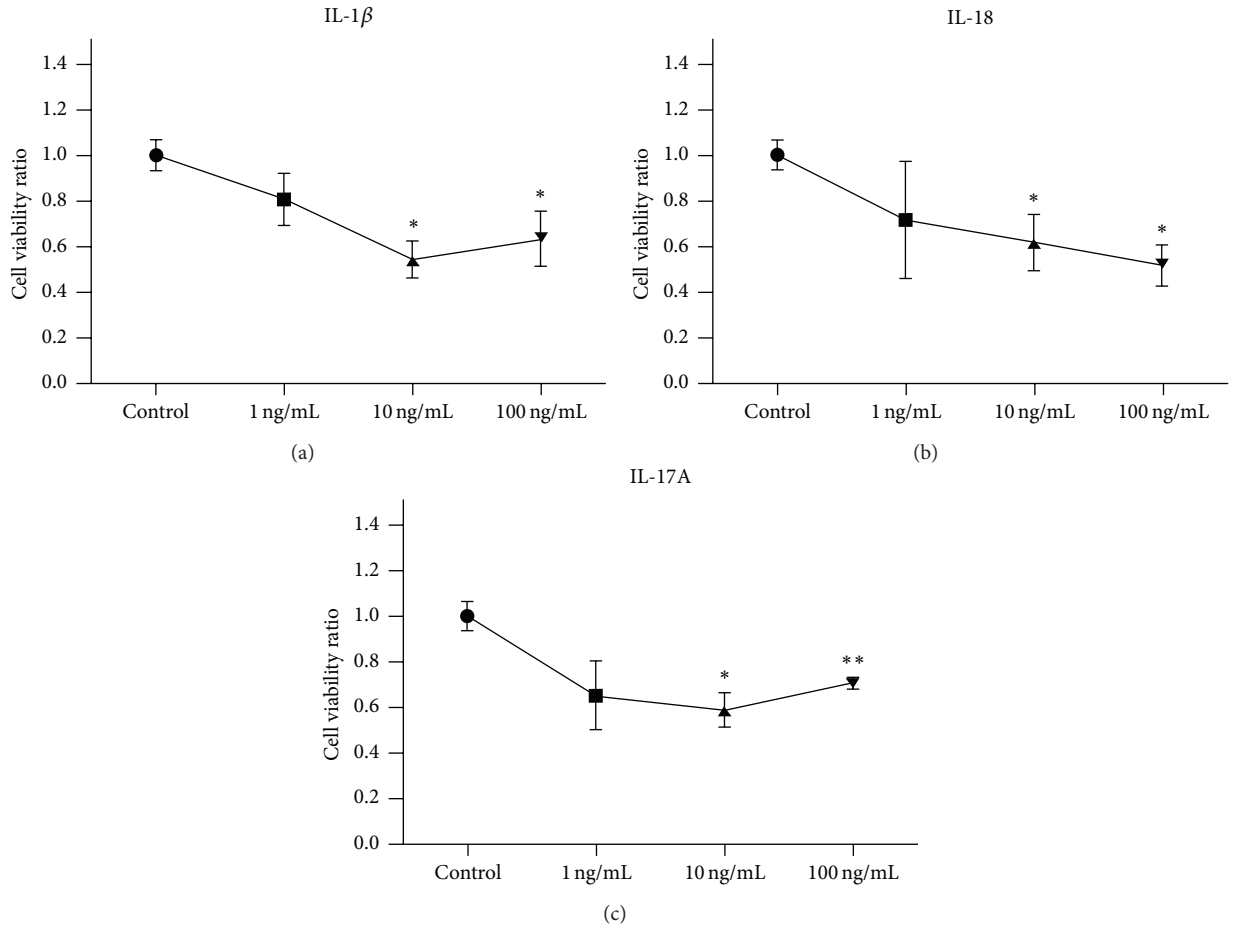

Figure 3: RSCs viability was detected with MTT assay. The RSCs were treated with IL-1β (a), IL-18 (b), or IL-17A (c) at different concentrations. $^{*}p < 0.05$; $^{**}p < 0.01$ compared to control.

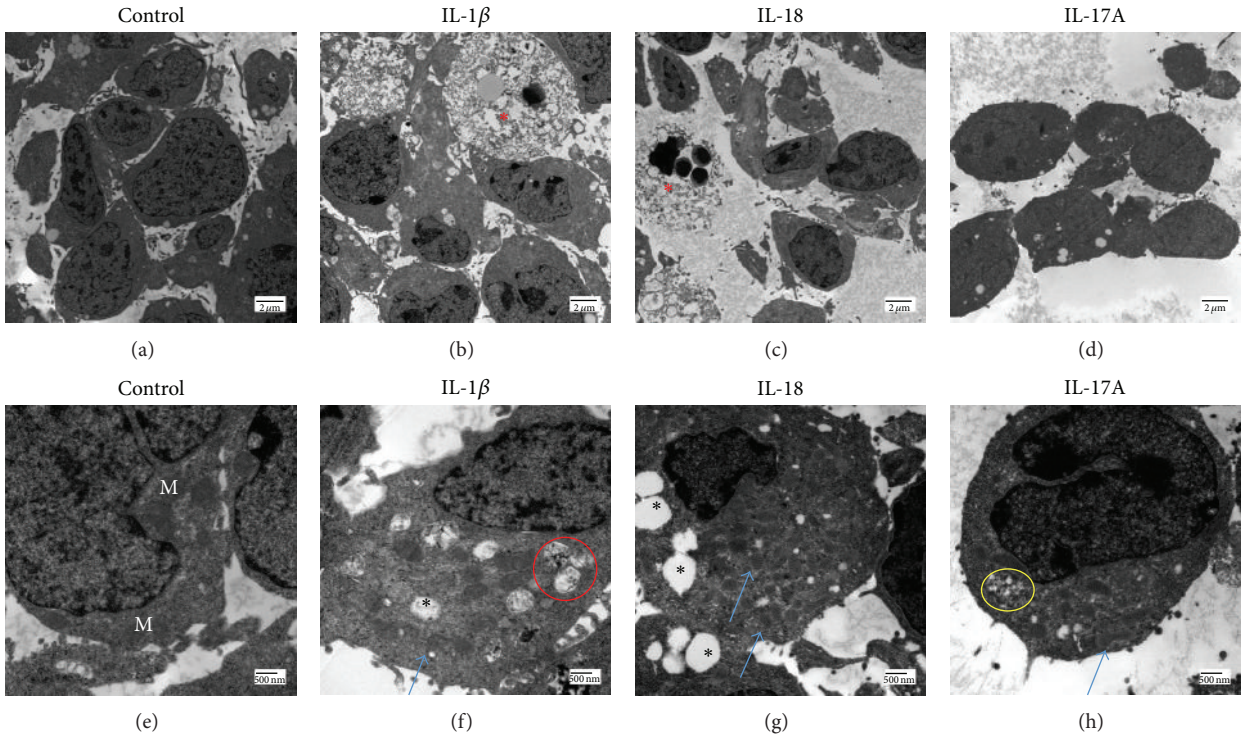

Figure 4: RSC ultrastructure change after stimulation. Control ((a), (e)), 100 ng/mL IL-1β ((b), (f)), 10 ng/mL IL-18 ((c), (g)), and 10 ng/mL IL-17A ((d), (h)) (M, mitochondria; black asterisks, cytoplasmic vacuoles; red asterisks, necroptotic cells; blue arrows, degenerated mitochondria; red circle, autophagosome; yellow circle, glycogen deposits).

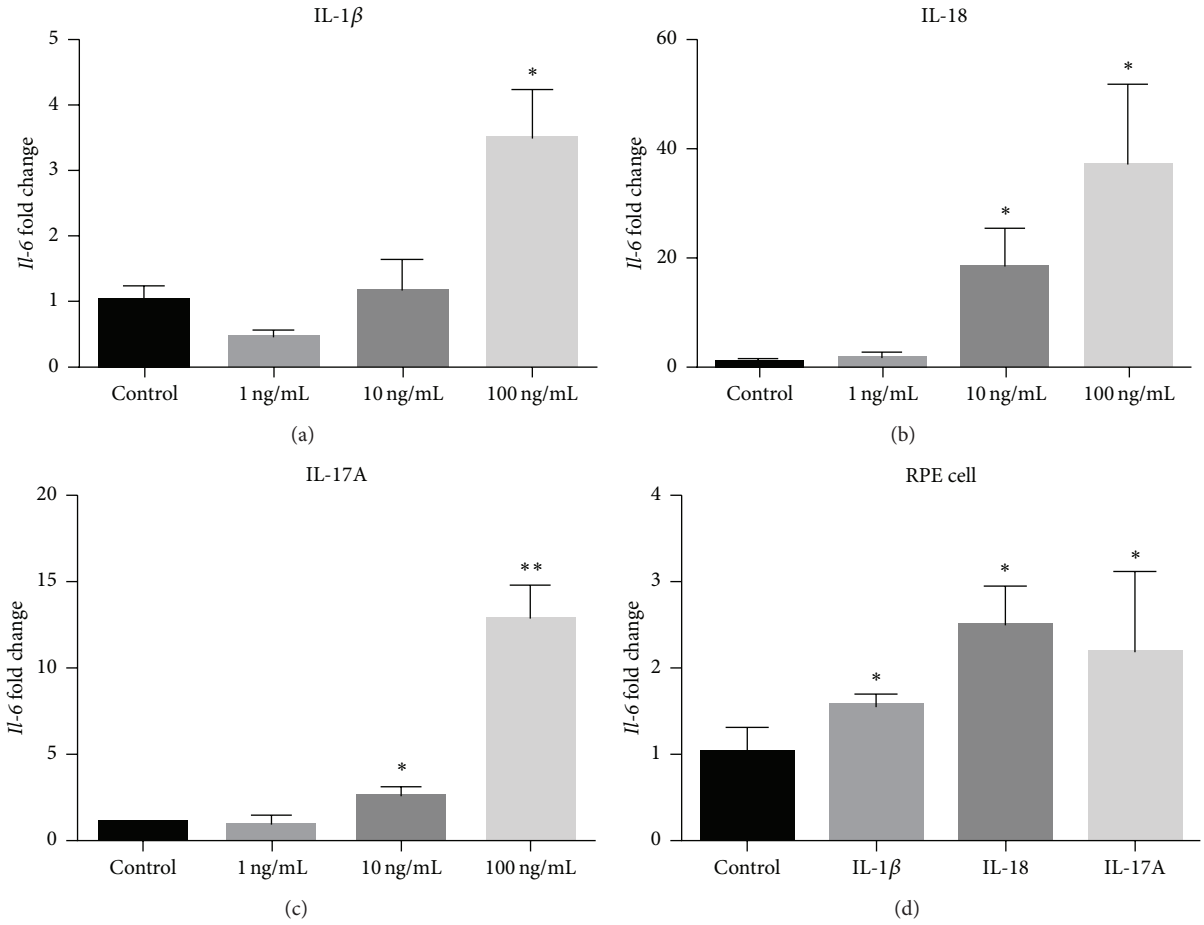

Figure 5: Proinflammatory effect of IL-1β, IL-18, or IL-17A. *Il-6* mRNA expression after stimulation with IL-1β (a), IL-18 (b), or IL-17A (c) with different concentrations in RSCs. (d) *Il-6* mRNA was induced after the stimulation of 100 ng/mL IL-1β, 10 ng/mL IL-18, or 10 ng/mL IL-17A in primary cultured mouse PRE cells. The mRNA levels of the *Il-6* were measured by quantitative RT-PCR. $^{*}p < 0.05$; $^{**}p < 0.01$ compared to control.

IL-17RC serves as an essential subunit of the IL-17 receptor complex and mediates the signal transduction and proinflammatory activities of IL-17A and IL-17F [26], which have been implicated in autoimmune and neurodegenerative diseases [27–29]. Recent research has also implicated the IL-17A/IL-17RC pathway in the pathogenesis of AMD [13, 30]; however, the exact role of IL-17A still remains elusive. In a previous study, we found that IL-17A is cytotoxic to ARPE-19 cells and decreases cell viability. Silencing of IL-17RC could prevent upregulation of cleaved caspase-3 and cleaved caspase-9 and was protective against IL-17A-mediated cell death [12]. In RSCs, IL-17A did not induce measurable proapoptotic proteins but did still decrease cell viability. This may imply that IL-17A-induced effect in RSCs proceeds through pathways other than apoptosis.

One of the most notable roles of IL-17 is its involvement in inducing and mediating proinflammatory response [31]. In synoviocytes, IL-17A could induce IL-6 expression, and knockdown of IL-17RC reversed the effect [32]. Interestingly, we found that not only IL-17A but also IL-1β and IL-18 could induce *Il-6* expression in RSCs and RPE cells. Generally, IL-6 is an important proinflammatory cytokine and has been associated with incidence of early AMD [33]. Furthermore, elevated plasma IL-6 was found in AMD patients with the CC variant in the CFH Y402H polymorphism, indicating a potential role for IL-6 in inflammation-related damage in AMD pathogenesis [34]. It has also been shown that IL-6 can contribute to Th17 cell differentiation from naïve T cells [35]. IL-1β combined with IL-23 can promote IL-17 production in naïve and memory T cells [36, 37]. Thus, IL-6 secretion by RSCs or RPE cells could result in a positive feedback loop through which Th17 and $\gamma\delta$ cells are locally induced. Although neither IL-1β nor IL-18 led to increased expression of *Il-17a* in RSCs, both could independently induce *Il-17rc* expression, which may amplify the effect of IL-17A. Interestingly, primary cultured RPE cells could also express notably higher *Il-17rc* and *Il-6* under the stimulation of IL-1β, IL-18, or IL-17A. These findings may account for a potential mechanism of IL-17A-induced pathogenesis in AMD via IL-6 production.

There are some limitations in this study. First, we only explored the response of RSCs, not the differentiated mature neuroretinal cells to IL-1β, IL-18, and IL-17A; in future studies, we plan to differentiate the RSCs to photoreceptor

cells and explore their response to these cytokines, which will be a better model for photoreceptor changes in AMD. Additionally, this study only evaluates the *in vitro* effects of IL-1β, IL-18, and IL-17A; in the future, we hope to explore the effect of these cytokines *in vivo*.

5. Conclusions

In conclusion, we demonstrated that IL-1β, IL-18, and IL-17A have cytotoxic (necroptosis, pyroptosis, and apoptosis) effect and induce proinflammatory response in RSCs. Inflammasome promotes the maturation of IL-1β and IL-18 via caspase-1 activation. Though IL-1β, IL-18 alone could not induce IL-17A expression in RSCs, they all induce IL-17RC expression, which may mediate the effect of IL-17A.

Conflict of Interests

There is no conflict of interests in this research.

Authors' Contribution

Chi-Chao Chan and Shida Chen were responsible for analysis and interpretation of data and drafted the paper. Chi-Chao Chan, Jingsheng Tuo, and Shida Chen designed the study. Shida Chen, Defen Shen, Nicholas A. Popp, and Alexander J. Ogilvy performed experiments. Mones Abu-Asab and Ting Xie took part in analyzing data and revised the paper. All authors reviewed the paper.

Acknowledgment

This research received the NEI intramural research fund. The authors would like to thank Dr. Chun Gao of the Biological Imaging Core, NEI, who helped them with the confocal experiments.

References

[1] J. L. Dunaief, T. Dentchev, G.-S. Ying, and A. H. Milam, "The role of apoptosis in age-related macular degeneration," *Archives of Ophthalmology*, vol. 120, no. 11, pp. 1435–1442, 2002.

[2] J. Ambati, B. K. Ambati, S. H. Yoo, S. Ianchulev, and A. P. Adamis, "Age-related macular degeneration: etiology, pathogenesis, and therapeutic strategies," *Survey of Ophthalmology*, vol. 48, no. 3, pp. 257–293, 2003.

[3] J. Ambati, J. P. Atkinson, and B. D. Gelfand, "Immunology of age-related macular degeneration," *Nature Reviews Immunology*, vol. 13, no. 6, pp. 438–451, 2013.

[4] V. Tarallo, Y. Hirano, B. D. Gelfand et al., "DICER1 loss and Alu RNA induce age-related macular degeneration via the NLRP3 inflammasome and MyD88," *Cell*, vol. 149, no. 4, pp. 847–859, 2012.

[5] S. L. Doyle, M. Campbell, E. Ozaki et al., "NLRP3 has a protective role in age-related macular degeneration through the induction of IL-18 by drusen components," *Nature Medicine*, vol. 18, no. 5, pp. 791–798, 2012.

[6] O. A. Anderson, A. Finkelstein, and D. T. Shima, "A2E induces IL-1β production in retinal pigment epithelial cells via the NLRP3 inflammasome," *PLoS ONE*, vol. 8, no. 6, Article ID e67263, 2013.

[7] S. J. Lalor, L. S. Dungan, C. E. Sutton, S. A. Basdeo, J. M. Fletcher, and K. H. G. Mills, "Caspase-1-processed cytokines IL-1beta and IL-18 promote IL-17 production by gammadelta and CD4 T cells that mediate autoimmunity," *The Journal of Immunology*, vol. 186, no. 10, pp. 5738–5748, 2011.

[8] L. S. Dungan and K. H. G. Mills, "Caspase-1-processed IL-1 family cytokines play a vital role in driving innate IL-17," *Cytokine*, vol. 56, no. 1, pp. 126–132, 2011.

[9] J.-M. Doisne, V. Soulard, C. Bécourt et al., "Cutting edge: crucial role of IL-1 and IL-23 in the innate IL-17 response of peripheral lymph node NK1.1-invariant NKT cells to bacteria," *The Journal of Immunology*, vol. 186, no. 2, pp. 662–666, 2011.

[10] L. Campillo-Gimenez, M.-C. Cumont, M. Fay et al., "AIDS progression is associated with the emergence of IL-17-producing cells early after simian immunodeficiency virus infection," *The Journal of Immunology*, vol. 184, no. 2, pp. 984–992, 2010.

[11] B. Liu, L. Wei, C. Meyerle et al., "Complement component C5a promotes expression of IL-22 and IL-17 from human T cells and its implication in age-related macular degeneration," *Journal of Translational Medicine*, vol. 9, article 111, 12 pages, 2011.

[12] D. Ardeljan, Y. Wang, S. Park et al., "Interleukin-17 retinotoxicity is prevented by gene transfer of a soluble interleukin-17 receptor acting as a cytokine blocker: implications for age-related macular degeneration," *PLoS ONE*, vol. 9, no. 4, Article ID e95900, 2014.

[13] L. Wei, B. Liu, J. Tuo et al., "Hypomethylation of the IL17RC promoter associates with age-related macular degeneration," *Cell Reports*, vol. 2, no. 5, pp. 1151–1158, 2012.

[14] T. Li, M. Lewallen, S. Chen, W. Yu, N. Zhang, and T. Xie, "Multipotent stem cells isolated from the adult mouse retina are capable of producing functional photoreceptor cells," *Cell Research*, vol. 23, no. 6, pp. 788–802, 2013.

[15] Y. Wang, D. Shen, V. M. Wang et al., "Enhanced apoptosis in retinal pigment epithelium under inflammatory stimuli and oxidative stress," *Apoptosis*, vol. 17, no. 11, pp. 1144–1155, 2012.

[16] A.-J. F. Carr, M. J. K. Smart, C. M. Ramsden, M. B. Powner, L. da Cruz, and P. J. Coffey, "Development of human embryonic stem cell therapies for age-related macular degeneration," *Trends in Neurosciences*, vol. 36, no. 7, pp. 385–395, 2013.

[17] K. Bharti, M. Rao, S. C. Hull et al., "Developing cellular therapies for retinal degenerative diseases," *Investigative Ophthalmology & Visual Science*, vol. 55, no. 2, pp. 1191–1202, 2014.

[18] A. Kaczmarek, P. Vandenabeele, and D. V. Krysko, "Necroptosis: the release of damage-associated molecular patterns and its physiological relevance," *Immunity*, vol. 38, no. 2, pp. 209–223, 2013.

[19] A. Linkermann and D. R. Green, "Necroptosis," *The New England Journal of Medicine*, vol. 370, no. 5, pp. 455–465, 2014.

[20] A. Degterev, Z. Huang, M. Boyce et al., "Chemical inhibitor of nonapoptotic cell death with therapeutic potential for ischemic brain injury," *Nature Chemical Biology*, vol. 1, no. 2, pp. 112–119, 2005.

[21] D. Ofengeim and J. Yuan, "Regulation of RIP1 kinase signalling at the crossroads of inflammation and cell death," *Nature Reviews Molecular Cell Biology*, vol. 14, no. 11, pp. 727–736, 2013.

[22] S. W. G. Tait, G. Ichim, and D. R. Green, "Die another way—non-apoptotic mechanisms of cell death," *Journal of Cell Science*, vol. 127, part 10, pp. 2135–2144, 2014.

[23] C. P. Ardeljan, D. Ardeljan, M. Abu-Asab, and C. C. Chan, "Inflammation and cell death in age-related macular degeneration: an immunopathological and ultrastructural model," *Journal of Clinical Medicine*, vol. 3, no. 4, pp. 1542–1560, 2014.

[24] D. Ling, B. Liu, S. Jawad et al., "The tellurium redox immunomodulating compound AS101 inhibits IL-1beta-activated inflammation in the human retinal pigment epithelium," *The British Journal of Ophthalmology*, vol. 97, no. 7, pp. 934–938, 2013.

[25] W. A. Tseng, T. Thein, K. Kinnunen et al., "NLRP3 inflammasome activation in retinal pigment epithelial cells by lysosomal destabilization: implications for age-related macular degeneration," *Investigative Ophthalmology and Visual Science*, vol. 54, no. 1, pp. 110–120, 2013.

[26] S. H. Chang and C. Dong, "Signaling of interleukin-17 family cytokines in immunity and inflammation," *Cellular Signalling*, vol. 23, no. 7, pp. 1069–1075, 2011.

[27] Y. Hu, F. Shen, N. K. Crellin, and W. Ouyang, "The IL-17 pathway as a major therapeutic target in autoimmune diseases," *Annals of the New York Academy of Sciences*, vol. 1217, no. 1, pp. 60–76, 2011.

[28] R. Gold and F. Lühder, "Interleukin-17—extended features of a key player in multiple sclerosis," *The American Journal of Pathology*, vol. 172, no. 1, pp. 8–10, 2008.

[29] W. T. Hu, A. Chen-Plotkin, M. Grossman et al., "Novel CSF biomarkers for frontotemporal lobar degenerations," *Neurology*, vol. 75, no. 23, pp. 2079–2086, 2010.

[30] C.-C. Chan and D. Ardeljan, "Molecular pathology of macrophages and interleukin-17 in age-related macular degeneration," *Advances in Experimental Medicine and Biology*, vol. 801, pp. 193–198, 2014.

[31] D. V. Jovanovic, J. A. Di Battista, J. Martel-Pelletier et al., "IL-17 stimulates the production and expression of proinflammatory cytokines, IL-beta and TNF-alpha, by human macrophages," *The Journal of Immunology*, vol. 160, no. 7, pp. 3513–3521, 1998.

[32] S. Zrioual, M.-L. Toh, A. Tournadre et al., "IL-17RA and IL-17RC receptors are essential for IL-17A-induced ELR^+ CXC chemokine expression in synoviocytes and are overexpressed in rheumatoid blood 1," *The Journal of Immunology*, vol. 180, no. 1, pp. 655–663, 2008.

[33] R. Klein, C. E. Myers, K. J. Cruickshanks et al., "Markers of inflammation, oxidative stress, and endothelial dysfunction and the 20-year cumulative incidence of early age-related macular degeneration: the beaver dam eye study," *JAMA Ophthalmology*, vol. 132, no. 4, pp. 446–455, 2014.

[34] S. Cao, A. Ko, M. Partanen et al., "Relationship between systemic cytokines and complement factor H Y402H polymorphism in patients with dry age-related macular degeneration," *American Journal of Ophthalmology*, vol. 156, no. 6, pp. 1176–1183, 2013.

[35] E. Bettelli, Y. Carrier, W. Gao et al., "Reciprocal developmental pathways for the generation of pathogenic effector TH17 and regulatory T cells," *Nature*, vol. 441, no. 7090, pp. 235–238, 2006.

[36] C. E. Sutton, S. J. Lalor, C. M. Sweeney, C. F. Brereton, E. C. Lavelle, and K. H. G. Mills, "Interleukin-1 and IL-23 induce innate IL-17 production from gammadelta T cells, amplifying Th17 responses and autoimmunity," *Immunity*, vol. 31, no. 2, pp. 331–341, 2009.

[37] C. Sutton, C. Brereton, B. Keogh, K. H. G. Mills, and E. C. Lavelle, "A crucial role for interleukin (IL)-1 in the induction of IL-17-producing T cells that mediate autoimmune encephalomyelitis," *The Journal of Experimental Medicine*, vol. 203, no. 7, pp. 1685–1691, 2006.